DESIGN AND EVALUATION OF A PLANNING AID FOR PORT PLACEMENT IN ROBOT-ASSISTED LAPAROSCOPIC SURGERY

A thesis

submitted by

Jose Bañez

In partial fulfillment of the requirements

for the degree of

Master of Science

in

Human Factors

TUFTS UNIVERSITY

August 2012

ADVISER: Caroline G.L. Cao

Copyright © 2012 Jose Bañez

Abstract

Robot-assisted laparoscopic surgery is gaining popularity because it has been associated with reduced blood loss and shorter hospital stays for patients while providing ergonomic advantages to the surgeon over conventional laparoscopic surgery. However, it can result in a longer pre-operative planning process. The goal of this research was to provide an aid for placing ports and posing the robot. A field study was conducted with observations and interviews with expert surgeons to understand the challenges associated with the robot. A symbolic model of the robot was created along with a simplified method to model the patient torso to enable calculation of a suitable port placement and robot pose plan. A prototype planning aid incorporating patient modeling, port placement, and posing the robot was created and tested. Results indicate that providing a view of the robot pose from above helped subjects replicate the recommended pose on a model of the robot.

Keywords: da Vinci Surgical System, Patient Specific Port-placement, Robot-Assisted Laparoscopic Surgery, Robotic Surgery Simulation

Acknowledgements

Dr. Caroline G.L. Cao, Department of Mechanical Engineering, Tufts University

Dr. Jason Rife, Department of Mechanical Engineering, Tufts University

Dr. Steven Schwaitzberg, Chief of Surgery, Cambridge Health Alliance

Pr. Jean-Marc Classe, MD, PhD and the surgical staff at Département Chirurgie Oncologique, Institut de Cancérologie de l'Ouest

Dr. Stéphane Caro, Researcher, Institut de Recherche en Communications et Cybernétique de Nantes (IRCCyn)

Dr. Daniel Hannon, Department of Mechanical Engineering, Tufts University

Dr. Amine Chellali, Post-Doctoral Associate, Cambridge Health Alliance

Dr. Tad Brunye, Visiting Scholar, Spatial Cognition Laboratory, Tufts University

Stacey Cunningham, MS Human Factors E12, Tufts University

Bertrand Lamiré, clinical sales representative, Intuitive Surgical

Dr. Chris Rogers, Director, Tufts University Center for Engineering Education and Outreach (CEEO)

Mike Kokko, Senior Systems Integration Engineer, Simbex

Dr. Paul M. Hendessi, MD, Director of Gynecology, Boston Medical Center

Katarina Morowsky, Erin Davis, Cristol Grosdemouge, Likun Zhang, Seth Studer

Table of Contents

List of Tables

List of Figures

DESIGN AND EVALUATION OF A PLANNING AID FOR PORT PLACEMENT IN ROBOT-ASSISTED LAPAROSCOPIC SURGERY

1. Introduction

Laparoscopic surgery is a form of minimally invasive surgery (MIS) performed in the abdominal and pelvic areas for general abdominal surgery, gynecology, and urology (Kenngott et al, 2011). Benefits of laparoscopic surgery generally include decreased pain, decreased blood loss, less scarring, a lower risk of infection, and a shorter hospital stay (Advincula & Wang, 2009). It is performed using specially-designed tools that are inserted into the patient abdomen through narrow openings that are strategically placed around the target area. These openings are commonly referred to as ports.

When placing the ports, surgeons must consider the variations in patient size and anatomy, and also the spatial requirements of the planned intervention. The ports limit the movement of the surgical instruments to five (5) degrees of freedom (DOF): pitch, yaw, rotation, and extraction/insertion plus the actuation of the tool's manipulator at the tip. Proper port placement affords easy access to the target areas, an optimal view of the target area, reduced time and effort to perform the procedure, and a decrease in mental and physical fatigue (Ferzli & Fingerhut, 2004). When placed improperly, surgeons could experience difficulty performing the procedure, have to assume difficult positions, or add additional ports which increases patient trauma.

Robot-assisted laparoscopic surgery is becoming increasingly popular with patients because of its perceived advantages over other forms of minimally invasive surgery. According to Kenngott et al. (2011), over 70% of procedures

performed with the da Vinci System are for prostatectomy and hysterectomy as stated by Intuitive Surgical Inc. in their 2010 Annual Report. However, the comparison is more accurately between open and robot-assisted for prostatectomy and especially hysterectomy which have not been commonly performed using conventional laparoscopy (Kenngott et al, 2011). So the advantages commonly for robotic surgery are the same advantages conventional laparoscopic surgery has over open techniques. Nevertheless, the robot introduces additional variables that surgeons must consider during the critical act of port placement. Ports must be placed so that the surgical instruments attached to each robot arm can have the same access to the target area as a surgeon would in conventional laparoscopic surgery. However, each robot arm has multiple joints that allow a multitude of arrangements or poses. Ports must be placed so that the robot arms can be posed to avoid collisions with vulnerable patient anatomy, with other robot arms, and with other objects in the operating room (Adhami & Coste-Manière, 2003).

The process of positioning the robot, posing and connecting each robotic arm to the trocars, and the insertion of the surgical instruments to perform the intervention is referred to as docking (Dal Moro, Secco, Valotto, Artibani, & Zattoni, 2011). It is difficult to pose the robot in such a way that provides the surgeon unrestricted visual and physical access to the surgical field. It is also difficult to maximize the separation between the robot arms, and to anticipate collisions, both internal and external to the patient. For this reason, robotic surgery can increase the time surgeons spend in pre-operative planning.

Although Intuitive Surgical, the manufacturer of the da Vinci Surgical System provides guidelines and training for use, guidelines are inadequate, if only because they are not tailored for the variations of each patient and each surgical intervention. Likewise, training cannot necessarily account for these variations. Thus, when the ports are poorly placed or when the robot is posed incorrectly, it may become necessary to reposition the robot to improve access to the target area. Once it has been docked, the robot cannot be repositioned easily. This will further extend the total duration of the operation (Zorn et al., 2007).

The goal of this project was to provide surgeons with a real-time or near real-time port-placement aid for pre-operative planning in robot-assisted laparoscopic surgery. The objective was to design an intelligent software tool that accepts both patient characteristics and the planned intervention as inputs, then given the inputs, provides recommendations for port placement, and, finally, provides guidance in the positioning and posing of the robot. In order to accomplish this objective, four distinct phases of research were conducted. The first phase consisted of field observations. The second phase focused on modeling the robot arms of the da Vinci Si Surgical System, the only system currently approved by the FDA to perform robot-assisted laparoscopic surgery. The third phase focused on modeling the patient anatomy to allow for calculation of a port placement recommendation. During the final phase, a prototype planning aid was designed to address the ergonomic challenges associated with pre-operative planning, especially the posing of the robot arms. A usability test

was conducted to determine its ease of use and effectiveness in the pre-operative planning process. The results indicate that showing the recommended arrangement of the robot arms from a perspective about the robot could be helpful to achieving the recommended pose.

2. Background

In laparoscopic surgery, small incisions are made in the patient's abdomen around the target area to gain access to the abdominal cavity. In comparison to open surgery, this method has several major advantages to the patient including reduced blood loss, shorter hospital stay, faster recovery time, and smaller scars (Kenngott et al, 2011). Examples of procedures performed laparoscopically include cholecystectomy or removal of the gallbladder and prostatectomy or removal of all or part of the prostate gland (Ferzli & Fingerhut, 2004). The first documented laparoscopic cholecystectomy was performed in Germany in 1985. It was first performed in the United States in 1988 (Reynolds, 2001). Since then, cholecystectomy became one of the most common procedures performed in the US and is performed primarily laparoscopically ("Patient Information for Laparoscopic Gall Bladder Removal," 2011). Patients who undergo cholecystectomies laparoscopically typically experience a short hospital stay of one (1) day or less. This is compared to two (2) or three (3) days with open surgery.

One (1) in six (6) men in the US is diagnosed with prostate cancer and it is

the second leading cause of death from cancer for men. In one treatment option for prostate cancer, the entire prostate gland and some of the surrounding tissue is removed. The procedure is called a radical prostatectomy. Demand is rising for this procedure to be performed laparoscopically because patients perceive that this approach would require smaller incisions and result in shorter hospital stays versus open radical prostatectomy (Hu et al, 2008).

The target organs of both these laparoscopic procedures are in different parts of the abdominal and pelvic areas. Surgeons must consider the requirements for the specific procedure as well as the variations in patient anatomy when selecting sites for the incisions. This is to ensure that they will have adequate visual and physical access to the target area to perform the procedure. This process is referred to as port placement.

2.1. Port Placement in Laparoscopic Procedures

Laparoscopic surgery is performed using specially designed tools that are inserted through narrow openings in the abdomen. These openings are created using a device with two components: a hollow cannula or port, and the trocar which is inserted in the cannula and used to cut through the abdominal wall. The port remains in place after the trocar is removed and can vary in size to accommodate different surgical instruments (Shafer , Khajanchee, Wong, & Swanstrom, 2006). Typical port sizes are 5, 8, 10, and 12mm in diameter (Covidien Surgical, 2012).

The view of the operative field is provided by an endoscope which is a

surgical instrument that allows surgeons to view inside a patient. When inserted in the abdominal or pelvic cavity, it is also called a laparoscope. A laparoscope is inserted into one port while surgeons operate using surgical instruments in additional ports (Coste-Manière, Adhami, Mourgues & Carpentier, 2003).

In order to have more room operate, surgeons expand the abdominal cavity by introducing carbon dioxide, a process called insufflation. The condition of having gas in the abdominal or peritoneal cavity is called pneumoperitoneum. Depending on the port placement method, the initial port may be inserted before or after pneumoperitoneum.

Methods to insert ports in conventional laparoscopic procedures are grouped into three categories: blind or closed, visual or open, and hybrid visual and closed methods. The blind or closed method is further divided into two methods: needle or direct trocar insertion. With the needle insertion method, a Veress or other needle is inserted into the peritoneum to insufflate the abdomen before the insertion of the initial trocar. This is the access method most commonly used in gynecology. The direct method uses the first trocar to insufflate the abdominal area. In the visual or open technique, also called the Hasson technique, incisions are made carefully to reach the peritoneal cavity before insertion of a blunt trocar. With the hybrid visual and closed methods, an optical trocar or optical needle is used before gas insufflation to inspect the abdominal cavity (Lalchandani & Philips, 2008)

Care must be taken during the insertion of the ports to avoid injury to the

arteries and veins, especially the aorta and the iliac vessels. The aortic bifurcation, the separation of the aorta into the common iliac arteries, can be above, below, or at the same level as the umbilicus, depending on the patient habitus, or body type, and body mass index (BMI). For thinner patients, the depth or distance from the abdominal wall to the aorta and iliac arteries is less than in other patients. Injury may also occur during port placement due to adhesions to the abdominal wall. To minimize the risk of injury when placing additional ports, the laparoscope is inserted into the first port and used to monitor the abdominal cavity (Shafer et al., 2006). The initial port is usually placed near the umbilicus. The positions of the other ports are dependent on the planned surgical procedure, the patient's characteristics, and surgeon's habitus or body type (Ferzli & Fingerhut, 2004).

2.2. Port Placement Objectives

Proper port placement in conventional laparoscopy results in optimal view of the surgical area and optimal access to the target organs. Optimal view of the surgical area not only allows the surgeon to see the surgical area but also eases the surgeon's ability to recognize target organs. It also reduces the risk of injury and allows the surgeon to immediately see and recognize any problems as they occur such as an injury to the patient or internal bleeding. Optimal view also reduces the mental fatigue that may result from "working opposite" or "against" the camera, requiring increased mental effort to coordinate the movement of the instruments (Ferzli & Fingerhut, 2004).

Ports restrict the movements of the surgical instruments at the abdominal wall (Figure 1). The surgical instruments pivot at the port to access the target region. The amount of room necessary for the instrument to access the target region defines its work envelope inside the abdominal cavity. Optimal port placement provides the surgeon access to the surgical area and the target organs, without the need to move instruments between ports or to relocate ports because instruments cannot reach the target area. A suitable port placement ensures that instruments including the camera do not compete with each other for the same work volume to minimize the risk of collisions. Finally, it allows the surgeon to perform the procedure without assuming a difficult stance or pose which can contribute to physical and mental fatigue (Ferzli & Fingerhut, 2004).

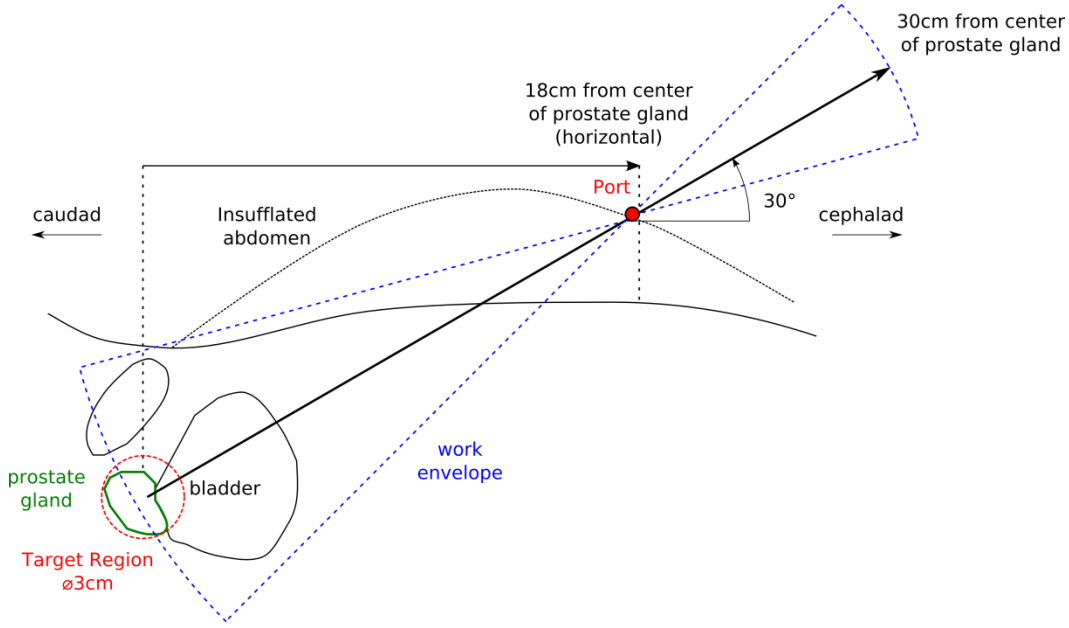

Figure 1. Example of Port Placement and Work Volume

Ferzli and Fingerhut (2004) provided a standardized technique for port placement in laparoscopic abdominal procedures. Using this technique, the abdominal area is divided into four quadrants (anterior and lateral) and two triangles: thoracic or cephalad, and pelvic or caudad, as shown in Figure 2.

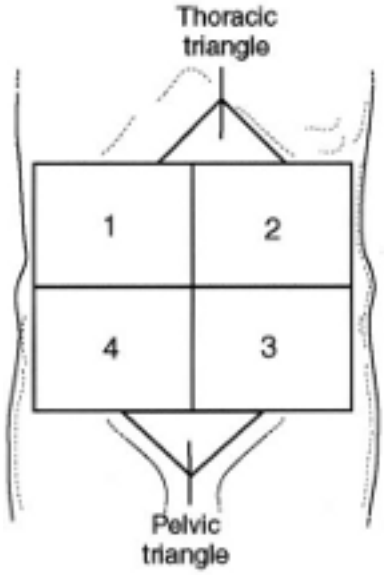

Figure 2. Abdominal quadrants and triangles (Ferzli and Fingerhut, 2004).

Trocars are placed along a semi-circular line centered on the target organ with a radius between 16 and 18 cm. This distance is intended to provide a suitable ratio between the length of the laparoscopic tool that is inside the patient cavity and the length that is outside the patient cavity for a standard length laparoscopic tool, about 30 – 35cm. This is referred to as the intracorporeal-extracorporeal tool length ratio. A study by Emam, Hanna, Kimber, Dunkley, & Cuschieri (2000) and cited by Ferzli & Fingerhut (2004) indicated that a reduction of this ratio below 1:1 in conventional laparoscopic surgery can negatively affect the dexterity of the

surgeon in performing the surgical procedure. In addition, the ports should be separated to achieve a suitable manipulation angle. A study by Hanna, Shimi, & Cuschieri (1997), also cited by Ferzli & Fingerhut (2004), indicated that the optimal manipulation angle for endoscopic knot-tying, the angle between two instruments with their tips at the center of the target region, is about 60 degrees.

In the illustration in Figure 1 with a 30° elevation angle, the intracorporeal tool length is 20cm and the extracorporeal tool length is 10cm. The intracorporeal-extracorporeal tool length ratio in this example is 2:1. Shorter instruments are available and typically used for pediatric surgery. Longer instruments, about 45cm long, typically used for larger patients, are also available. Ports should be placed so that the resulting intracorporeal:extracorporeal tool length ratio and manipulation angle are suitable for the planned procedure using the desired instrument length (Ferzli & Fingerhut, 2004).

An example of port placement for procedures in the patient's right upper quadrant (e.g., a laparoscopic cholecystectomy) is shown in Figure 3. The laparoscope is at port C. Instruments can access the gallbladder from ports A, B, and D. Ports A and B may be optimal positions while port D may be restricted due to collision with the rib-cage. The resulting manipulation angles between instrument ports A & B, A & D, or B & D may also be sub-optimal. Surgeons are advised to consider the length of the instruments and the trocars, the surgeon's habitus or body type, and the size of the work area in selecting suitable port placement for optimal ergonomics (Ferzli & Fingerhut, 2004).

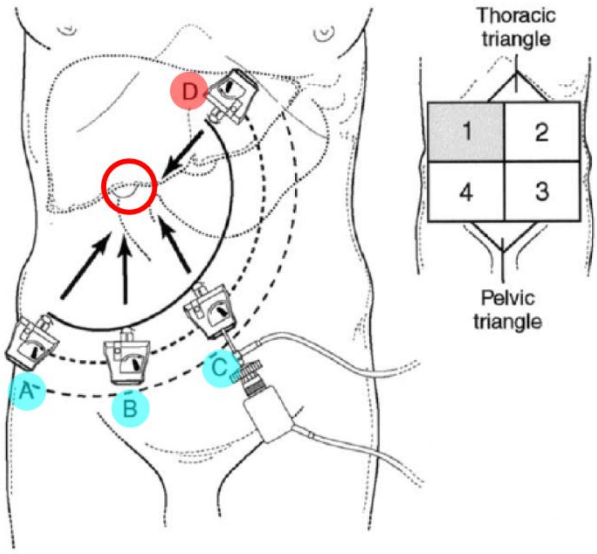

Figure 3. Port Placement for Laparoscopic Cholecystectomy (Ferzli & Fingerhut, 2004).

2.3. Variations in Patient Characteristics

Port placement in minimally invasive surgery (MIS) is based on the preference of the primary surgeon. His or her preference may be guided by experience, training, textbooks, or research papers. Basing port placement on personal preference may work in many situations but does not take into account the variations in patient characteristics that even an experienced surgeon may not have yet encountered (Ferzli & Fingerhut, 2004), (Trejos, Patel, Ross & Kiaii, 2007).

For patients with previous abdominal surgical procedures, ports must be placed to avoid scars where there may be adhesions to the abdominal wall. Port placement must be modified and the port that will be farthest from the scars or

possible adhesions be inserted first, prior to other ports to allow visual inspection of the abdominal wall and guide the safe insertion of additional trocars (Ferzli & Fingerhut, 2004).

Surgeons often use the umbilicus as a key reference point. But variation of umbilical position and abdominal dimensions vary widely with patient body mass index (BMI). Tall, heavy, short, and thin patients vary from the abdominal topography in textbooks. In a study conducted over a 9 month period, the BMI of 259 patients was calculated at New York -Presbyterian Hospital and Ben Taub General Hospital and each patient was classified in one of four groups: underweight, normal, overweight, and obese. The average position of the umbilicus for all four groups was below the vertical midpoint, and was lower as the BMI increased. In women with above-normal BMI, the location of the umbilicus shifted caudally, but the internal organs did not. Further, abdominal dimensions also increased with increased BMI (Ambardar et al., 2008).

Torso length also affects ideal port placement. For women who have relatively short dimensions below the umbilicus, one researcher found it necessary to place several ports above the umbilicus to accommodate the recommended 10cm separation between ports to avoid collisions between surgical instruments (Matthews, Schubert, Woodward, & Gill, 2010). An example for a laparoscopic prostatectomy is shown in Figure 4. In this example, for male patients who are taller than average (over 6 feet tall), the distance between the umbilicus and the target organs, marked by a Z, may be greater after insufflation

than expected. Thus, instruments may not be able to reach the target area in such a patient, because it will be too far away from the port (Pick, Lee, Skarecky & Ahlering, 2004).

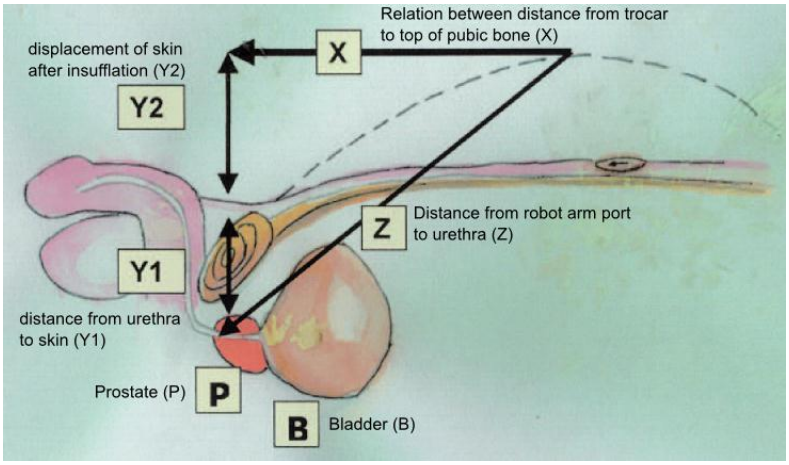

Figure 4. Relation between trocar and pubic bone (Pick, Lee, Skarecky & Ahlering, 2004)

2.4. Surgical Robotics

In 1985, the first use of a robot in surgery occurred with the PUMA 560. It was used to perform stereotactic brain biopsy under computed tomography guidance. In 1992, ROBODOC was used to perform total hip replacements. In 2000, the US Food and Drug Administration (FDA) approved the da Vinci surgical system from Intuitive Surgical Inc. The ZEUS system from Computer Motion, Inc, was developed in 1999 for use in cardiac operations and approved by the FDA for use in general surgery in 2001. The PUMA 560, ROBODOC, and other early designs performed their tasks autonomously using pre-operative imaging. In contrast, the da Vinci and ZEUS systems were designed to be tele-

operated by a surgeon using a remote console, located in the same room or a long distance away (Advincula & Wang, 2009).

The ZEUS surgical system was a master-slave system with two robotic arms in addition to the camera. It was based on the AESOP (Automated Endoscopic System for Optimal Positioning) from the same company that was simply a robotic camera holder. The surgeon controlled the slave robotic instruments from a master console using handles similar to joysticks and viewed the operation from a monitor with special glasses to achieve three-dimensional (3D) visualization. The computer interface reduced physiological tremors and allowed the surgeon's movements to be scaled from 2:1 to 10:1 to improve precision (Advincula & Wang, 2009).

The da Vinci® Surgical System from Intuitive Surgical is similar to the ZEUS with a master-slave configuration. It consists of the surgical console, the imaging system, and the patient-side cart with three or four robotic arms, depending on the model (Advincula & Wang, 2009). The patient-side cart is commonly referred to as the robot. The latest model of the da Vinci system, the Si model, is shown in Figure 5 with the surgeon operating console on the left and an assistant at the operating table on the right. The patient-side cart is behind the operating table (Intuitive Surgical, 2011). Numerous surgical instruments are available for use with the system that allows the surgeon to perform the same procedures as in conventional laparoscopic surgery.

In 2003, Intuitive Surgical, Inc. acquired Computer Motion, Inc. and

phased out the ZEUS system. The da Vinci Surgical System is the only system currently approved by the FDA to perform robot-assisted laparoscopic surgery. Thus, this study is limited to only the patient side cart, or robot, component of the da Vinci Surgical System in discussing robot-assisted laparoscopic surgery (Kenngott et al, 2011).

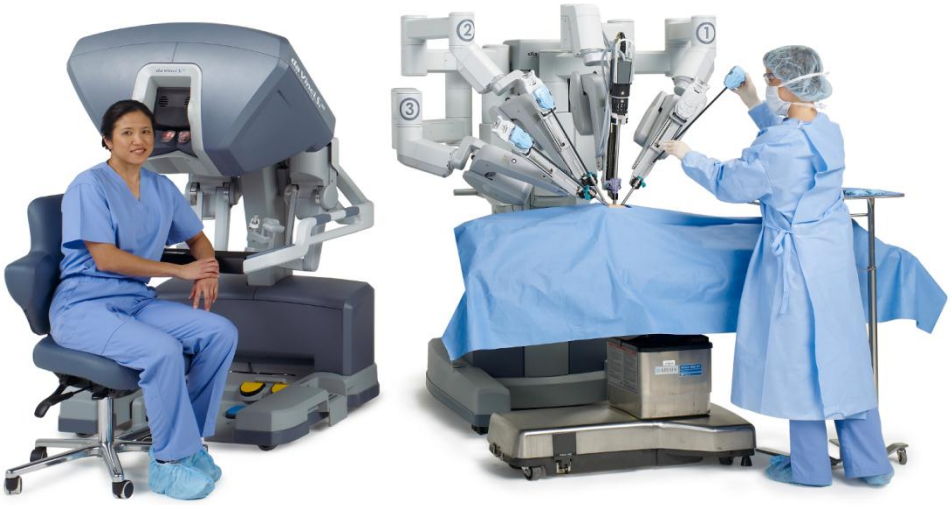

Figure 5. da Vinci Si HD Surgical System©2011 Intuitive Surgical, Inc.

2.5. Disadvantages of Laparoscopic Surgery

Surgeons performing conventional laparoscopic surgery experience several disadvantages over open surgery. As laparoscopic procedures have become more advanced, the duration of operations and the physical and mental stress on the surgical teams have likewise increased. However improvements in the ergonomics of surgical instruments used and the operating room in general, originally designed for conventional surgery, have not kept pace.

The instruments themselves have several disadvantages. Laparoscopic

instruments reduce haptic sense to minimal tactile feedback. Because laparoscopic instruments are restricted by the diameter of the ports, actions at the handle are transmitted by cables to the end-effector. This requires surgeons to apply up to six times more force to perform a task than is required in open surgery. Non-ergonomically designed laparoscopic instruments can exacerbate the problem and lead to damage to the nerves of the thumb and the thenar muscle at the base of the thumb.

The two-dimensional (2D) view of the operative field is provided by the laparoscope. The lack of depth cues can impair hand-eye coordination. The position of the display monitor is often away from the hands and the instruments requiring mental rotations and can result in increased mental stress. The display monitor often is also positioned at a height to avoid its view being obstructed by equipment or other surgical team members which can increase physical fatigue and can also affect hand-eye coordination.

Laparoscopy limits the range of motion of the surgeon. The ports act like a spherical joint that constrains the motion of surgical instruments at a fixed point at the abdominal wall. This limits the degrees of freedom (DOF) of movement to five (5). There are four (4) DOF to move the tip of instrument: pitch, yaw, rotation, and translation. Pitch is the up and down motion at the tip of the instrument. Yaw is the side to side motion. Rotation is the twisting along the axis of the instrument and translation is the insertion and extraction of the instrument. The actuation of the tip of the instrument, usually called an end-effector, is the

fifth DOF. This is illustrated in Figure 6. Surgeons are sometimes forced to adapt awkward positions dictated by the placement of the ports. In addition, they sometimes perform awkward movements to use instruments within the limited range afforded by the ports. This can result in additional physical stress and neck and shoulder pain. After several hours of performing surgery, the physical and mental stresses result in fatigue that can reduce dexterity necessary to perform the procedure and affect mental judgment (Rassweiler, et al., 2010). Robot-assisted laparoscopic surgery attempts to address some these issues to the advantage of both surgeons and patients.

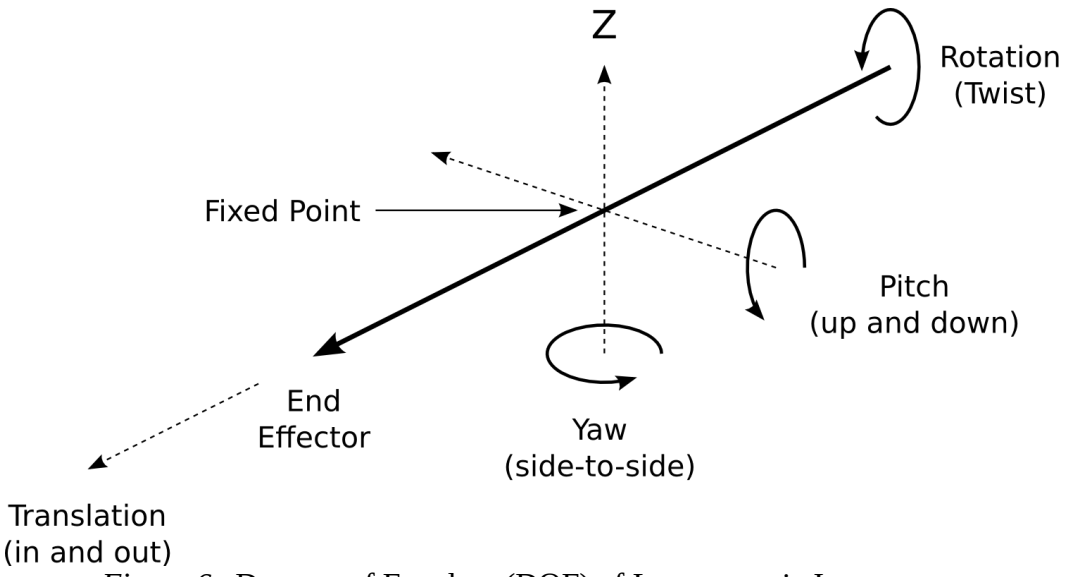

Figure 6. Degrees of Freedom (DOF) of Laparoscopic Instruments

2.6. Advantages of the da Vinci Surgical System

The da Vinci Surgical System affords the surgeon several ergonomic advantages over conventional laparoscopic surgery. First of all, the surgeon is seated at a console instead of standing while performing the procedure, reducing

the physical fatigue experienced by the surgeon. The surgeon also operates foot pedals while seated instead of standing so that the surgeon does not have to stand awkwardly with the surgeon's weight unevenly distributed between each leg (Rassweiler, et al., 2010).

Secondly the imaging system provides a three-dimensional (3D) stereoscopic view of the surgical field via the 12mm endoscope that is aligned with the workspace. This creates the illusion that the surgeon's hands are directly manipulating the end effectors inside the patient body without the necessary mental rotation or the strain of viewing a display monitor that may not be aligned with the surgeon's physical orientation. The imaging system can also provide up to ten times (10x) magnification for a closer view of the operative field (Rassweiler, et al., 2010).

The da Vinci system also provides increased precision and accuracy with regards to the surgeon's movements. It filters tremors unlike conventional laparoscopic tools which can magnify tremors due to the fulcrum effect (Rassweiler, et al., 2010). It can scale the surgeon's movements with ratios including 5:1, 3:1, and 1:1 so that a surgeon's movements at the console translates into smaller movements at the end effectors, allowing for greater accuracy (Advincula & Wang, 2009). Conventional laparoscopic tools limit the surgeon to four (4) degrees of freedom but EndoWrist instruments provide seven (7) DOF for enhanced dexterity (Intuitive Surgical, 2011). In addition to these advantages the da Vinci system provides to surgeons, it offers several benefits to patients.

2.7. Benefits of Robot-Assisted Laparoscopic Surgery

Initial performance of robot assisted laparoscopic radical prostatectomy (RARP) was in 2001 by Pasticier, Rietbergen, Guillonneau, Fromont, Menon, & Vallancien (2001). By 2006, 31,500 cases or 35% of all radical prostatectomies were predicted to have been performed with the da Vinci system (Zorn et al., 2007). By 2010, based on the annual report from Intuitive Surgical as cited by Kenngott et al. (2011), it was estimated that over 80% of prostatectomies in the US were performed robotically as compared to conventional laparoscopic or open prostatectomy. An analysis of outcomes in published studies of open, laparoscopic, and robot-assisted radical prostatectomies between November 1994 and May 2009 showed higher continence and potency rates after robot-assisted radical prostatectomy as compared with open and laparoscopic (Coelho et al., 2010).

Minimally invasive techniques have not been widely used in gynecology due to difficulty in learning the advanced techniques and adjusting to the ergonomic issues. The use of robotics in gynecology is a possible solution to this problem as it addresses some of the limitations of conventional laparoscopic surgery such as the counterintuitive hand movement and limited degrees of freedom. The da Vinci system was approved by the US Food and Drug Administration (FDA) in gynecologic procedures in 2005 though one of the earliest reported robot-assisted laparoscopic hysterectomy was in 2002 (Advincula & Wang, 2009). Of the 538,722 hysterectomies reported in the United

States, 66% were performed open (abdominally) versus 33.8% vaginally or laparoscopically. While open surgery provided advantages to the surgeon from better depth perception and haptic feedback, patients experienced longer hospitalization, increased pain, longer recovery times, increased blood loss, and increased risk of wound inspection that with the non-abdominal procedures (Matthews, 2010).

Myomectomy is one procedure used for the removal of uterine fibroids, benign growths in the uterus ("ACOG Education Pamphlet AP074," 2011). In a study of 58 patients, the complication rates were lower and lengths of hospital stay were shorter for the 29 patients received robotic myomectomy compared with the standard laparotomy though the mean operative time was longer, 231.38 minutes vs. 154.41 minutes (Advincula & Wang, 2009).

Tubal anastomosis, a method for reversal of tubal ligation, is a complex procedure that requires careful manipulation and precise suturing of the Fallopian tubes. The enhanced accuracy and precision provided by robotic surgery makes it well-suited for performing this procedure. In a study in 2007, a comparison of patients undergoing tubal anastomosis, twenty-six (26) patients' procedures were performed with robot assistance compared with forty-one (41) patients' procedures performed using mini laparotomy, the patients who underwent the robotic method experienced longer operative and anesthesia times but were able to return to normal activity sooner, mean 0.8 versus 2.8 weeks (Advincula & Wang, 2009).

In 2009, 205,000 procedures were performed with the da Vinci robot. This is up fifty-one percent from the previous year and continues to increase with patients demanding the latest medical technology (Gomes, 2011). Surgeons are adopting robot-assisted laparoscopic surgery in procedures in urology and gynecology still commonly performed via a laparotomy in an attempt to overcome limitations of conventional laparoscopy that have hindered wider application of minimally invasive techniques (Advincula & Wang, 2009). While providing benefits to both patients and surgeons, robot-assisted laparoscopic surgery presents additional challenges including port placement.

2.8. Overview of Port Placement and Docking the da Vinci Surgical System

Intuitive Surgical, the manufacturer of the da Vinci Surgical System, provides training and guidance to surgeons in placing ports for various robot-assisted laparoscopic surgical procedures. The recommendations differ slightly from conventional laparoscopic surgery for the same procedure. The endoscope port is also placed near the umbilicus but the ports for the surgical instruments are positioned with different manipulation angles and at a distance greater than 16 – 18cm from the center of the target organ. However, the mechanics of the robot and the instruments used are different. EndoWrist® laparoscopic instruments manufactured by Intuitive Surgical for use with the da Vinci Surgical System are approximately 50cm in length and provide seven (7) degrees of freedom (DOF) instead of five (5) DOF with conventional laparoscopic instruments (Kenngott et al, 2011). So, the recommended intracorporeal-extracorporeal tool length ratio

and optimal manipulation angle for conventional laparoscopic surgery may not apply.

In general the procedure starts with placing the 12mm port for the endoscope that will be attached to the arm at the center of the patient side cart during the docking process. It cannot be moved around to the other instrument ports which are usually 5 or 8mm. A visual inspection is performed while the endoscope is held manually and the image is shown on display monitor. Instrument ports are inserted while still viewing the abdomen from the display monitor. Additional 5 or 12mm ports are also inserted for the assistant or assistants to manipulate organs or perform other tasks and for a suction device. The position of these ports and the arrangement of the instrument arms have to be considered with the patient variables in avoiding collisions: between the instruments, with the patient, with the operating environment, or between the robot arms (Adhami & Coste-Manière, 2003).

The guide provided for a radical hysterectomy shown in Figure 7 in recommends placing the endoscope (12mm) port at the umbilicus about 20cm from the pubic bone. It suggests placing the right and left instrument (8mm) ports corresponding to arm 1 and 2 of the robot at about 10cm to the left and right of the endoscope. It recommends placing the assistant (12mm) port 1cm inferior to the costal margin and at least 6cm away from robotic ports. Finally it recommends placing the third instrument port corresponding to arm 3 approximately 20 cm from the umbilicus (Intuitive Surgical, 2008).

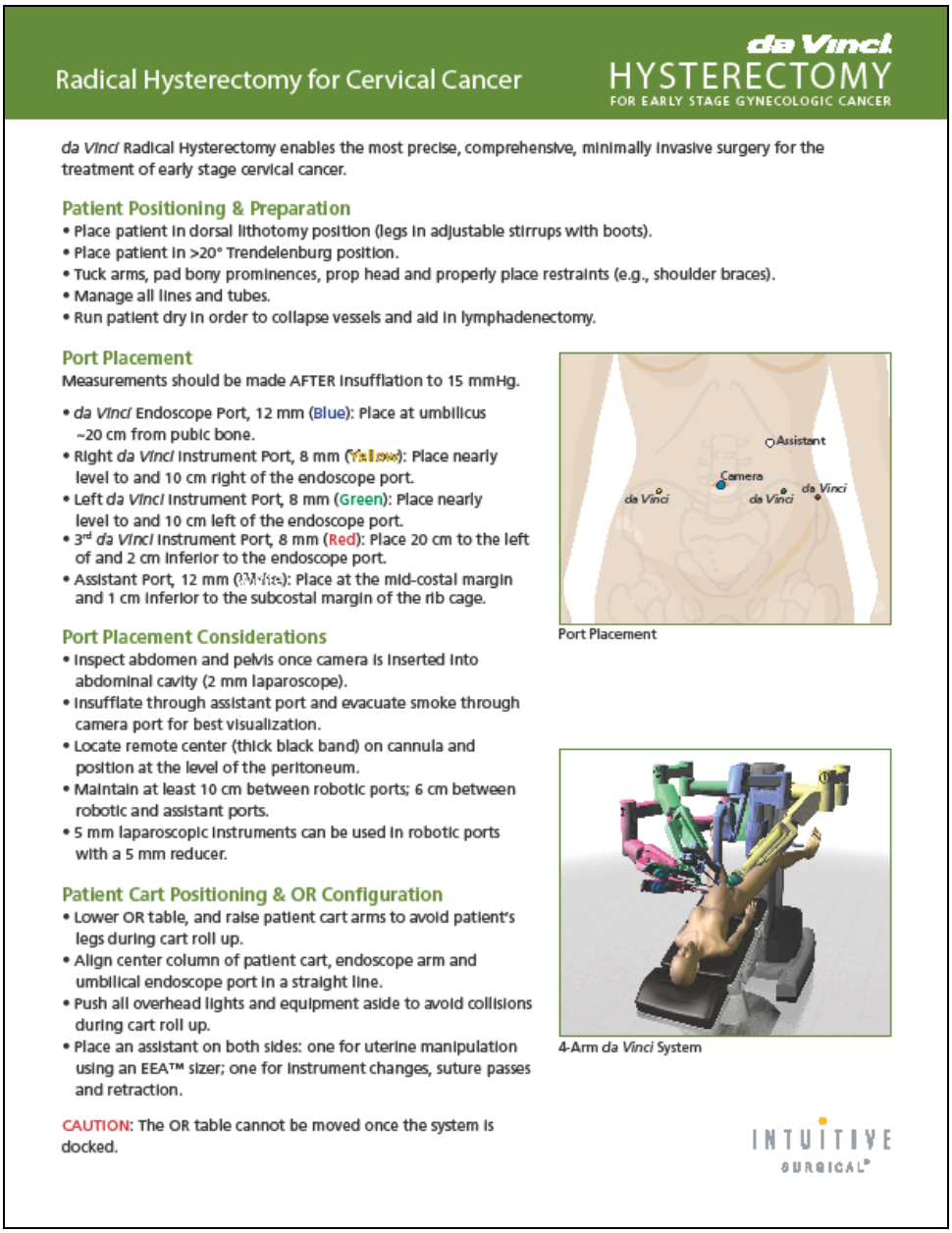

Radical Hysterectomy for Cervical Cancer

da Vinci HYSTERECTOMY
FOR EARLY STAGE GYNECOLOGIC CANCER

da Vinci Radical Hysterectomy enables the most precise, comprehensive, minimally invasive surgery for the treatment of early stage cervical cancer.

Patient Positioning & Preparation

- Place patient in dorsal lithotomy position (legs in adjustable stirrups with boots).
- Place patient in >20° Trendelenburg position.
- Tuck arms, pad bony prominences, prop head and properly place restraints (e.g., shoulder braces).
- Manage all lines and tubes.
- Run patient dry in order to collapse vessels and aid in lymphadenectomy.

Port Placement

Measurements should be made AFTER insufflation to 15 mmHg.

- *da Vinci* Endoscope Port, 12 mm (Blue): Place at umbilicus ~20 cm from pubic bone.
- Right *da Vinci* Instrument Port, 8 mm (Yellow): Place nearly level to and 10 cm right of the endoscope port.
- Left *da Vinci* Instrument Port, 8 mm (Green): Place nearly level to and 10 cm left of the endoscope port.
- 3rd *da Vinci* Instrument Port, 8 mm (Red): Place 20 cm to the left of and 2 cm inferior to the endoscope port.
- Assistant Port, 12 mm (White): Place at the mid-costal margin and 1 cm inferior to the subcostal margin of the rib cage.

Port Placement

Port Placement Considerations

- Inspect abdomen and pelvis once camera is inserted into abdominal cavity (2 mm laparoscope).
- Insufflate through assistant port and evacuate smoke through camera port for best visualization.
- Locate remote center (thick black band) on cannula and position at the level of the peritoneum.
- Maintain at least 10 cm between robotic ports; 6 cm between robotic and assistant ports.
- 5 mm laparoscopic instruments can be used in robotic ports with a 5 mm reducer.

Patient Cart Positioning & OR Configuration

- Lower OR table, and raise patient cart arms to avoid patient's legs during cart roll up.
- Align center column of patient cart, endoscope arm and umbilical endoscope port in a straight line.
- Push all overhead lights and equipment aside to avoid collisions during cart roll up.
- Place an assistant on both sides: one for uterine manipulation using an EEA™ sizer; one for instrument changes, suture passes and retraction.

CAUTION: The OR table cannot be moved once the system is docked.

4-Arm *da Vinci* System

INTUITIVE SURGICAL®

Figure 7. Procedure Card Hysterectomy

After the ports are placed, the docking procedure begins when the patient cart is brought to position at the operating table, the arms to be used for the procedure are posed, and the cannula mounts are mated to the ports in the patient's abdomen. An example of the robot docked with a patient in position for

a hysterectomy is shown in Figure 8. Only after docking is complete will work begin at the console for the surgeon to perform the intervention (Dal Moro et al, 2011).

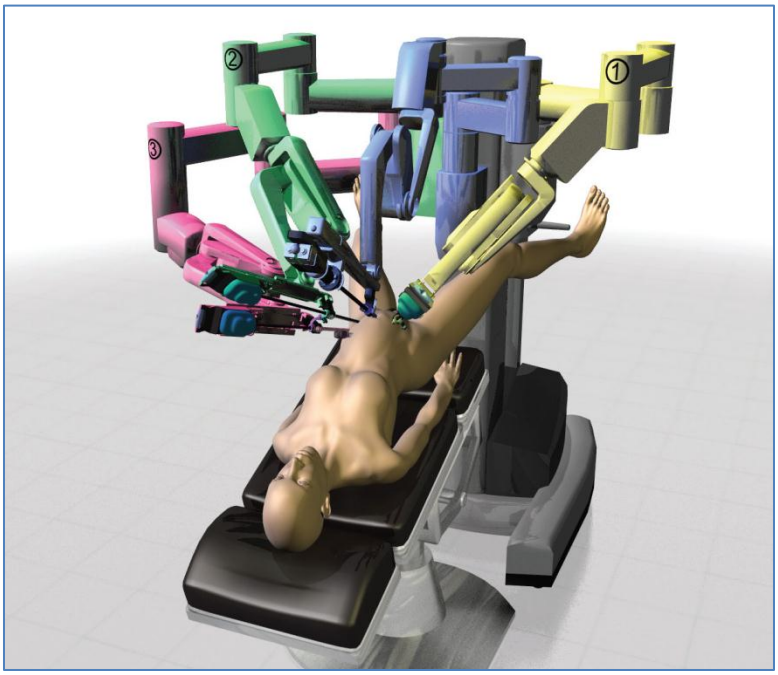

Figure 8. Patient Cart Pose Guide Example (Intuitive Surgical, 2008)

3. Problem Statement

The difficulty in port placement is best illustrated when the guidelines are applied to a patient undergoing a gynecologic procedure whose torso may be smaller than average as shown in Figure 9. The patient's torso is very narrow and it would be difficult to apply the port placement recommendations from the sample procedure card for a hysterectomy shown in Figure 7.

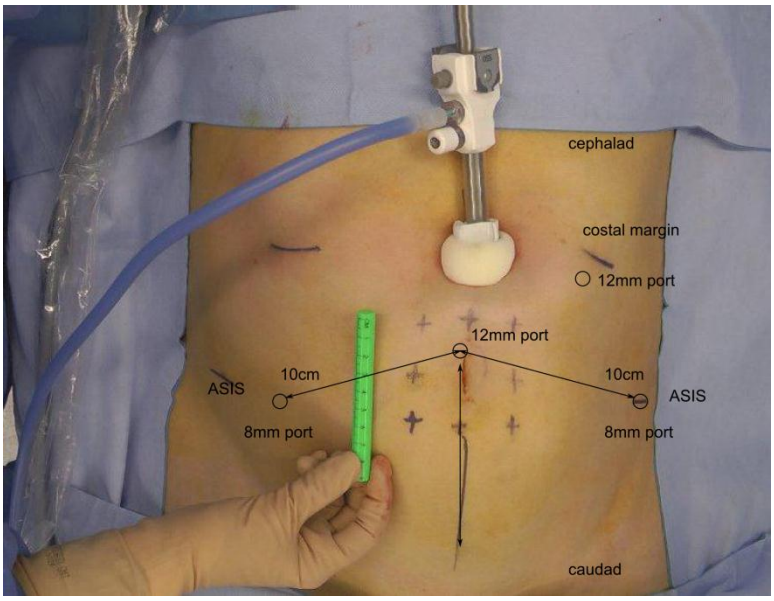

Figure 9. Patient Torso Marked for Hysterectomy

The process of determining suitable location of ports is complex and the guides are insufficient for avoiding collisions between the robot arms and surgical instruments. An integrated solution is needed provide guidance to the surgical team through the duration of the pre-operative planning process from the time the patient is brought into the operating room until docking is complete and the surgeon begins work at the console. It must integrate the patient specific characteristics, the requirements of the intervention, and the details of the operating room and present recommendations with the purpose of reducing duration of pre-operative planning and avoiding collisions.

4. Review of Literature

4.1. Port Placement in Robot-Assisted Laparoscopic Surgery

Unlike human surgeons, the patient cart has limited flexibility in moving about the patient once it has been docked. Surgeons must visualize the work volume of each the robot arm necessary to perform the surgical procedure while avoiding collisions between them and obstacles in the operating room. Surgeons must place the ports such that they would allow for the robot arms to be posed as required to perform the procedure (Adhami & Coste-Manière, 2003). Several methods have been proposed to find optimal port placement in robot assisted laparoscopic surgery. Tabaie et al. (1999) provided initial guidance for port placement with the ZEUS Robotic Surgical System using external anatomical landmarks to estimate the patient's internal anatomy. Port placement was evaluated based on the following criteria:

1. Maintain the surgeon's relative orientation as with an open surgical procedure.
2. Consider the angles between instruments, endoscopes, and surgical sites based on the specific task.
3. Avoid collisions between instruments, the endoscope, and patient tissue.
4. Position the endoscope to utilize a gravity-fed drip system to keep the lens clear.

Cannon, et al. (2003) considered the above criteria for evaluating port position in proposing an algorithm for calculating optimal port placement in cardiothoracic surgery based on preoperative imagery instead of relying on external landmarks to estimate the patient's internal landmarks. However, this

method does not consider the changes as a result of insufflation.

Adhami and Coste-Manière (2003) provided a method for calculating optimal port placement for use of the da Vinci robot in cardiothoracic surgery. It utilized pose planning algorithms based on robot kinematics often used in industrial plants and manufacturing environments. During pre-operative planning, anatomical models of the patient were created based on imaging. A surgeon defined target cones which are the areas of operation based on this model. The base of the cone was centered at the target area with the radius of the base indicating the size of the target area. The direction of the height of the cone defined the optimal direction to reach the target area. The surgeon also defined admissible locations for the location and position of the port. The algorithm considered distances between target cones and admissible locations, distances between admissible locations, angles of the target cone and admissible locations, and the model of the patient anatomy (Adhami and Coste-Manière, 2003).

After the performance of port placement and pose planning calculations, goodness of port locations were evaluated using the following criteria: reachability, dexterity, visibility, patient trauma, surgeon comfort, and feasibility. Reachability refers to the ability of the instruments to reach the target organs from any of the ports. Dexterity refers to the ease with which the surgeon will be able to perform the required movements. Visibility is how easily the surgeon can see the target area when the cavity has been insufflated. Patient trauma is a measure of the extent of trauma as a result of the MIS setup such as the number and size of

the incisions or the requirement to move the trocars. Surgeon comfort incorporates the ergonomics and the visibility and reach. Finally, feasibility is a measure of how realizable is the proposed placement. These criteria served as cost functions in the optimization problem. The above method first calculated optimal port placement and then tried to solve a pose planning problem. This was to limit the influence of the structure of the robot and the resulting pose planning from the optimal port placement problem (Adhami and Coste-Manière, 2003).

Falk et al. (2005), a team that includes the previous authors, used fiducials to register a patient into an augmented reality visualization for port placement in cardiac surgery. This was an improvement over the previous method. Fiducials were placed on the patient prior to performing the computed tomography (CT) scan. Organs, ribs, and other areas of interest were isolated from the CT scan and a three-dimensional (3D) model was created. A model of the robot was also created. Using the patient and robot models, optimal port placement was calculated based on reachability, dexterity, and visibility, the cost functions from the previous algorithm from Adhami and Coste-Manière (2003).

Next the positions of the different joints of the robot were considered to avoid collisions. The patient's whole body, the operating table, and other obstacles were also considered in the collision avoidance calculations. The results of the port placement and robot position were transferred to the operating room by converting the coordinate frames of the CT image, the patient, the robot, and the operating room into a single frame of reference the authors call registration using

the same fiducials still attached to the patient. The da Vinci system was used to point at the fiducials which allows the position of the robot to be measured relative to the patient, the imagery, and the calculated port placement. The arm of the robot was then used to indicate the suggested positions of the ports (Falk et al., 2005).

The first human trial of this method was performed in 2003. Errors were found in the transfer process due to patient deformation at the operating table. Also, adjustments were necessary in the weighting of the factors in the optimization algorithm. The surgeon was able to make adjustments to the augmented reality display by adding additional landmark information in real-time. However, with technology available at the time, patient modeling and planning was a two-hour process (Falk et al., 2005).

Cestari et al. (2010) provided a simplified way of port placement for robot-assisted laparoscopic prostatectomy (RALP) based on the umbilicus without use of computer algorithms or imagery. A double-equilateral triangle with each border measuring 8 cm was positioned on the patient's abdomen based on the umbilicus and the midpoint of the iliac crest as shown in Figure 10. This method was tested with a randomly assigned group of 30 consecutive patients. Ports were placed using the double-triangle technique for one group of 15 patients. For the second group, ports were placed based on the recommendation of the surgeon. In this trial, the average time from the completion of the anesthesia to the start of the procedure was shorter, 17 minutes versus 24 minutes. The second group also

required repositioning of one or two trocars in two patients. The authors continued to apply this method for patients ranging in height between 1.58 and 2.1 meters and with BMI between 21 and 38 without difficulty (Cestari et al., 2010).

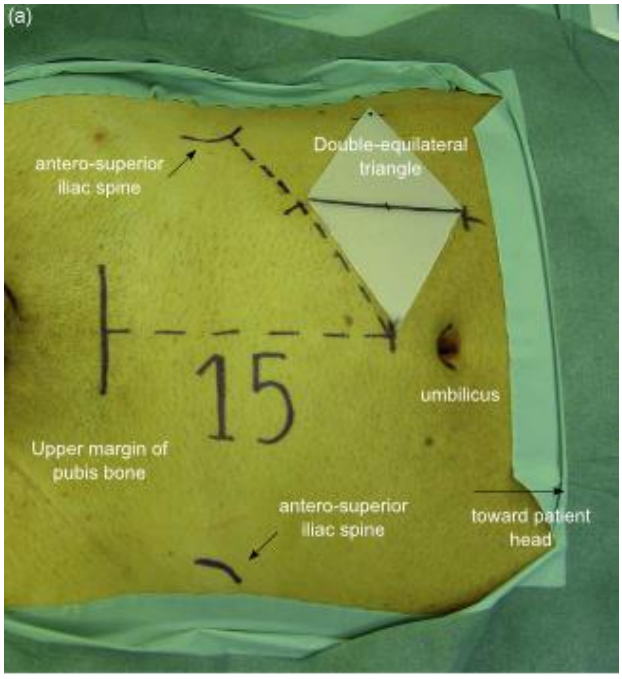

Figure 10. Simplified port placement using a double-equilateral triangle (Cestari et al., 2010)

However, the umbilicus as a reference point is not always reliable due to variations in the patient anatomy. As patients get older and in overweight patients, the umbilicus can descend. Ports are also often placed parallel to the umbilicus but too far laterally in patients with larger abdominal girth when applying methods used for patients of average size (Pick et al., 2004). Dal Moro et al. (2011) did not find methods recommended by Cestari et al. (2010) or Pick et

al. (2004) to be beneficial in port placement in RALP. They found that the distances between the anterior superior iliac spine, umbilicus, and pubis were too variable to use a standardized method.

Hayashibe et al. (2005) developed a system for pre-operative planning and posing of the robot. The system was intended for pre-operative simulation and training. It was based on a previous model of the da Vinci surgical system and, as with previous researchers mentioned above, their method relied on creating a detailed model of the patient from CT scan or magnetic resonance imaging. Sun et al (2007) designed and developed a simulation system for training surgeons based on a previous model of the da Vinci system. In addition, Sun and Yeung (2007) proposed another method for determining the port placement and robot pose using two performance measures: the global isotropy index (GII), and the efficiency index (EI). These measures were intended to maximize reachability, dexterity, and visibility, the criteria defined by Adhami and Coste-Manière (2003). They were able to validate their performance measures but did not provide a way to present the information for use in the operating room. The da Vinci system also imposes other ergonomic disadvantages in addition to the complex cognitive task of port placement.

4.2. Challenges of Robot-Assisted Laparoscopic Surgery

One of the disadvantages with robotic surgery is the lack of haptic feedback. The surgeon operating at the console has to rely instead on visual cues. In addition, the surgeon is dependent upon an assistant at the operating table and

communication can be difficult due to various factors such as lack of face to face contact and differences in frame of reference. The assistant and other surgical staff experience the same ergonomic disadvantages from their perspective. In addition, they have to contend with the robot arms which occupy a large volume over the patient, as shown in Figure 11, when trying to access the patient to perform suction or other tasks (Rassweiler, et al., 2010). Compare this with the idealized scene in Figure 5.

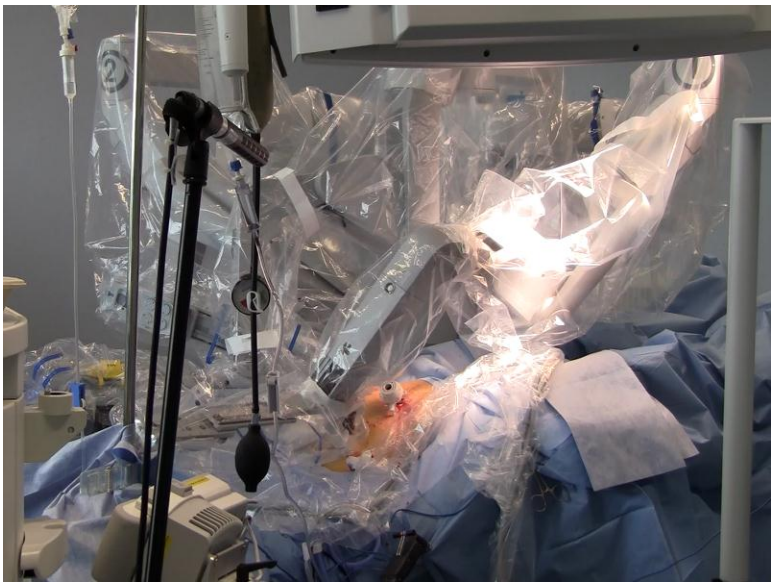

Figure 11. Patient Side Cart over Surgical Table

Another ergonomic challenge with the da Vinci system is in the docking process which has been mentioned briefly. This is the process of bringing the patient cart into position after the ports are placed and connecting the instrument arms to the ports. Driving the patient cart into position is done from the rear and the view of the person driving is obstructed, relying on the directions from other

members of the surgical team. It is just as difficult to see the team member behind the patient cart driving it in Figure 12 as it is for her to see what is in front of the cart.

Figure 12. Driving the Patient Cart

After the patient cart has been brought into position, the robot arms have to be posed and connected to the ports (Dal Moro et al, 2011). The methods for port placement discussed in the previous section do not address the task of posing the instrument arms and connecting them to the trocars, shown Figure 13. Each of the three instrument arms has multiple joints that have to be arranged to achieve a pose that at a minimum allows each instrument, when inserted in the instrument arm, to reach the target area. The pose must also maximize the work volume that each instrument arm would have without colliding with the other arms so as not to restrict the amount of pitch and yaw that each instrument arm

can move during the operation. This process can be difficult as it requires team members to perform mental rotations and visualize the work volume required by each instrument arm for the planned procedure.

Figure 13. Connecting the Instrument Arms.

Patient positioning is discussed only briefly in literature. It is the process after the patient is placed on the operating table but before port placement begins. The patient is secured to the operating table and the legs are moved apart and lowered to position the robot between the legs. The operating table is adjusted so that patient is placed in a maximal Tredelenburg position with the head close to the floor (Dal Moro et al, 2011). In some procedures, the robot is positioned at the patient side or the patient is positioned in a reverse Tredelenburg position with the feet close to the floor (S. Schwaitzberg, personal communication, 2011). These are additional factors that must be taken into consideration while posing the cart. After successfully placing the ports and docking the patient cart, there still exists

the possibility of complications.

4.3. Complications

In addition to the challenges associated with port placement and physical configuration of the robotic arms, surgeons must also consider the risk of converting from robotic surgery to either conventional laparoscopic surgery or open surgery due to system failure or complications. Device failure rates of 2% to 5% have been used when counseling patients. In one review of over 800 cases of robot-assisted laparoscopic radical prostatectomy (RALP) performed with the da Vinci in 2006, system failure occurred in 0.5% and the study authors recommend using the lower failure rate when counseling patients. The authors do advise surgeons to consider the possibility during pre-operative planning, specifically making sure that the da Vinci system is set up before patient enters the operating room to avoid unnecessary general anesthesia (Zorn et al., 2007). In another study of 526 RALPs performed between April 2005 and May 2010, 257 cases were considered for the study and 3 out of 257 cases required conversion, an overall rate of 1.17%. Of the three cases requiring conversion, one was due to an unsolvable collision of the robot instruments. Another one was due to a technical problem with one of the robot arms and the third was due to bleeding from Santorini's venous complex (Dal Moro et al, 2011). However, the likelihood of any complications requiring conversion to conventional laparoscopic surgery or open surgery was considered minimal that it was not deemed a critical factor for consideration in the port placement.

Methods proposed by other researchers to solve this problem require intensive computer calculations to create a 3D reconstruction that relies on pre-operative imagery taken before insufflation. The height that the abdomen will rise varies between patients and algorithms based on preoperative imaging may result in ports placed too far from the target area (Coste-Manière, Adhami, Mourgues, Fabien & Bantiche, 2004). In addition, most patients are diagnosed only using an ultrasound to minimize unnecessary exposure to radiation (S. Schwaitzberg, personal communication, 2011). These ultrasound images do not have sufficient detail to use in a 3D reconstruction. Their reliance on pre-operative imagery would also prevent real-time adjustments during the operation (Moglia et al, 2011) and none provide way for surgical teams to transfer the pose and position plan into the operating room.

5. Methodology

The complexity of the problem required that the methodology be divided into smaller tasks. In addition to the review of literature, a field study was conducted consisting of informal observations and a study of videos of cases of robot-assisted laparoscopic surgery. Expert interviews were conducted and a generalized task analysis of port placement was created. This was followed by research into patient and robot modeling. Finally, the research was concluded with the design, creation, and usability testing of a planning aid prototype.

5.1. Field Study

The review of previous related work provided insight into the overall problem and difficulties encountered in port-placement for robotic surgery. Several observations of conventional laparoscopic procedures were conducted at hospitals in Boston, USA to better understand port placement. No notes or photographs were taken. Videos of two (2) robot-assisted laparoscopic procedures with a novice team in a hospital in Nantes, France were also analyzed. While the surgeons in France were experienced surgeons in laparoscopic surgery, they were novices with regards to robot assisted laparoscopic surgery, having only performed less than five cases at the time. While reviewing the videos, the researcher focused on the difficulties the surgical team experienced with regard to port placement and variations in patient anatomy. In addition the difficulties in the docking process were also noted.

5.2. Task Analysis

The field observations were conducted at teaching hospitals. In some instances the surgical team included residents and fellows and the lead surgeons would verbalize their decision process and the factors they considered as they placed each port. This provided an opportunity to conduct an informal cognitive task analysis of the port placement process. Interviews with expert surgeons were conducted to elicit additional information regarding the procedure observed, as well as from past experience to refine the cognitive task analyses of the port placement process. A task analysis was also conducted in an operating room with

a surgeon at the hospital in France with a da Vinci Si Surgical System without a patient present. This provided additional information than was unavailable during an operation and outside the operating room.

5.3. Product Design

Elements of a generic product development process were used in the design of the planning aid, specifically, identifying customer needs, defining requirements, generating a product concept, decomposing of the requirements definition, and defining a conceptual process flow of the software. Decomposing the requirements dictated the need to research the sub-problems of modeling the patient and the robot.

5.4. Patient Model

One of the primary requirements was that the decision aid be patient specific. Thus it was necessary to determine what measurements would be useful in modeling a patient torso and in determining where to place ports, based on the same criteria listed in 4.1 but specifically criteria 1 and 2 which can be summarized as have sufficient access to the target area while avoiding collisions.

5.4.1 Data Collection

A protocol was designed to collect measurements based on the above tables from actual patients undergoing laparoscopic surgery (with approval from Tufts Institutional Review Board (IRB)). It was difficult to execute in practice due to the lack of rulers and body calipers in the operating room, the time required

in collecting the measurements, and concerns of violating the sterile field.

Therefore, a second method was devised that depends only on disposable rulers available in most operating rooms, avoids violating the sterile field, and expedites the process to minimize impact on the surgery. Measurements are calculated from images of the abdomen taken with reference rulers from above and from the side of the patient on the operating table, before and after insufflation (Figure 14 and Figure 15). The patient abdomen is marked to indicate the subcostal plane and the iliac crests which are used as landmarks.

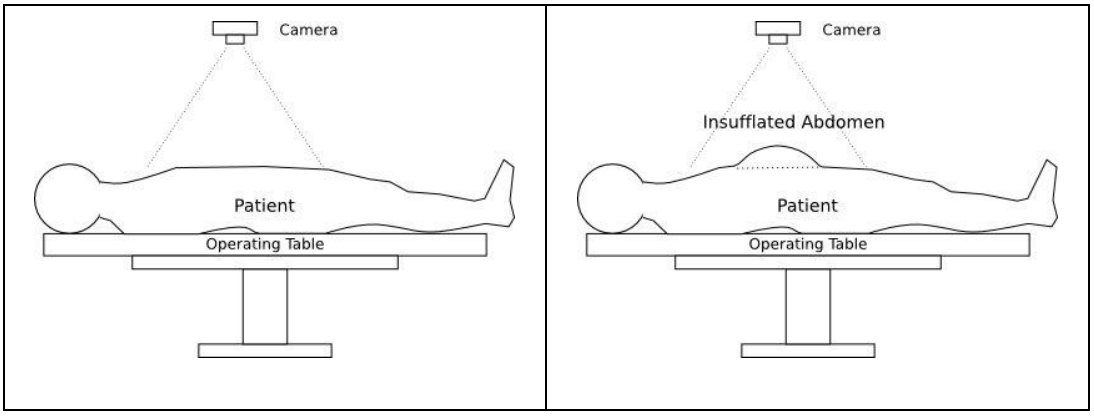

Figure 14. Images of patient front (pre and post insufflation)

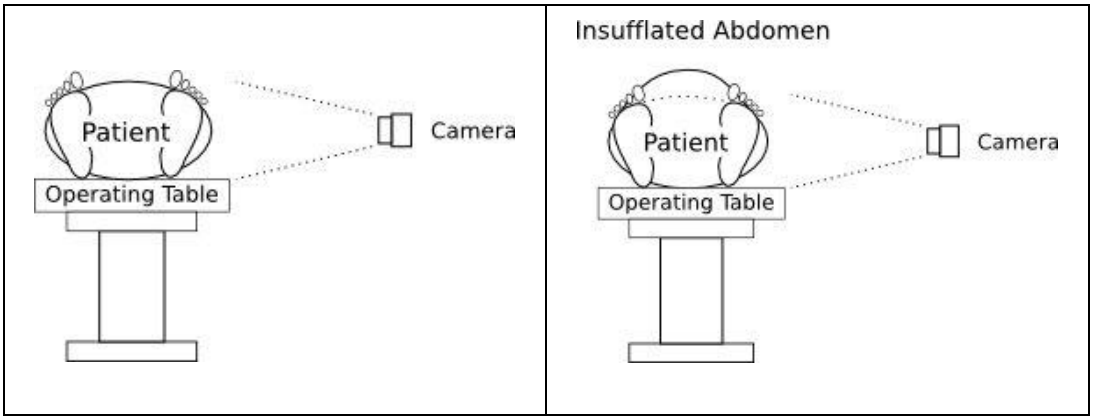

Figure 15. Images of patient side (pre and post insufflation)

The patient dimensions were calculated from the images taken using the method described below:

1. Import the image into GIMP, the GNU Image Manipulation Program (http://www.gimp.org/).

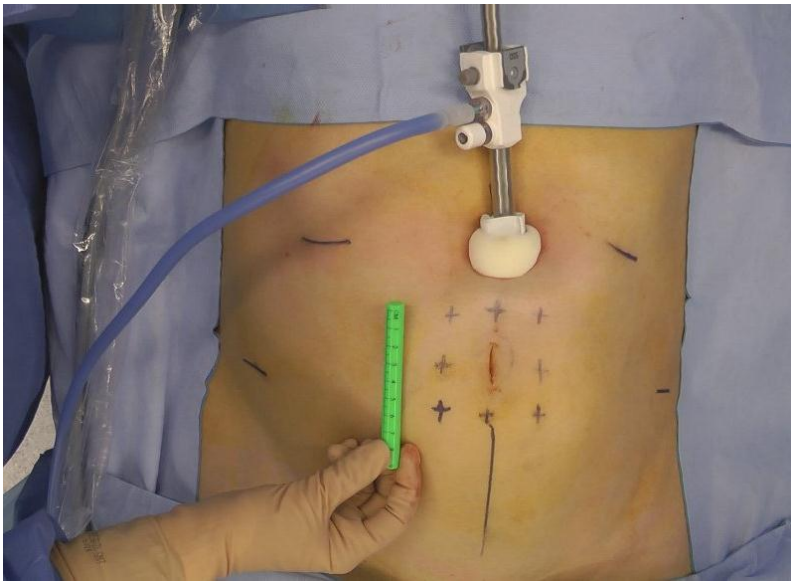

Figure 16. Patient torso front

2. Use the Measure tool to determine the length in pixels of the reference rule. Divide the number of pixels by the length of the reference rule. For example, if the reference rule is 7cm long and the measurement tool indicates it is 230 pixels long, divide 230 pixels by 7 cm. In this example, the scale is $\frac{230}{7} = 32.9$ pixels per cm.
3. Use the Measure tool to determine other lengths in the image. For example, the horizontal width of the draping at the costal margin is

876 pixels wide. The equivalent in centimeters is $\frac{876}{32.9} = 26.6$ cm.

The recorded measurements and images were combined with the patient's height, weight, and age in an individualized model. This method was designed to expedite data collection to minimize any impact on the total duration of the operation, and has the added advantage of providing the patient's abdominal deformation data during surgery for individualized, intra-operative planning.

After some practice, the second method was used successfully by the author to collect measurements from three (3) patients undergoing laparoscopic procedures at CHA (after IRB approval). The resultant data were also used to create use cases for testing the decision aid.

5.4.2 Creating the 3D Model

The next phase of the research involved creating a model of the anatomy from the patient measurements. The initial concept for this model was a box with the width, height, and length corresponding to the torso width, sagittal thickness, and distance between the subcostal plane and the pubic symphysis. The volume necessary to perform the procedure was approximated by a sphere. The work volume of each instrument was represented by a right circular cone with the base a circular cross-section of the sphere and the axis of the cone passing through the center of the sphere. The tip of the cone was the remote center of motion of an instrument arm of the robot. This was similar to the concept employed by Adhami and Coste-Manière (2003) for optimal port placement in cardiac surgery.

The model of the anatomy would then be combined with the robot kinematic model discussed later to calculate a port placement recommendation so a brief survey of methods to create a computer model based on the initial concept was undertaken. Methods investigated included developing an application using Python and C or using numerical computation software such as Matlab, GNU Octave, and Mathematica. Mathematica was selected because it provided an easier path to developing computational applications with a user-friendly interface. The other methods investigated also allowed for development of computational applications but required more effort to provide a user-friendly interface.

Using Wolfram Mathematica 7, several prototypes of a user interface for accepting patient measurements were created based on the initial concept. The first prototype combined a tube with an elliptical cross section combined with a sphere to approximate insufflation. The tube was an improvement over the box in approximating the cross section of a patient's torso. A small red sphere can be moved independently in three dimensions to designate the area of interest for the surgery. The result is shown in Figure 17.

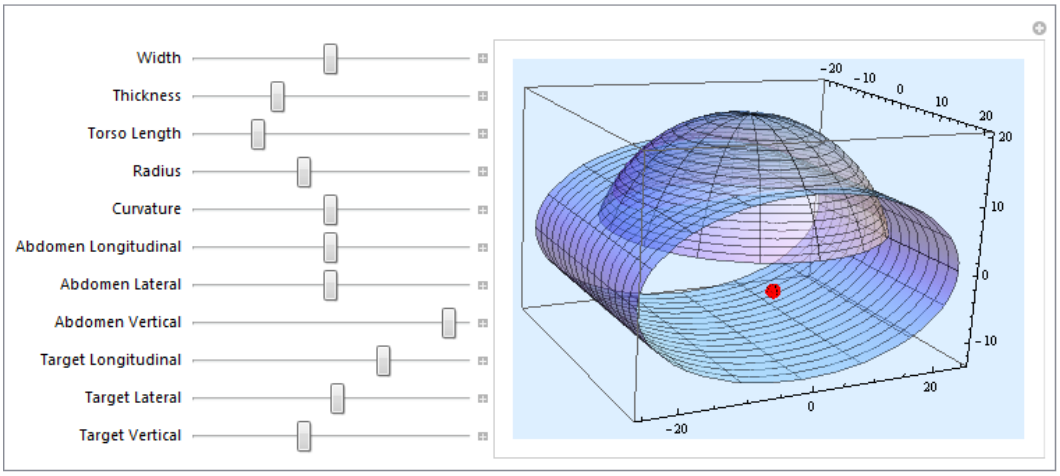

Figure 17. 3D Model with Ellipse, Sphere, and Target Sphere (in Red)

Ideally, a member of the surgical team would take measurements of the patient on the operating table while another member would enter the settings in the user interface to create the torso model. The location of the target region in 3D space and the dimensions of the abdomen after insufflation are also input variables. When the surgeon is satisfied with the model, the software could be used to calculate the optimal port placement and pose plan.

Additional user interface prototypes using different algorithms were created in an effort to better approximate mathematically the shape of the patient torso. Another example is shown in Figure 18. This torso was exported to a Virtual Reality Modeling Language (VRML) format file. This format was chosen because it is supported natively by many 3D modeling and visualization platforms such as OpenSceneGraph and Blender. The Mathematica instructions to create the torso models are found in Appendix A. It is shown in Figure 19 after it has been imported into Blender and combined with the patient cart. In Figure 20, the

torso has been combined with the model of the patient. The intent was to not only support the calculation of optimal port placement but also support the creation of a user-friendly interface to display the results.

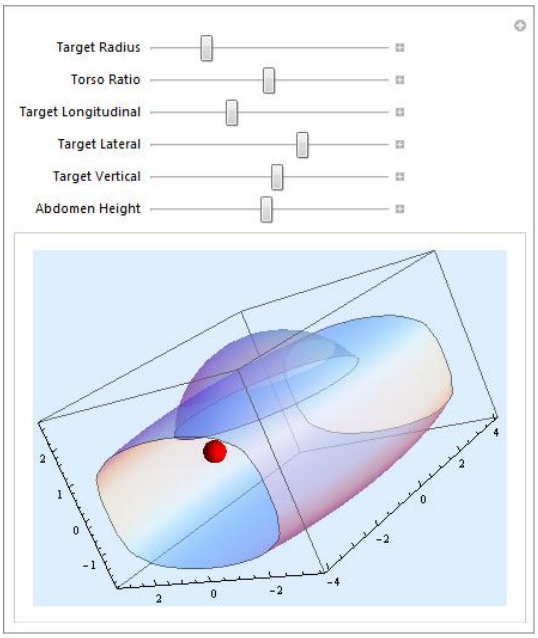

Figure 18. Revised torso prototype.

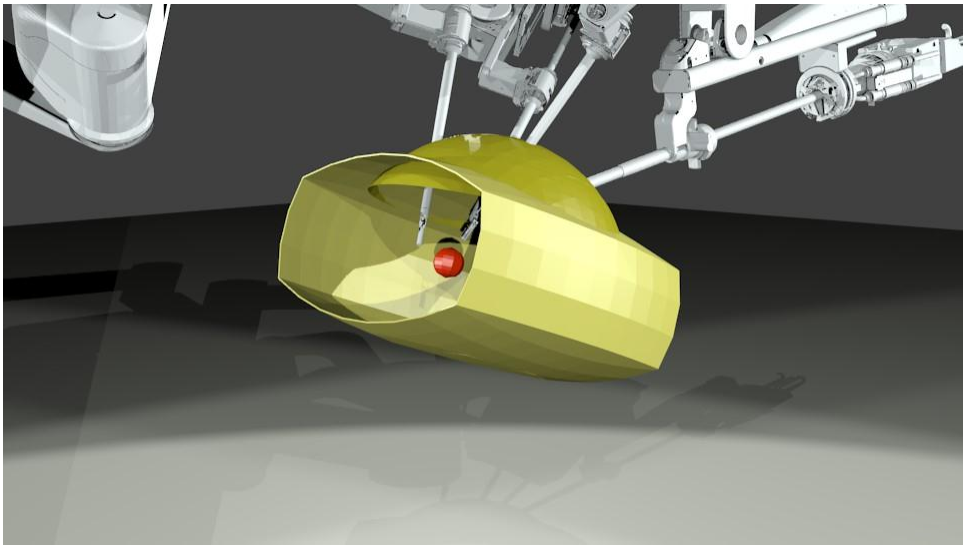

Figure 19. Torso Model in 3D Simulation

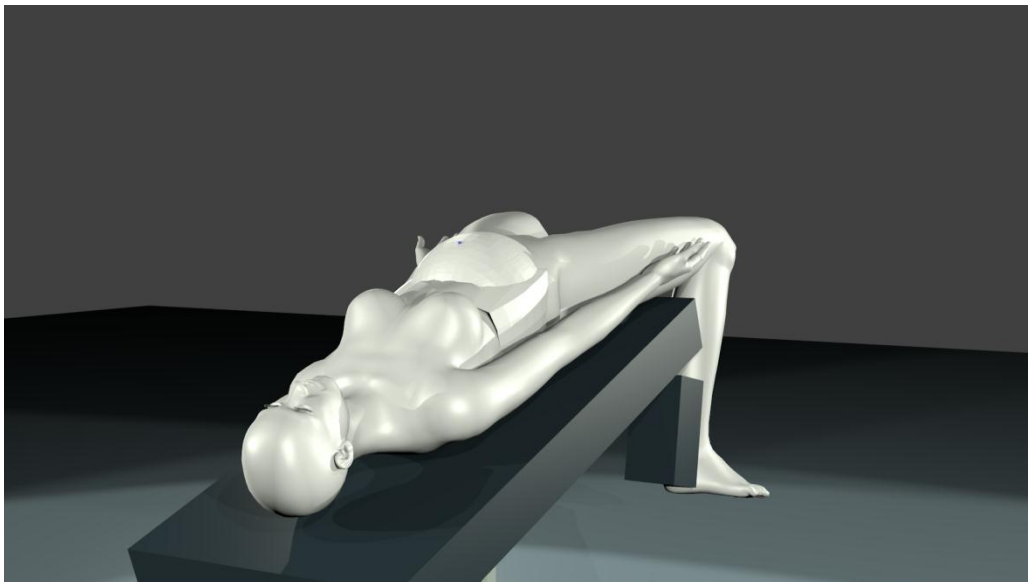

Figure 20. Patient and Torso Combined in 3D simulation

5.5. Robot Model

Port placement must consider not only the patient but also the surgical instruments and camera used to perform the surgery. For robot-assisted laparoscopic surgery, this also includes the definition of the robot workspace, the dimensions of the robot components and the end effectors, and poses necessary to accomplish specific procedures.

From June 2011 to August 2011, access to a da Vinci Si surgical system for use in modeling the robot was available courtesy of Pr. Jean-Marc Classe and the surgical staff at Institut de Cancérologie de l'Ouest in Nantes, France. An initial attempt to capture the range of motion and the workspace volume of the da Vinci Si surgical system patient-side cart was performed using OptiTrack from NaturalPoint. This method required attaching passive retro-reflective markers to multiple facets of each joint and tracking the motion using six infrared cameras

with active infrared illumination. However, this method had several disadvantages and was quickly abandoned. The main problem with this method was that it was difficult to position the cameras around the patient cart in such a way that each marker was visible to at least three cameras to track its movement without being obscured by a part of the robot. Furthermore, the data collected had to be converted into a form that could be analyzed and used in a 3D model.

Instead of recording the workspace volume using optical tracking of the movement of each arm, a symbolic model of the robot was created using the modified Denavit-Hartenberg (DH) parameters for each of the three instrument arms and the endoscope arm. This is a commonly accepted way of modeling the motion of robot joints and was used by Sun et al. (2007) and Sun and Yeung (2007) to model older versions of the da Vinci Surgical System. This method could be used to calculate the work volume of each robot arm. It could also be used to calculate a suitable pose plan using inverse kinematics (IK) to calculate the angle and position of each of the robot arm joints knowing the position of the instrument holder.

The four arms of the patient cart, the endoscope arm and the three instrument arms, were analyzed and a symbolic model was created for each of the four arms separately. Each joint of the arm was modeled as a series of prismatic or revolute joints using the notation employed in SYMORO+, an application for symbolic modeling of robots and shown in Table 1 and Figure 21

Table 1. SYMORO+ Symbolic Model Notation (Khalil and Lemoine, 2003)

Symbol	Description
σ_j	$\sigma_j = 0$ if joint j is revolute, $\sigma_j = 1$ if joint j is prismatic,
Z_j	the axis of joint j
x_j	the axis along the common normal between z_j and z_j+1
α_j	angle between z_j-1 and z_j around x_j-1 (in radians)
d_j	distance between z_j-1 and z_j along x_j-1,
θ_j	angle between x_j-1 and x_j around z_j (in radians)
r_j	distance between x_j-1 and x_j along z_j.
O_j	the intersection of z_j and x_j
P_j/R_j	Instead of using the Link j notation L_j,P_j are R_j are used to designate revolute and prismatic joints respectively.

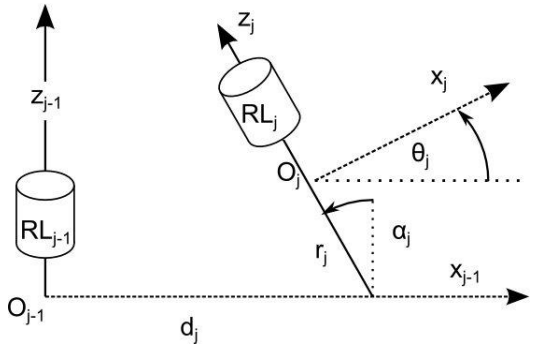

Figure 21. Symbolic Model Parameters (Khalil and Lemoine, 2003)

Intuitive Surgical distinguishes between the links that are powered and move during surgery and the links that are unpowered and are positioned manually during the docking phase. They are referred to as the instrument arm for the former and setup joint for the latter and the separation is noted in Figure 22 for instrument arm 2. Analysis of the unpowered joints is shown in Figure 22. The measurements for some links were taken from a SolidWorks drawing and verified with measurements taken in the hospital.

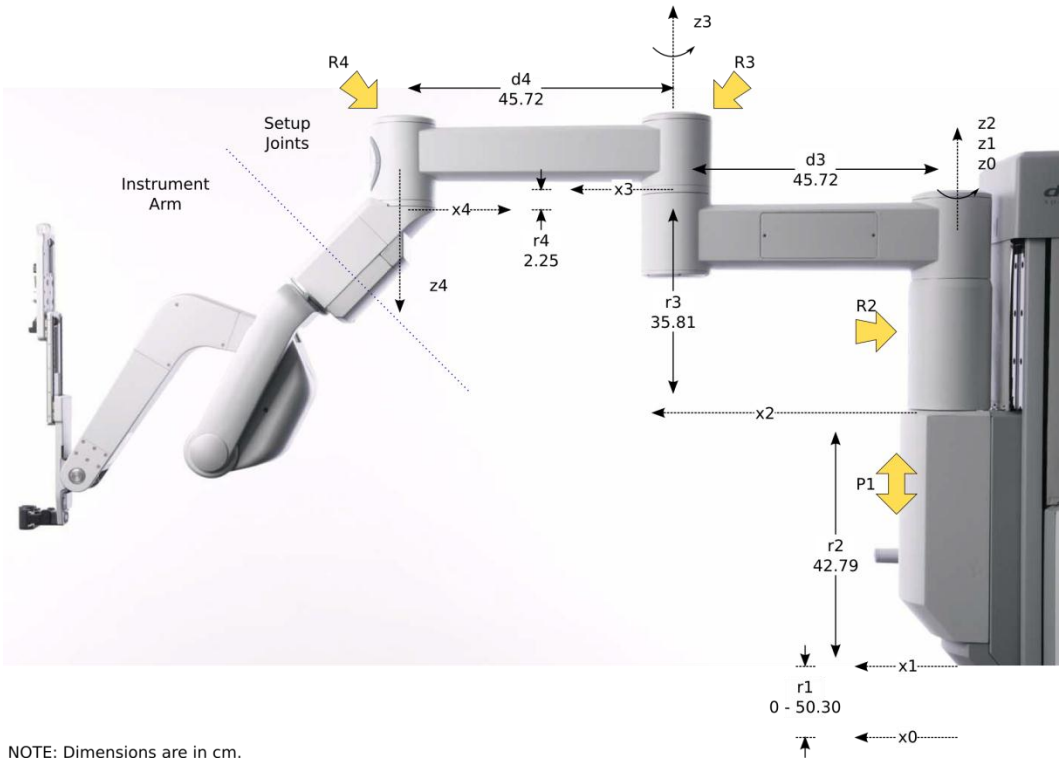

Figure 22. Modeling Instrument Arm 2 with Setup Joints (Unpowered) revolute and prismatic joints indicated by arrows.

The powered joints were analyzed to understand the mechanism by which the surgical instruments are manipulated. The analysis is shown in Figure 23. Based on observation of its movement, the powered joints were believed to be equivalent to revolute joints (R6, R7, and R8) arranged in a parallelogram. This configuration is similar to how previous models of the da Vinci patient side cart were able to keep the remote center of motion (RCM) at the port fixed while moving the surgical instrument. For the purposes of this model, the prismatic joints P9 and P10 that control the insertion and extraction of the surgical

instruments were not included. These joints would be treated as fixed to simplify the model.

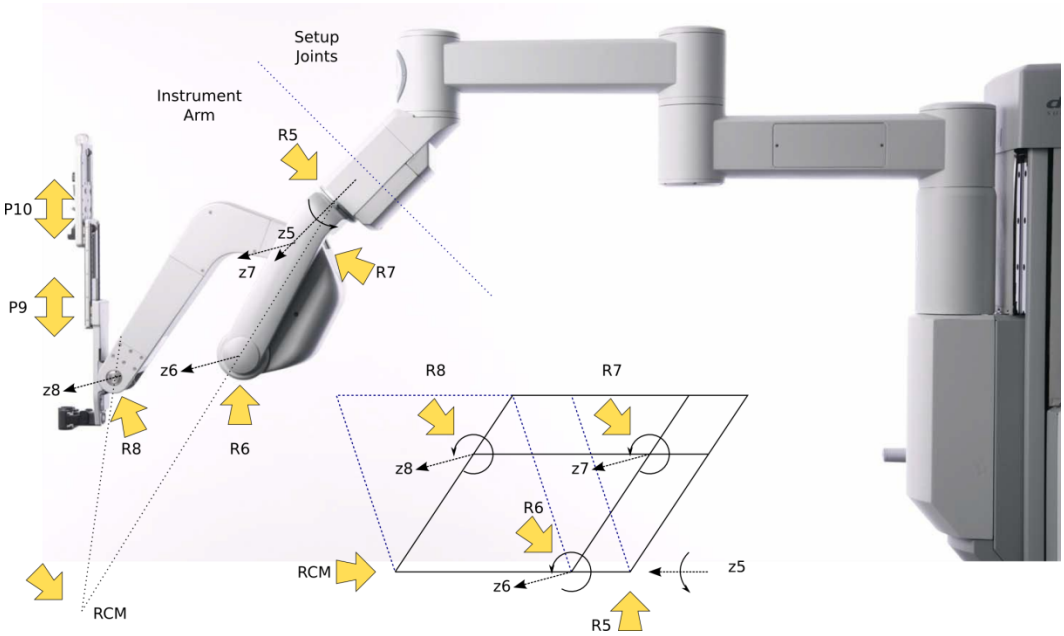

Figure 23. Modeling Instrument Arm 2 with Instrument Arm (Powered) showing parallelogram arrangement, revolute and prismatic joints indicated by arrows.

The endoscope arm was analyzed in the same way as the instrument arms. Unlike the instrument arms, it does not have two prismatic joints to extract and insert the endoscope. The partial symbolic model of the endoscope arm showing the joints is shown in Figure 24. Note that it has shorter links and a different joint at the junction at R4 and R5.

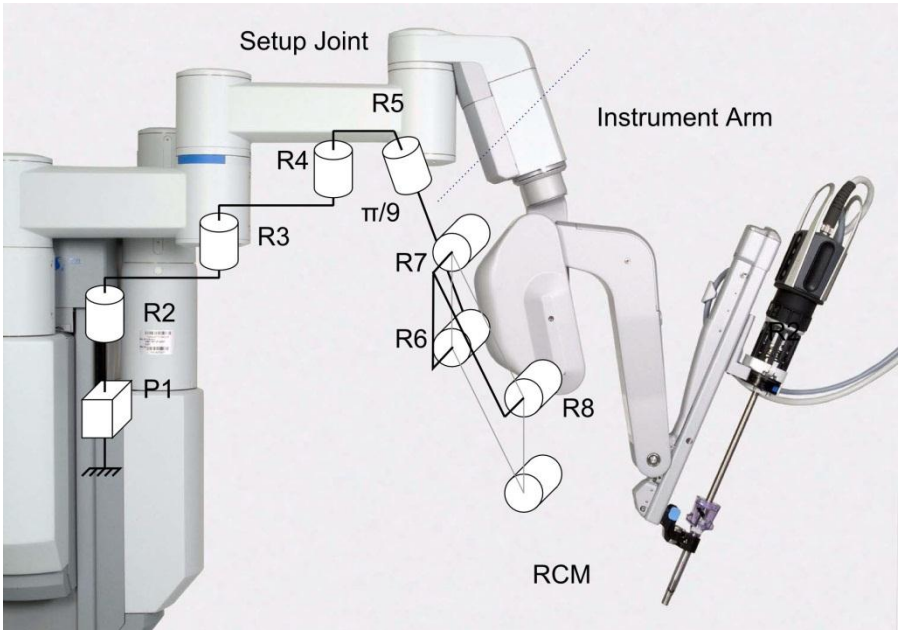

Figure 24. Modeling the Endoscope Arm

5.6. Combining the Patient Model with the Robot Model

In order to calculate the angles of each of the joints of the robot arms using inverse kinematics (IK), it would be necessary to know the location, in x, y, z, of the tip and the port as the fixed point. However, the choice of the origin can be any arbitrary point in space. For this illustration, the remote center of motion (RCM) of the endoscope arm was selected as the origin at height z_1 (0, 0, z_1), then the location of the other ports and the center of the target region relative to the origin can be calculated. Example locations are shown in Figure 25 and listed in Table 2 below:

Table 2. Location of Ports and Target Example

Object	Location (x, y, z)
Endoscope (Port 1)	0, 0, z_1
Instrument Arm 1 (Port 2)	-6.9, -4, z_2
Instrument Arm 2 (Port 3)	6.9, -4, z_3
Instrument Arm 3 (Port 4)	-13.8, 0, z_4
Target	0, -18, z_T

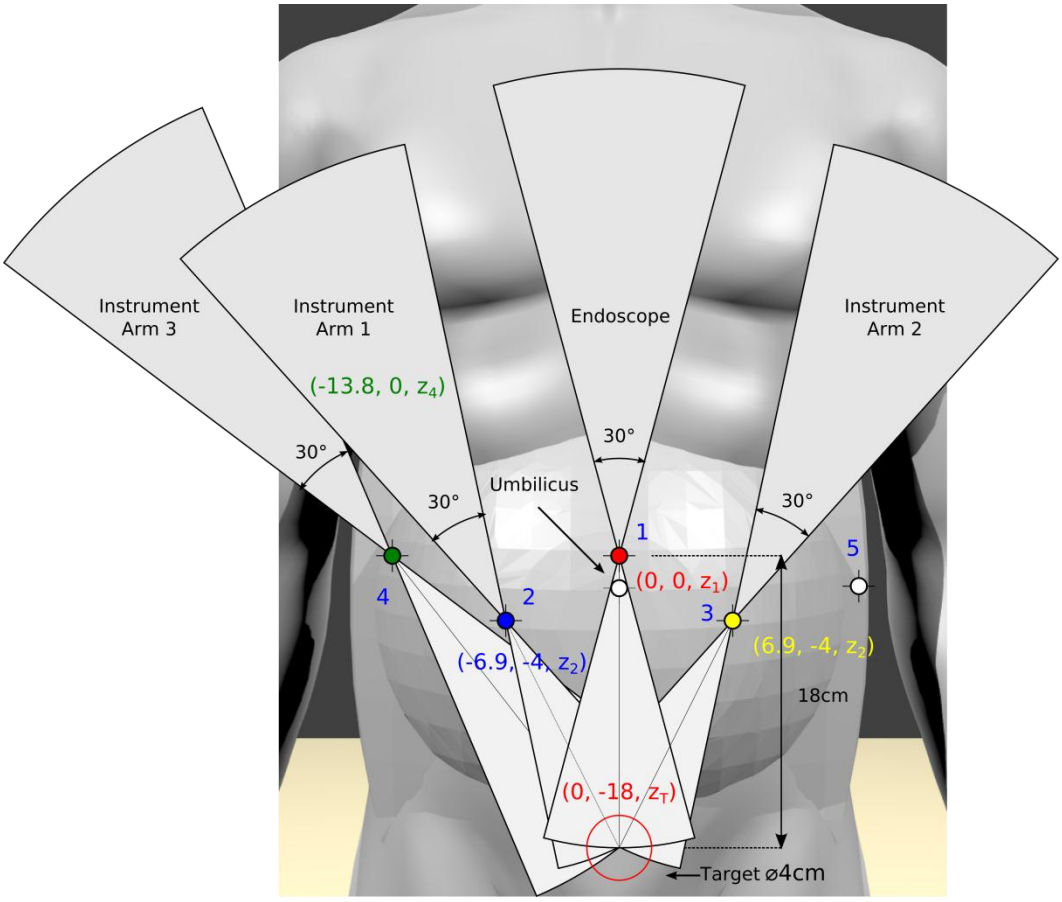

Figure 25. Work volume in the horizontal plane for a ±15º yaw movement of the endoscope and instrument arms of the patient cart and surgical instruments shown with the patient model.

It is also necessary to calculate the angle of the parallelogram joint θ_7 (instrument arms 1 and 2, and the endoscope arm) and θ_8 (instrument arm 3).

These are parameters in the DH models listed in the results section for each of the

robot arms. These values are based on the elevation angle of each of the surgical instruments (Figure 26). The method to calculate θ_7 and θ_8 is illustrated by Figure 27.

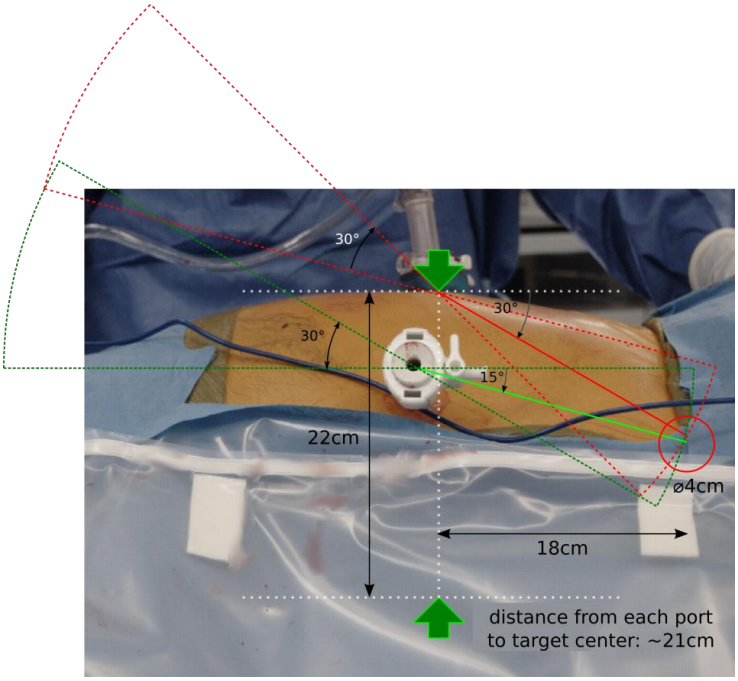

Figure 26. Work volume in the vertical plane for a ±15º pitch movement of the endoscope (red) and one instrument arm of the patient cart and surgical instrument (green) shown with a patient use case.

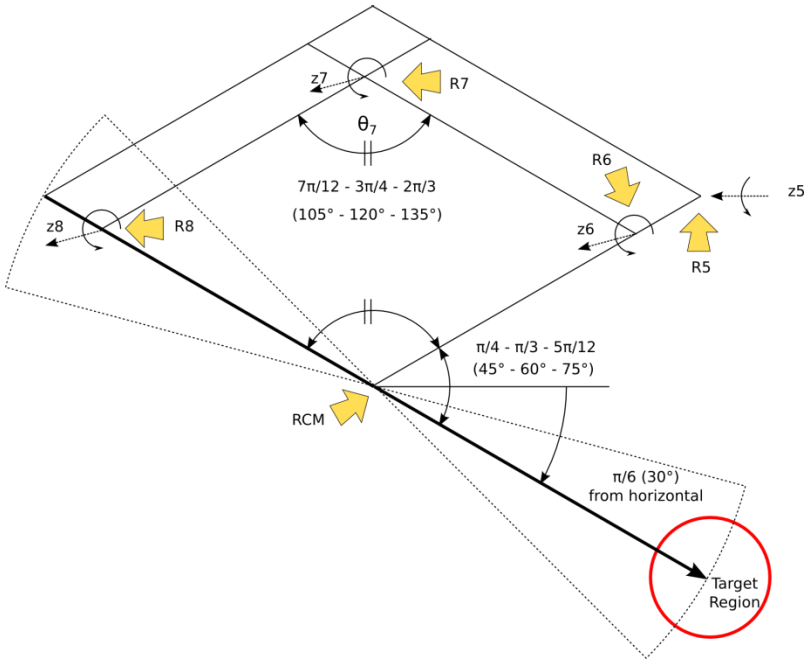

Figure 27. Values for θ_7, given a ±15º pitch movement of the surgical tool

5.7. Comparison of Port Locations Based On Instrument Work Volumes

A computational method was devised to compare possible port locations in robot-assisted laparoscopic procedures. This method calculated the intracorporeal work envelope volume of each instrument and the overlap between each instrument (Figure 25). Each instrument port location was varied methodically and the resulting volume of overlap between the work envelopes of each instrument was compared. By reducing the volume of overlap, potential intracorporeal instrument collisions could also be reduced. For completeness, this analysis was performed using port placement guidelines used in conventional and robot-assisted laparoscopic surgery.

5.7.1 Model of Patient Torso and Surgical Instruments

An analytical model of the patient abdominal and pelvic regions, the target of interest, the laparoscopic instruments, and the ports was developed for this computation. The insufflated patient torso was modeled as a cylinder with an elliptical cross-section across the width of the torso. The following simplifications for this model were also made:

- The thickness of the abdominal wall was considered negligible.
- Other internal organs have been shifted out of the way as a result of patient positioning, insufflation, organ retraction or another method.
- The ports were modeled as dimensionless points.
- The surgical instruments were modeled as lines occupying no volume. The specific work volume requirements of the end effectors were ignored.
- The region of interest was represented by a closed ball defined as a sphere and all the points inside of it.

The coordinate system of this model was defined as follows:

- The x-axis was parallel to the plane of the operating table with the positive direction toward the patient left.
- The y-axis was normal to the plane of the operating table with the positive direction toward the patient front.
- The z-axis was defined along the longitudinal axis of the patient parallel to the sagittal plane with the positive direction toward the patient head.
- The origin was at the center of the target region.

Surgeons mark a patient's abdomen for port placement prior to insufflation when the patient's abdomen is approximately flat. The amount a specific point on the abdomen shifts laterally or longitudinally (in this coordinate system, the x-z plane) after insufflation is small and negligible (P. Hendessi, personal communication, 2012). Thus the positions of each port in the x-z plane were considered to be unaffected by insufflation. The corresponding y-axis values

were calculated from the equation for an ellipse, $x^2/a^2 + y^2/b^2 = 1$, where *a* is half the width of the patient torso and *b* is half the sagittal thickness. The equation for positive values of y is $b\sqrt{1 + (x^2/a^2)}$.

This method only considered the instrument work volume internal to the patient abdomen. This is the intracorporeal space as compared to the extracorporeal space which is the volume external to the patient abdomen. The work volume of each instrument was represented by a single cone with the apex at the port. The axis of the cone was defined to pass through the center of the sphere encompassing the region of interest. The base was defined to be on a plane tangent to the sphere such that the height of each cone was the distance between the apex and the center of the sphere plus the radius of the sphere.

5.7.2 Patient Measurements

Patient measurements collected using the method described previously were selected for use in this analysis. Measurements of Patient 1, classified as average, and patient 2, classified as obese, were selected for use in this analysis. Their measurements, listed in Table 3, were applied to the analytical model. The radius of the target region for both patient models was estimated as 2cm, located half the distance between the patient front and the patient back.

Table 3. Patient Measurements

Measurement	**Patient 1**	**Patient 2**
Height	160.0cm (63in)	154.9cm (61in)
Weight	62.1kg (137lbs)	102.5kg (226lbs)
Body Mass Index	24.3 (Average)	42.7 (Obese)
Torso width	30cm	40cm
Sagittal thickness	22cm	28cm
Distance from the subcostal plane to the umbilicus	4cm	20cm
Distance from the umbilicus to the center of the target area	19cm	14cm
Distance from subcostal plane to center of target region	23cm	20cm

5.7.3 Port Placement Plans

The port placement guidelines provided by Ferzli & Fingerhut (2004) were applied to the two patient torso models. The resulting port placement plan is shown in Figure 28. In this arrangement, all ports are approximately 16 – 18cm from the target region in the horizontal (x-z) plane. In the same plane, the angle between instruments 1 and 2 is 60 degrees. The angle between instruments 1 and 3 is 30 degrees. The endoscope port is located approximately 18cm from the target region. The resulting work envelopes of the surgical instruments are shown in Figure 29.

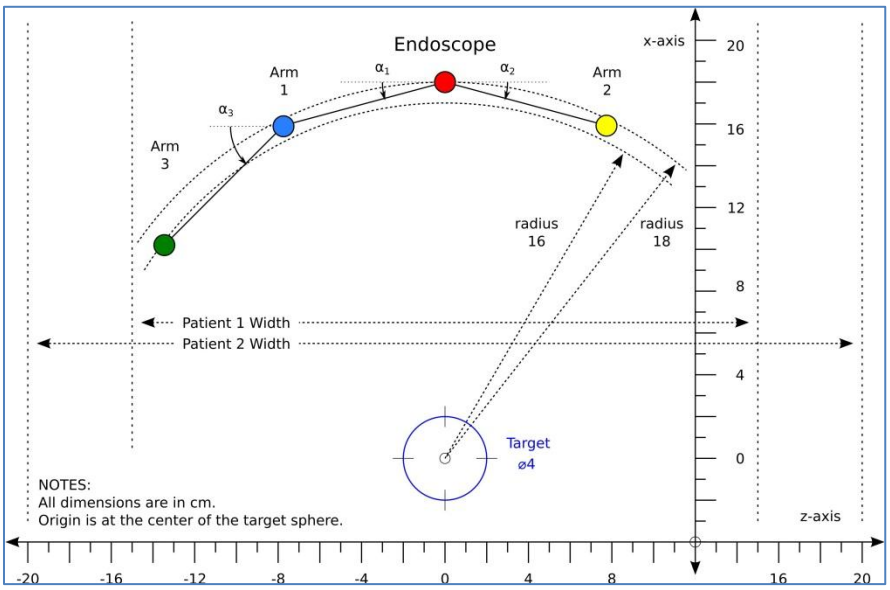

Figure 28. Port Placement Arrangement for Conventional Laparoscopic Surgery

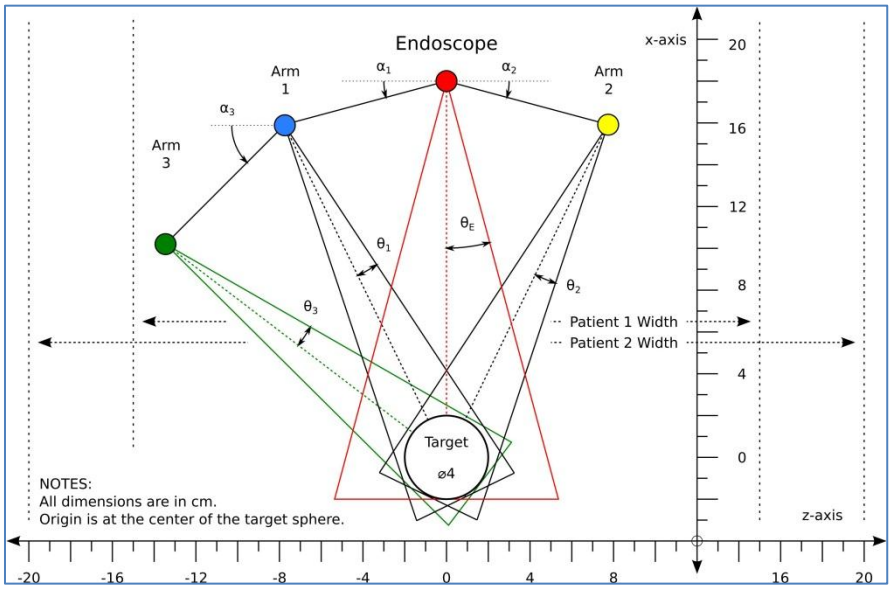

Figure 29. Instrument Work Envelopes for Conventional Laparoscopic Surgery

The recommendations for robot-assisted laparoscopic prostatectomy from Intuitive Surgical were also applied to the patient torso models. The resulting port

placement plan is shown in Figure 30. The manipulation angle between instrument 1 and 2 is approximately 53 degrees on the x-z plane. Intuitive Surgical recommends that ports be separated by a distance of 8 to 10cm. The torso width of patient 1 was narrow and only the 8cm distance between ports could be used. The torso width of patient 2 was enough to allow both 8 and 10cm separation distance between ports. These separation distances were applied to the robot-assisted port arrangement and also the arrangement for conventional surgery. This resulted in six port placement plans for analysis.

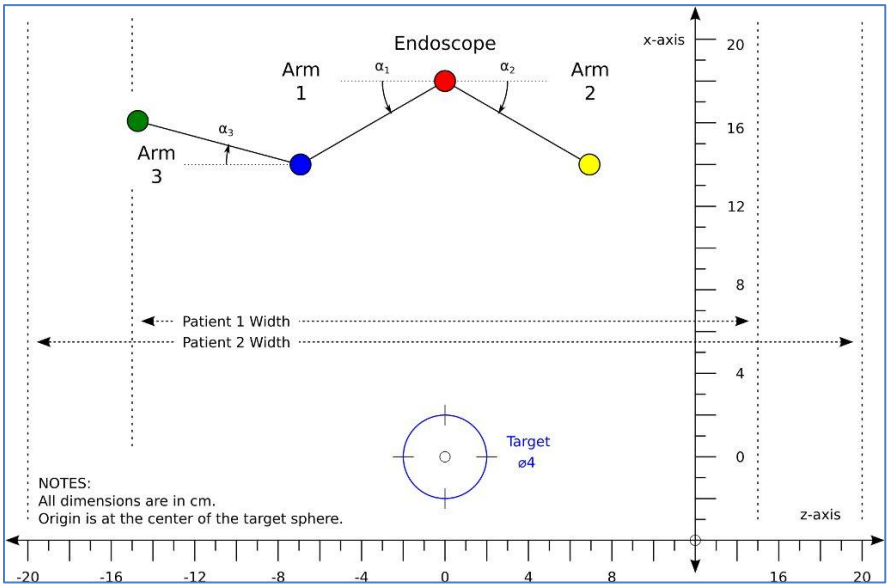

Figure 30. Port Placement Arrangement for Robot-Assisted Laparoscopic Surgery

5.7.4 Alternative Port Locations

It is not always possible to place ports where they were originally planned.

Inspection of the abdominal cavity after insufflation may require deviation from the original plan. Small changes will have some impact on the distance to the target organ and the manipulation angle between instruments. In order to analyze the effect these changes would have on the work volume and potential for collisions, the location of each instrument port in the six port placement plans were also varied from the initial position in the x and z direction. Port placement recommendations often specify dimensions with a 2cm range. By offsetting the x and z axis positions of each port from the base configuration by 2cm, separately, the different instrument work volume resulting from the eight different positions for each port could be compared with the initial position. The nine total possible positions, including the initial position for each of the three instrument ports, are shown in Figure 31 and Figure 32.

For convenience, each position was designated by a letter from A – I instead of referring to them by using the x,y,z coordinates or their relative offsets. For the patient 1, a 2cm negative offset in the x-axis for instrument arm 3 from the base position would exceed the lateral width of the patient. For patient 2, a 2cm negative offset in the x-axis with a 10cm distance between ports also would exceed the lateral width of the patient. The x-axis values for positions A, D, and G for instrument 3 were set equal to the minimum x-axis value in both cases and the corresponding y-axis values were set equal to zero.

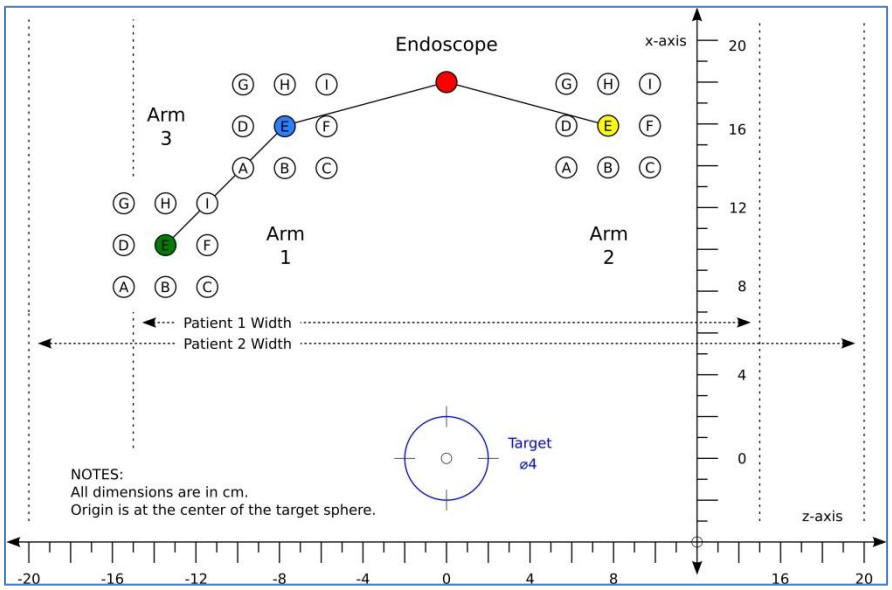

Figure 31. Port Placement Combinations for Conventional Laparoscopic Surgery

(8cm distance between ports)

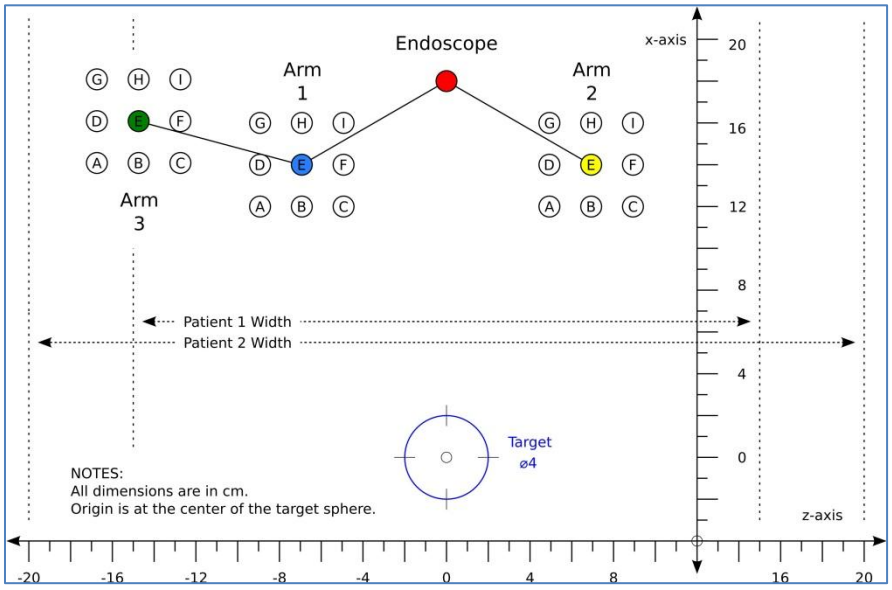

Figure 32. Port Placement Combinations for Robot-Assisted Laparoscopic Surgery

(8cm distance between ports)

This analysis of port placement was performed based on an insufflated abdomen, after the endoscope port has been placed. Thus the position of the endoscope was fixed for each of the six base configurations. For patient 1, the endoscope port was located at $\begin{bmatrix} 0 \\ 11 \\ 18 \end{bmatrix}$. For patient 2, it was located at $\begin{bmatrix} 0 \\ 14 \\ 18 \end{bmatrix}$. The different combinations of instrument port locations resulted in seven hundred twenty-nine (729) possible port placement configurations for each patient model. The complete list of possible port positions and their letter designation can be found in Table 13 - Table 18.

5.7.5 Metrics

Figure 33 shows the target sphere and the work volumes of instruments 1 and 2. The region of the target sphere encompassed by both instruments was shaded in red. The region outside the target sphere shaded in green was the work volume common between instruments 1 and 2 where potential collisions could occur. The blue and yellow regions were the portion of the work volumes of instrument 1 and 2 that were exclusive to each. For this analysis, reachability was extended from the definition used by Adhami and Coste-Manière (2003) to encompass both visual and physical access to the target region. It was calculated as the percentage of the total volume of the spherical target region that could be reached by all the instruments and the endoscope.

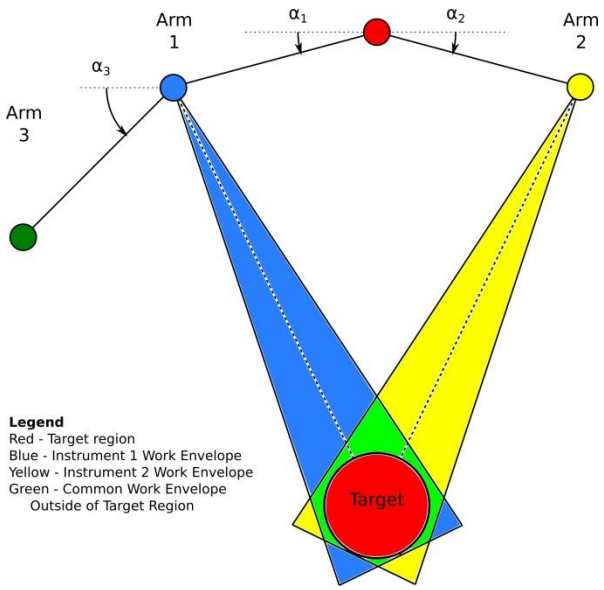

Figure 33. Overlapping Work Volumes of Two Instruments

The second metric used for comparing port locations was called interference. It was defined as the percentage of the total work volume occupied by two or more tools outside spherical target region, shown in green. This was where unwanted collisions could potentially occur. The general objective of port placement is to maximize reachability, the volume of the red target region, while minimizing potential interference, the volume of the green region.

Laparoscopic instruments inserted in different ports are often used differently, whether or not they are the same or different kind of instrument. Thus, they may have different work volume requirements. By assigning instruments a different priority, an analysis of the volume in common between two instruments as a percentage of the total volume of a primary instrument may result in a different port placement arrangement. For example, consider if the

work volume of instrument 1 were more important than the work volume of instrument 2 (Figure 33). The amount that instrument 2 could interfere with instrument 1 would provide a different way of comparing the work volumes. This could be measured as the volume of a secondary instrument that coincides with the work volume of primary instrument. Thus, the interference value would be the ratio of the green region with the total volume of instrument 1 in the blue, green, and red regions.

5.7.6 Computation Algorithm

Calculating the volume of intersection between cones with axes aligned arbitrarily in three-dimensional space was difficult to perform analytically (Balogun, Brunetti & Cesareo, 2000) so it was performed by approximation. A rectangular box that encompassed the spherical target region and the cones representing the work volumes of the instrument was defined as a region of analysis. This region was divided into smaller cubes. If a portion of the cube was within the cone or sphere, then its volume was counted toward the volume of the cone or sphere. The sum of the volume of the cubes was used to approximate the volume of the cone or sphere. By progressively reducing the size of the cubes and, consequently increasing their number, a more accurate estimate of volume could be achieved.

To determine if all or part of a cube was within the volume of the cone or sphere, the point that defined the position of the cube was tested if it was on the

surface or inside of a cone or sphere. The algorithm for determining whether a point in space was on or inside a cone or sphere is explained in the section that follows with examples. Four sample points were defined for use in the calculation to see if they were on or inside the work volume cone of the endoscope (Figure 34) or instrument 1 (Figure 35).

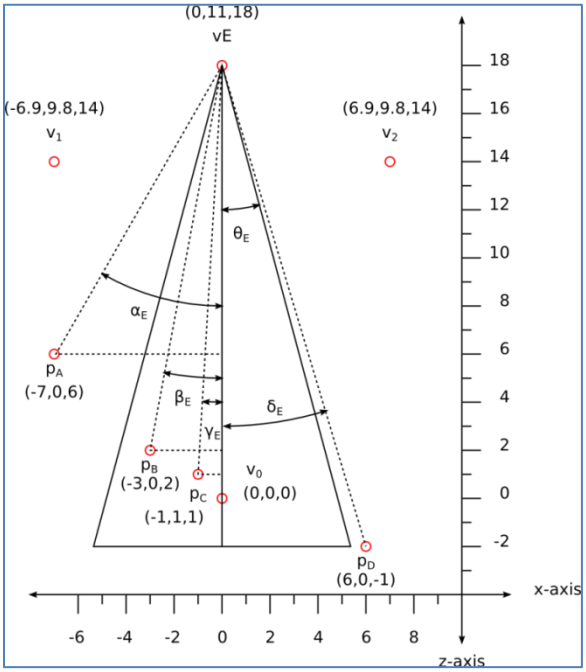

Figure 34. Work volume of endoscope with port at V_E and target at V_0

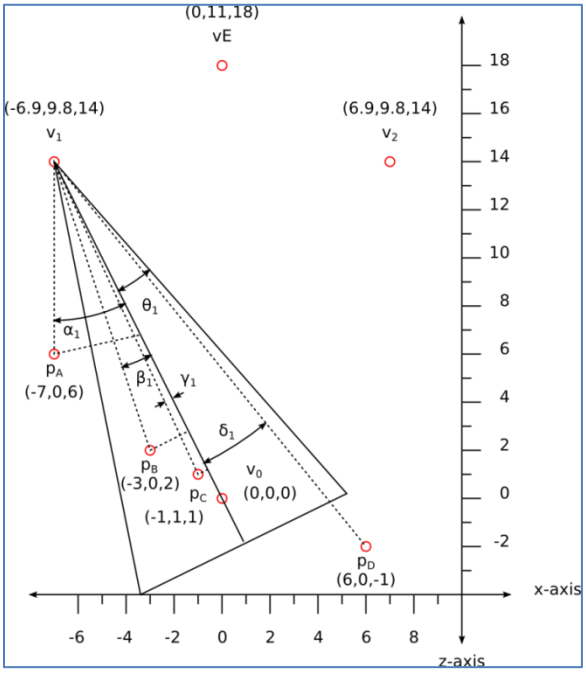

Figure 35. Work volume of instrument arm 1 with port at V_1 and target at V_0

5.7.7 Test if a Point is On or Inside a Sphere or Cone

1. Define vectors for the endoscope port and instrument arm 1 port as follows:

$$\overrightarrow{V_E} = \begin{bmatrix} 0 \\ 11 \\ 18 \end{bmatrix} \qquad \overrightarrow{V_1} = \begin{bmatrix} -6.928 \\ 9.756 \\ 14 \end{bmatrix}$$

2. Define the four sample points to test as follows:

$$P_A = \begin{bmatrix} -7 \\ 0 \\ 6 \end{bmatrix} \qquad P_B = \begin{bmatrix} -3 \\ 0 \\ 2 \end{bmatrix} \qquad P_C = \begin{bmatrix} -1 \\ 1 \\ 1 \end{bmatrix} \qquad P_D = \begin{bmatrix} 6 \\ 0 \\ -1 \end{bmatrix}$$

3. Calculate the vectors from the center of the target region V_0 to each sample point.

$$\overrightarrow{V_0} - P_A = \begin{bmatrix} 0 \\ 0 \\ 0 \end{bmatrix} - \begin{bmatrix} -7 \\ 0 \\ 6 \end{bmatrix} = \begin{bmatrix} 7 \\ 0 \\ 6 \end{bmatrix} = \overrightarrow{V_{PA}}$$

4. Calculate the magnitude of each vector. If the magnitude exceeds the radius of the target sphere, in this case 2cm, then the sample point is outside the target sphere.

$$\left\|\overrightarrow{V_{PA}}\right\| = \sqrt{\overrightarrow{V_{PA}} \cdot \overrightarrow{V_{PA}}} = 9.22$$

$$\left\|\overrightarrow{V_{PB}}\right\| = 3.61$$

$$\left\|\overrightarrow{V_{PC}}\right\| = 1.73$$

$$\left\|\overrightarrow{V_{PD}}\right\| = 6.08$$

From the above calculations, only the magnitude $\left\|\overrightarrow{V_{PC}}\right\|$ was less than 2. Therefore, only the point P_C is inside the target of interest.

5. Calculate the vectors from each port $\overrightarrow{V_E}$ and $\overrightarrow{V_1}$ and each sample point. For example,

$$\overrightarrow{V_E} - P_A = \begin{bmatrix} 0 \\ 11 \\ 18 \end{bmatrix} - \begin{bmatrix} -7 \\ 0 \\ 6 \end{bmatrix} = \begin{bmatrix} 7 \\ 11 \\ 12 \end{bmatrix} = \overrightarrow{V_{EA}}$$

The remaining vectors are as follows:

$$\overrightarrow{V_{EA}} = \begin{bmatrix} 7 \\ 11 \\ 12 \end{bmatrix} \qquad \overrightarrow{V_{EB}} = \begin{bmatrix} 3 \\ 11 \\ 16 \end{bmatrix} \qquad \overrightarrow{V_{EC}} = \begin{bmatrix} 1 \\ 10 \\ 17 \end{bmatrix} \qquad \overrightarrow{V_{ED}} = \begin{bmatrix} -6 \\ 11 \\ 19 \end{bmatrix}$$

$$\overrightarrow{V_{1A}} = \begin{bmatrix} 0.072 \\ 9.756 \\ 8 \end{bmatrix} \quad \overrightarrow{V_{1B}} = \begin{bmatrix} -3.928 \\ 9.756 \\ 12 \end{bmatrix} \quad \overrightarrow{V_{1C}} = \begin{bmatrix} -5.928 \\ 8.756 \\ 13 \end{bmatrix} \quad \overrightarrow{V_{1D}} = \begin{bmatrix} -12.928 \\ 9.756 \\ 15 \end{bmatrix}$$

6. Calculate the magnitude of each vector defined by the port and the sample points.

$$\left\|\overrightarrow{V_E}\right\| = \sqrt{\overrightarrow{V_E} \cdot \overrightarrow{V_E}} = 21.10$$

$$\left\|\overrightarrow{V_1}\right\| = \sqrt{\overrightarrow{V_1} \cdot \overrightarrow{V_1}} = 18.42$$

$$\left\|\overrightarrow{V_{EA}}\right\| = 17.72 \quad \left\|\overrightarrow{V_{EB}}\right\| = 19.65 \quad \left\|\overrightarrow{V_{EC}}\right\| = 19.78 \quad \left\|\overrightarrow{V_{ED}}\right\| = 22.76$$

$$\left\|\overrightarrow{V_{1A}}\right\| = 12.62 \quad \left\|\overrightarrow{V_{1B}}\right\| = 15.96 \quad \left\|\overrightarrow{V_{1C}}\right\| = 16.76 \quad \left\|\overrightarrow{V_{1D}}\right\| = 22.08$$

7. Calculate the angle in degrees between each vector.

$$\cos^{-1}\frac{\overrightarrow{V_E} \cdot \overrightarrow{V_{EA}}}{\left\|\overrightarrow{V_E}\right\| \left\|\overrightarrow{V_{EA}}\right\|} * \frac{180}{\pi} = \alpha_E = 25.64°$$

$$\alpha_E = 25.64° \quad \beta_E = 9.30° \quad \gamma_E = 3.06° \quad \delta_E = 15.34°$$

$$\alpha_1 = 27.19° \quad \beta_E = 8.82° \quad \gamma_E = 1.62° \quad \delta_E = 13.84°$$

8. Compare the angles with the angle of each cone corresponding to the endoscope and instrument arm 1. Only angles that are less than or equal to θ_E and θ_1 would correspond to points that are valid if the cone were infinitely long. For this example, θ_E and θ_1 are 15°. The angles that are less than or equal to 15° are listed in bold below:

$$\alpha_E = 25.64° \quad \boldsymbol{\beta_E = 9.30°} \quad \boldsymbol{\gamma_E = 3.06°} \quad \delta_E = 15.34°$$

$$\alpha_1 = 27.19° \quad \boldsymbol{\beta_1 = 8.82°} \quad \boldsymbol{\gamma_1 = 1.62°} \quad \boldsymbol{\delta_1 = 13.84°}$$

9. Calculate the scalar projection of the vectors of the test points that are valid based on the previous step. The scalar projection is compared to the magnitude of the vector of the cone plus the radius of the sphere. If the

scalar projection exceeds the magnitude of the vector of the cone, then it is not valid.

From step 5, $\left\|\overrightarrow{V_E}\right\| + r = 23.10$ and $\left\|\overrightarrow{V_1}\right\| + r = 18.42 = 20.42$.

Both $s\overrightarrow{V_{EB}} = \left\|\overrightarrow{V_{EB}}\right\| * \cos^{-1}\beta_E = 19.38$ and $s\overrightarrow{V_{EC}} = \left\|\overrightarrow{V_{EC}}\right\| * \cos^{-1}\gamma_E = 19.72$ are less than 23.10. They are both inside the work volume of the endoscope. Both $s\overrightarrow{V_{1B}} = 15.77$ and $s\overrightarrow{V_{1C}} = 16.75$ are less than 20.42. They are inside the work volume of instrument 1. However, $s\overrightarrow{V_{1D}} = 21.43$ exceeds 20.42 and is not inside the work volume of instrument 1. Therefore, points P_B and P_C are inside the work volume of both the endoscope and instrument 1 in their current positions.

5.7.8 Calculating Accuracy of Estimate

The method for determining the accuracy based on the estimate of the volume of the sphere is detailed below:

1. Calculate the volume encompassing the target sphere. For a cube with sides equal to the diameter of the sphere this is simply the diameter cubed.

$$V_C = (2r)^3$$

1. Calculate the volume of the sphere.

$$V_S = \frac{4}{3}\pi r^3$$

2. Calculate the theoretical ratio.

$$V_T = \frac{V_S}{V_C} = \frac{\pi}{6}$$

3. Calculate the actual ratio of points on and inside the sphere versus outside the sphere

$$V_A = \frac{points\ on\ or\ inside}{points\ outside}$$

4. Compare the ratio to determine the percent error.

$$\frac{V_T - V_A}{V_T} * 100 = \%\ error$$

5. Decrease the size of the cubes until the desired accuracy is achieved.

Based on sample calculations, an accuracy of less than 2% error could be achieved using a cube measuring 0.1cm on each side or 1000 samples per cubic centimeter. The region of analysis that encompasses the instrument work volumes and target region for both patient 1 and patient 2 was defined as follows:

- x-axis: -20 to 20
- y-axis: -6 to 14
- z-axis: -6 to 20

A cross-section of this region in the x-y plane is shown in Figure 36. The volume of this region is 20,800cm^3, requiring 20.8 million cube positions to be calculated.

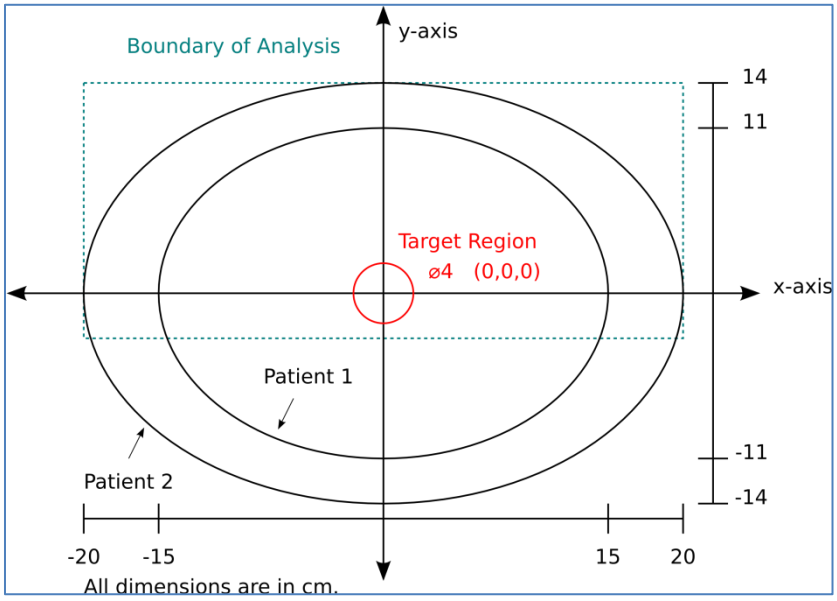

Figure 36. Elliptical Cross-Section of Patient Torso (Patient 1 and 3)

5.7.9 Software Program

A program was written in GNU Octave to calculate the different reachability and interference values for all the possible combinations of the different instrument port placement positions. A complete listing of the program and supporting functions are included in Appendix C. Parameters that were adjusted to suit a specific analysis along with some suggested values are listed below:

- Distance between the ports: 8 or 10cm
- Angle from horizontal between ports:

Table 4. Port Placement Angles from Horizontal

Angle	Conventional	Robot-Assisted
α_1	$\pi/12$ (15°)	$\pi/6$ (30°)
α_2	$\pi/12$ (15°)	$\pi/6$ (30°)
α_3	$\pi/4$ (45°)	$\pi/12$ (15°)

- The x, y, z-axis coordinates defining the boundary of the analysis
- Resolution of the partition of the analysis region (cm): 0.1
- Location of target region in x-y-z dimensions: [0, 0, 0]
- Radius of target region (cm): 2
- Location of endoscope port in x-z plane: [0, Y_E, 18]
- Torso width (cm): Patient 1: 30, Patient 2: 40
- Torso thickness: Patient 1: 22, Patient 2: 28
- Cone angles (in radians) to cone axis

Table 5. Cone Angles to Cone Axis

Parameter	Value
θ_E	$\pi/12$ (15°)
θ_1	$\pi/24$ (7.5°)
θ_2	$\pi/24$ (7.5°)
θ_3	$\pi/24$ (7.5°)

6. Results and Analysis

6.1. Field Study

Intuitive Surgical provides training and provides experts on site to assist surgical teams while they are learning to use the da Vinci Surgical System. Based

on video of two early cases and an interview with the chief surgeon, the surgical team in France experienced a long setup time and collisions during the operation in the early cases. This occurred even with the assistance of experts brought in by Intuitive Surgical to provide guidance using the da Vinci Surgical System and the docking process.

6.1.1 Task Analysis

A generalized port placement process followed by the surgeons, based on the observations and interviews, is shown in Figure 37.

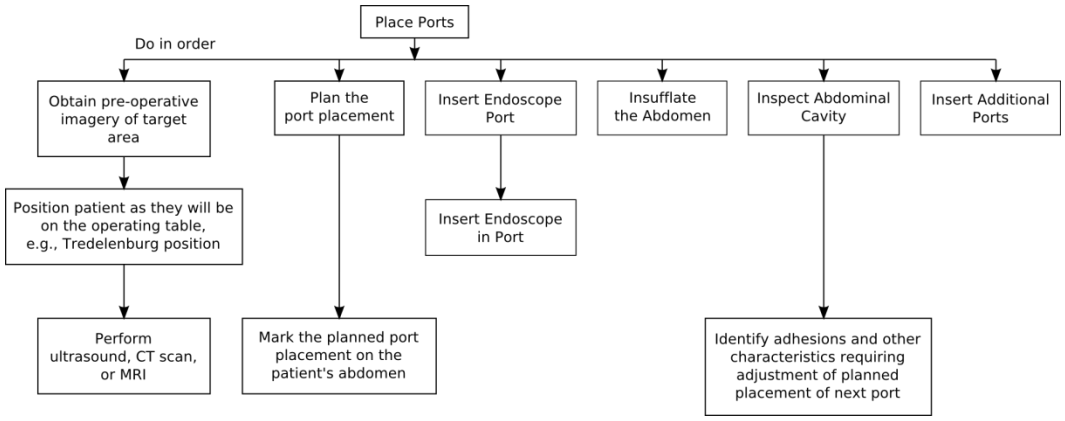

Figure 37. Hierarchical Task Analysis of Port Placement Process

The factors considered in the decision process vary depending on the specific intervention and often include co-morbidities. For example, in placing ports for a cholecystectomy, or removal of the gallbladder, the condition of the liver would be a consideration. A diseased liver will have different characteristics than a healthy liver and may not be as easily displaced as would be necessary to access

the gallbladder (S. Schwaitzberg, personal communication, 2011). A task analysis for a specific robotic gynecological procedure was planned but could not be performed due to lack of robotic procedures performed while in France.

6.2. Requirements Definition

Based on previous research, field observations, and task analyses, the following requirements were defined:

Table 6. Requirements for the Decision Aid

No.	Requirement	Importance
1	Accept individual patient dimensions.	Critical
2	Avoid internal and external tool collisions	Critical
3	Provide a recommended position of the ports on the patient	Critical
4	Provide a recommended pose plan for the robot	Critical
5	Allow for real-time adjustment of port placement	Highly desirable
6	Consideration of conversion to conventional laparoscopic surgery	Not important
7	Three-dimensional model of patient anatomy	Not important

The importance of each requirement was also noted. For example, the research revealed consideration of conversion to conventional laparoscopic surgery was not important because of the infrequency of occurrence. Consideration of the possibility of conversion could have resulted in sub-optimal port placement for robot assisted procedures.

Based on interviews and observations, high-fidelity 3D reconstruction of the patient torso was also deemed not important in laparoscopic procedures as it was in cardiac surgery where port placement had to contend with the rib cage.

The soft bodies in the abdominal and pelvic areas, as well as the effects of patient positioning -- commonly in the Tredelenburg position, and of insufflation make for a dynamic operating environment.

6.3. Design Concept

To clarify the problem, the requirements were decomposed as follows:

- Interface for input of patient measurements and relative position of target organ or region
- Combine patient model with intervention-specific robot model
- Calculate the inverse kinematics for collision-free port placement with access to target region
- Display the suggested port placement
- Allow adjustment of port placement after first inspection with endoscope
- Generate and display final pose plan to surgical team

From the design concept, a conceptual narrative of how it might be used was developed along with the conceptual process flow, shown in Figure 38. The narrative is as follows:

After the robot model has been adjusted for the specific intervention, it is combined with the patient model to derive a suitable port placement and pose plan. At the beginning of each procedure, when the endoscope is first inserted into the patient but before other incisions, the surgeon may discover additional

patient characteristics such as adhesions, scars from previous surgeries or other conditions. These conditions may require adjustment of the patient model, port placement, and pose plan for the desired operation.

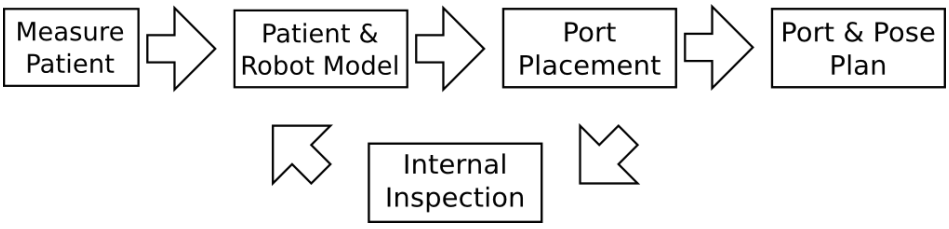

Figure 38. Pre-operative Planning Process

6.4. Patient Model

From the literature search and the task analysis performed, the patient information and measurements useful in modeling the patient torso are shown in Figure 39 and listed along with the method they are collected in Table 7. The measurements specific to female patients are shown in Figure 40 and listed Table 8. The measurements specific to male patients are shown in Figure 41 and listed in Table 9.

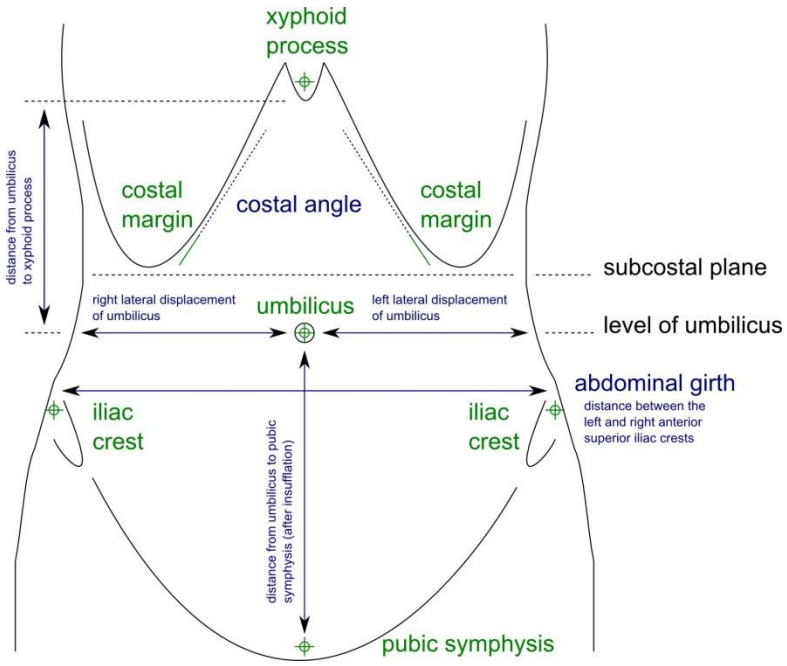

Figure 39. Patient Measurement (Front View)

Table 7. Patient Modeling Information

Metrics	**How Obtained**
Height	From patient record to calculate body mass index
Weight	From patient record to calculate body mass index
Body mass index (BMI)	Calculated from height and weight
Age	From patient record
Gender	From patient record
Race	Optional, self-reported. Some studies have shown correlation between race and position of the umbilicus.
Abdominal wall elasticity	Surgeon's observation
Abdominal girth	Measured using calipers across the front, above the iliac crests. Abdominal girth allows for placement of lateral ports.
Sagittal abdominal girth	Measured using calipers across from the front to the back of the subject at a position halfway between the subcostal plane and the iliac crests. This measure allows for modeling of the abdominal cavity.

Torso length	This is optional but with sufficient data will be analyzed for possible correlation with other patient metrics.
Patient habitus (gynecoid versus android)	Noted from surgeon's observation. Patients with gynecoid habitus have more truncal fat.
Position of the umbilicus in the horizontal plane	Measured from the right side. The umbilicus has been shown in a previous study to be laterally displaced.
Upper Abdomen	
Distance from umbilicus to xyphoid process	Measured during pre-operative consultation to model the abdominal cavity.
Distance from umbilicus to costal margin	Measured during pre-operative consultation to model the abdominal cavity to avoid collisions with the patient ribs.
Costal angle	Measured during pre-operative consultation to model the abdominal cavity to avoid collisions with the patient ribs.
Lower Abdomen and Pelvic area	
Distance between the left and right anterior superior iliac crests	Measured during pre-operative consultation to model the pelvic cavity.
Distance from umbilicus to pubic symphysis (before insufflation)	Measured during pre-operative consultation to model the pelvic cavity.
Distance from umbilicus to pubic symphysis (after insufflation)	Measured during pre-operative consultation to model the pelvic cavity.

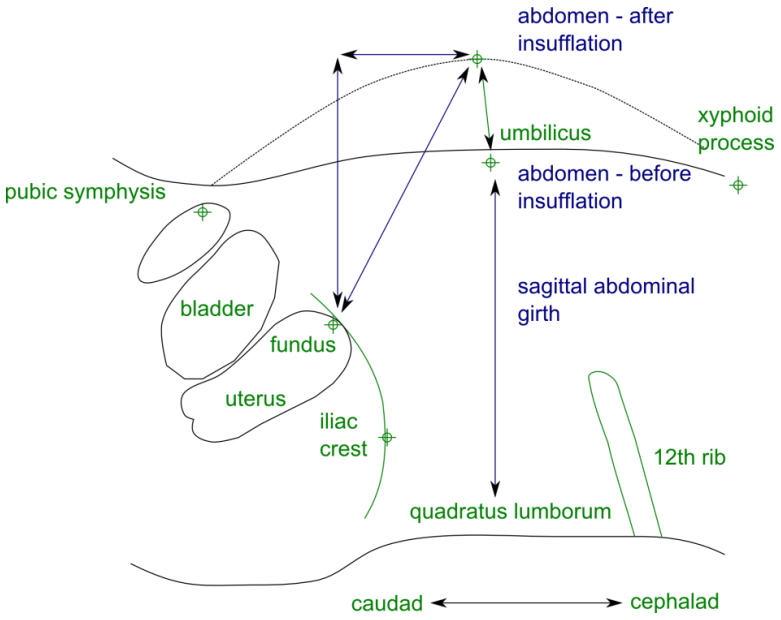

Figure 40. Patient Measurement, Female (Side View).

Table 8. Patient Modeling Information (Gynecological Procedures Only)

Gynecological Procedures Only	
Distance from umbilicus to fundus of uterus (after insufflation)	Surgeon or other surgical team member inserts the laparoscope and touches the fundus. The distance to the fundus is measured from the length of the scope inserted.
Angle from the horizontal plane from the umbilicus to fundus of uterus	Surgeon or other surgical team member inserts the laparoscope and touches the fundus. The angle of the scope relative to the operating table is measured.
Angle from the midline from the umbilicus to fundus of uterus	Surgeon or other surgical team member inserts the laparoscope and touches the fundus. The angle of the scope relative to patient midline is measured.

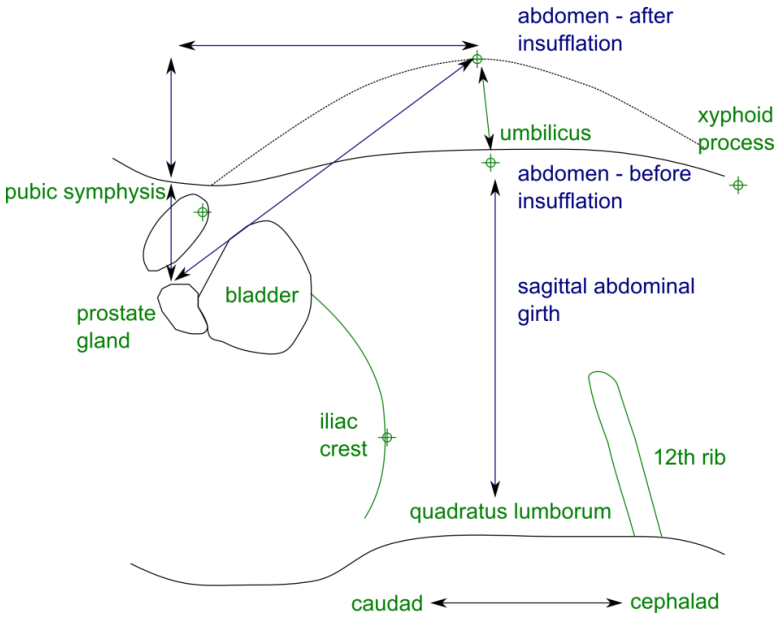

Figure 41. Patient Measurement, Male (Side View)

Table 9. Patient Modeling Information (Urological Procedures Only)

Urological Procedures ONLY	
Distance from umbilicus to prostate gland (after insufflation)	Surgeon or other surgical team member inserts the laparoscope and touches the fundus. The distance to the fundus is measured from the length of the scope inserted.
Angle from the horizontal plane from umbilicus to prostate gland	Surgeon or other surgical team member inserts the laparoscope and touches the fundus. The angle of the scope relative to the operating table is measured.
Angle from the midline from umbilicus to prostate gland	Surgeon or other surgical team member inserts the laparoscope and touches the fundus. The angle of the scope relative to patient midline is measured.

6.4.1 Patient Data Collected Using Simplified Method

The results from using the simplified method for collecting patient measurements are shown in Figure 44 - Figure 43 below:

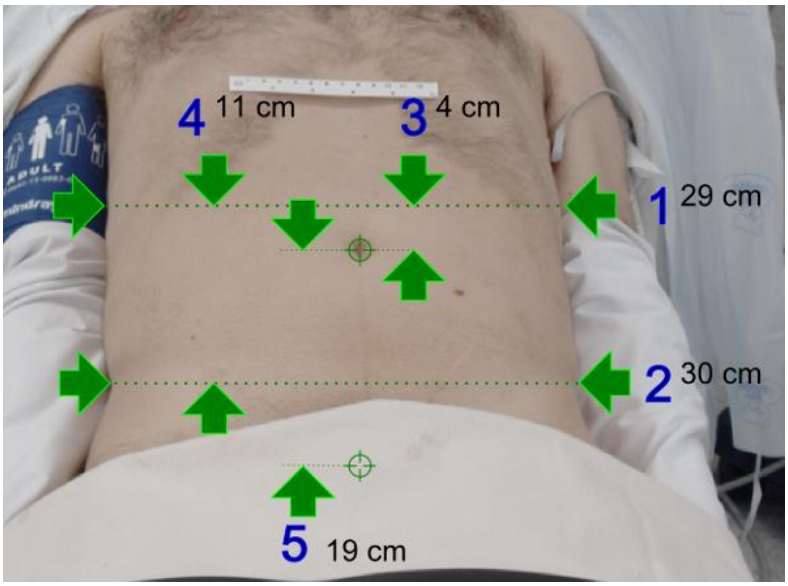

Figure 42. Patient 1 (Patient Front)

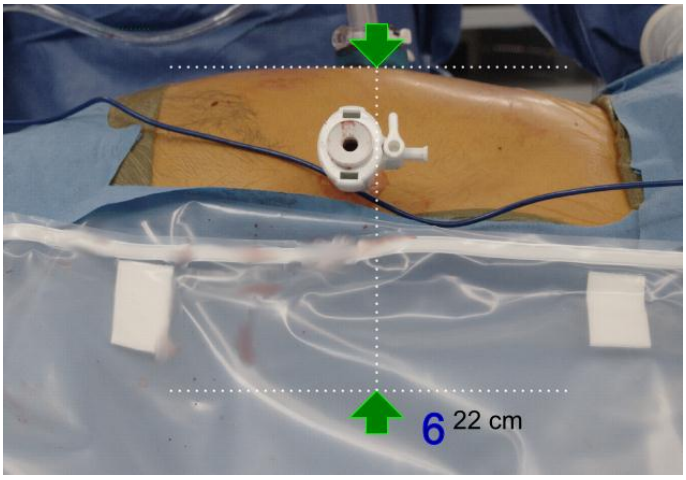

Figure 43. Patient 1 (Patient Side)

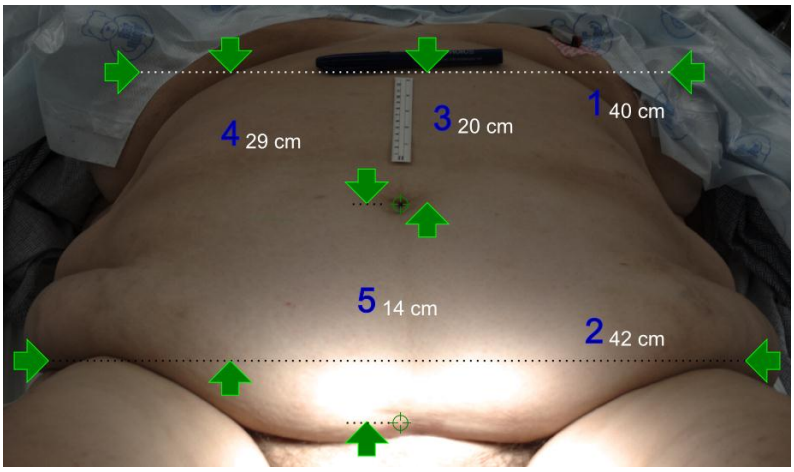

Figure 44. Patient 2 (Patient Front)

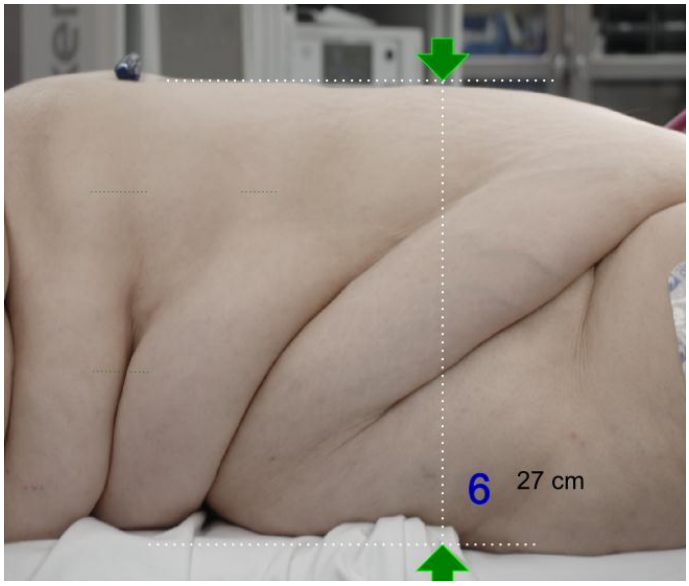

Figure 45. Patient 2 (Patient Side)

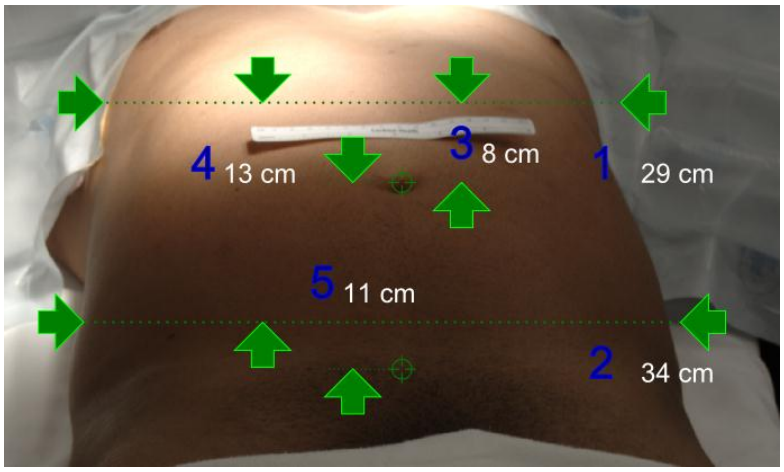

Figure 46. Patient 3 (Patient Front)

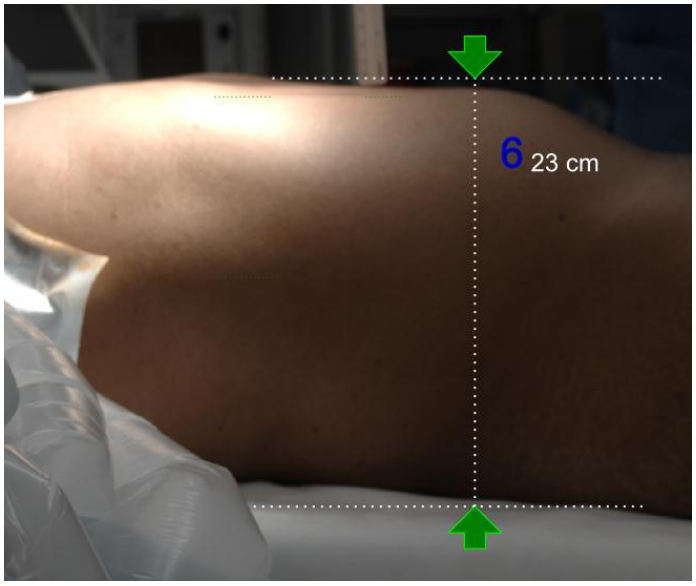

Figure 47. Patient 3 (Patient Side)

6.5. Robot Model

The symbolic model for instrument arm 2 is shown in Figure 48. The corresponding modified D-H parameters were derived for instrument arms 1 and 2, which are effectively identical, and are listed in Table 10. Instrument arm 3 has

an additional link which allows it to swivel to either side of the patient cart. The symbolic model for instrument arm 3 is shown in Figure 49. The modified D-H parameters for instrument arm 3 are listed in Table 11.

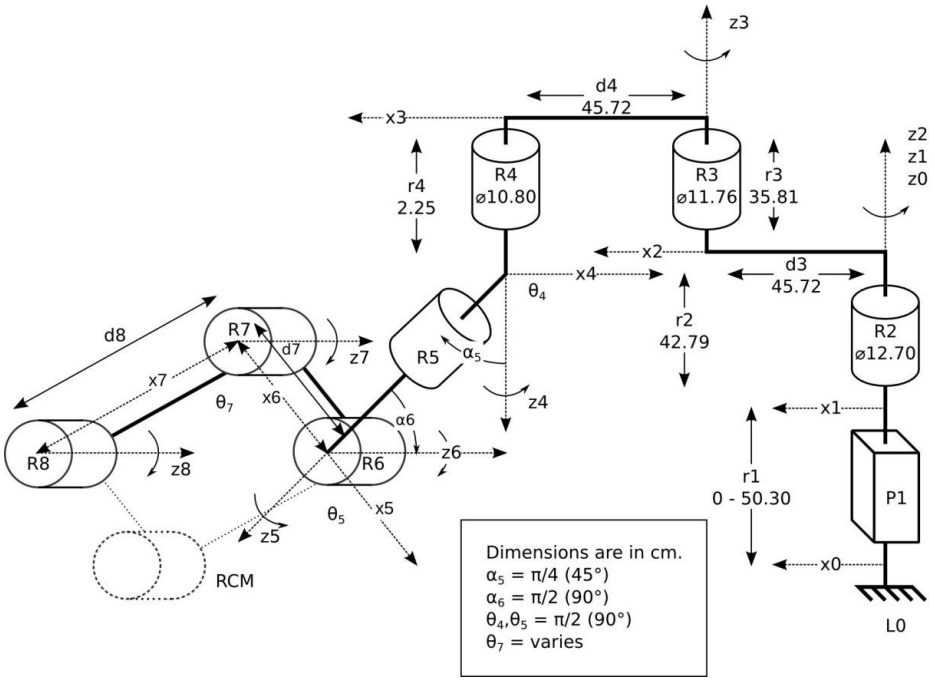

Figure 48. Symbolic Model of Instrument Arm 2

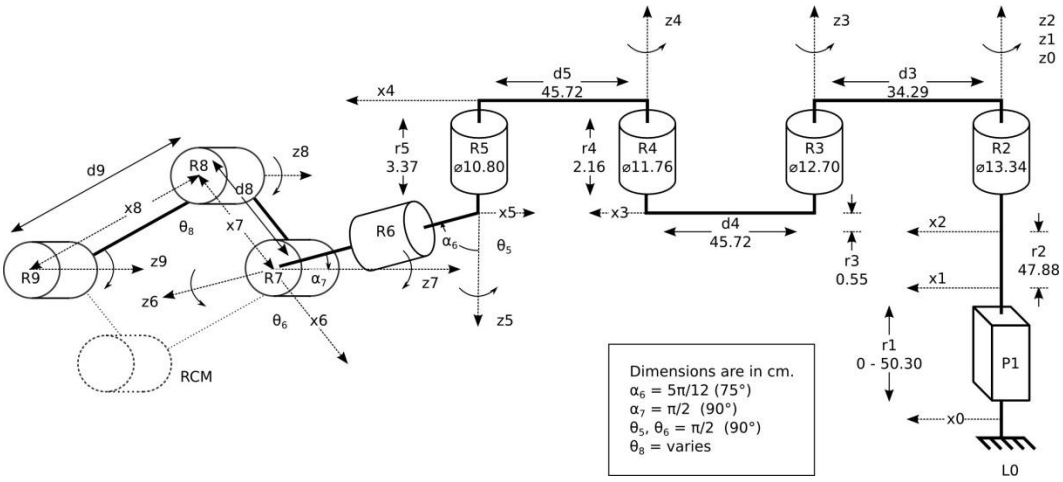

Figure 49. Symbolic Model of Instrument Arm 3

Table 10. Modified D-H parameters for Instrument Arm 1 & Arm 2

Setup Joint					
j	**σ_i**	**α_i**	**d_i (cm)**	**θ_i**	**r_i (cm)**
1	1	0	0	0	r1 = 0 – 50.30
2	0	0	0	0	r2=42.79
3	0	0	d3=45.72	0	r3=35.81
4	0	0	d4=45.72	$+\pi/2$	r4=2.25
5	0	$\pi/4$	0	$-\pi/2$	r5
Instrument Arm					
6	0	$-\pi/2$	0	0	0
7	0	0	d7	varies	0
8	0	0	d8		

Table 11. Modified D-H parameters for Instrument Arm 3

Setup Joint					
j	**σ_i**	**α_i**	**d_i (cm)**	**θ_i**	**r_i (cm)**
1	1	0	0	0	r1 = 0- 50.30
2	0	0	0	0	r2 = 47.88
3	0	0	d3 = 34.29	0	r3 = 0.55
4	0	0	d4 = 45.72	0	r4 = 2.16
5	0	0	d5 = 45.72	$+\pi/2$	r5 = 3.37
6	0	$-\pi/4$	0	$-\pi/2$	r6
Instrument Arm					
7	0	$-\pi/2$	0	0	0
8	0	0	d8	varies	0
9	0	0	d9		

The symbolic model for the endoscope arm is shown in Figure 50. The modified

D-H parameters for the endoscope arm are listed in Table 12.

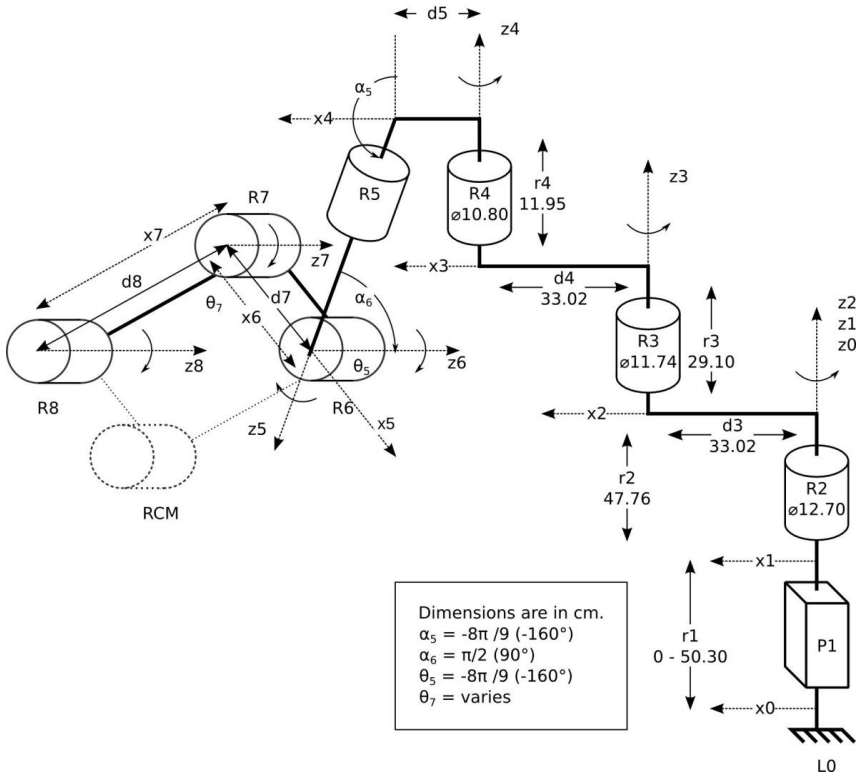

Figure 50. Symbolic Model of Endoscope Arm

Table 12. Modified D-H parameters for Endoscope Arm

Setup Joint					
j	**σ_i**	**α_i**	**d_i (cm)**	**θ_i**	**r_i (cm)**
1	1	0	0	0	r1= 0 – 50.30
2	0	0	0	0	r2 = 47.76
3	0	0	d3 = 33.02	0	r3 = 29.10
4	0	0	d4 = 33.02	0	r4 = 11.95
5	0	$-8/9\,\pi$	d5	$+\pi/2$	r5
Instrument Arm					
6	0	$-\pi/2$	0	$-\pi/2$	0
7	0	0	d7	varies	0
8	0	0	d8		

The positions of the bases of each of the instrument arms, relative to the base of the endoscope arm, was derived from a SolidWorks drawing and are shown in Figure 51.

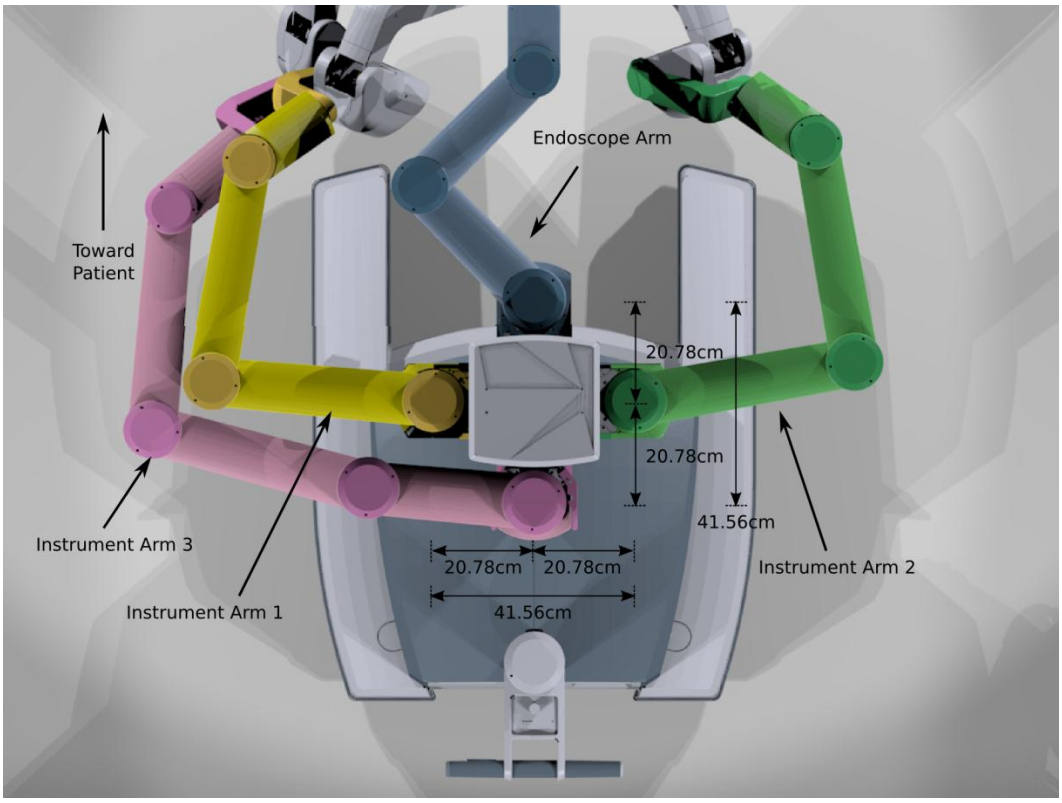

Figure 51. Positions of the center of the base of each instrument arm, relative to the center of the base of the endoscope arm.

Calculation of the pose of the robot could not be completed because the author was unable to derive the inverse kinematic equations from the forward kinematic equations using Symoro+. In addition, there were dimensions of the robot that were left in symbolic form because they could not be obtained. Due to issues at the hospital facility, the robot was unavailable after the preliminary symbolic

model was created. Thus the author could not verify that the parallelogram model of the instrument arms was valid and could not obtain the limits of the movements of the joints.

6.6. Comparison of Port Locations Based On Instrument Work Volumes

6.6.1 Port Placement Positions

The port placement positions calculated using guidelines for conventional and robot-assisted laparoscopic surgery are listed in Table 13 - Table 18. The base port position, the position from which the other port positions were calculated, was designated as position E. For each port position, the intracorporeal tool length (IL) and the intracorporeal:extracorporeal (I/E) tool length ratio, based on a standard laparoscopic tool length of 33cm, were also calculated and included.

Table 13. Instrument Port Positions, Intracorporeal Tool Length (IL), and Intracorporeal:Extracorporeal Length Ratio (I/E) for Conventional Laparoscopic Surgery (Patient 1, 8cm between ports)

	Instrument 1 Port					**Instrument 2 Port**					**Instrument 3 Port**				
Pos.	**X**	**Y**	**Z**	**I.L.**	**I/E**	**X**	**Y**	**Z**	**I.L.**	**I/E**	**X**	**Y**	**Z**	**I.L.**	**I/E**
A	-9.7	8.4	13.9	18.9	1.3	5.7	10.2	13.9	18.2	1.2	-15.0	0.0	8.3	17.1	1.1
B	-7.7	9.4	13.9	18.5	1.3	7.7	9.4	13.9	18.5	1.3	-13.4	5.0	8.3	16.5	1.0
C	-5.7	10.2	13.9	18.2	1.2	9.7	8.4	13.9	18.9	1.3	-11.4	7.2	8.3	15.8	0.9
D	-9.7	8.4	15.9	20.5	1.6	5.7	10.2	15.9	19.7	1.5	-15.0	0.0	10.3	18.2	1.2
E	-7.7	9.4	15.9	20.1	1.5	7.7	9.4	15.9	20.1	1.5	-13.4	5.0	10.3	17.6	1.1
F	-5.7	10.2	15.9	19.7	1.5	9.7	8.4	15.9	20.5	1.6	-11.4	7.2	10.3	16.9	1.1
G	-9.7	8.4	17.9	22.0	2.0	5.7	10.2	17.9	21.4	1.8	-15.0	0.0	12.3	19.4	1.4
H	-7.7	9.4	17.9	21.7	1.9	7.7	9.4	17.9	21.7	1.9	-13.4	5.0	12.3	18.8	1.3
I	-5.7	10.2	17.9	21.4	1.8	9.7	8.4	17.9	22.0	2.0	-11.4	7.2	12.3	18.2	1.2

Table 14. Instrument Port Positions, Intracorporeal Tool Length (IL), and Intracorporeal:Extracorporeal Length Ratio (I/E) for Conventional Laparoscopic Surgery (Patient 2, 8cm between ports)

	Instrument 1 Port					Instrument 2 Port					Instrument 3 Port				
Pos.	**X**	**Y**	**Z**	**I.L.**	**I/E**	**X**	**Y**	**Z**	**I.L.**	**I/E**	**X**	**Y**	**Z**	**I.L.**	**I/E**
A	-9.7	12.2	13.9	20.9	1.7	5.7	13.4	13.9	20.2	1.6	-15.4	8.9	8.3	19.6	1.5
B	-7.7	12.9	13.9	20.5	1.6	7.7	12.9	13.9	20.5	1.6	-13.4	10.4	8.3	18.9	1.3
C	-5.7	13.4	13.9	20.2	1.6	9.7	12.2	13.9	20.9	1.7	-11.4	11.5	8.3	18.2	1.2
D	-9.7	12.2	15.9	22.3	2.1	5.7	13.4	15.9	21.6	1.9	-15.4	8.9	10.3	20.5	1.7
E	-7.7	12.9	15.9	21.9	2.0	7.7	12.9	15.9	21.9	2.0	-13.4	10.4	10.3	19.8	1.5
F	-5.7	13.4	15.9	21.6	1.9	9.7	12.2	15.9	22.3	2.1	-11.4	11.5	10.3	19.2	1.4
G	-9.7	12.2	17.9	23.8	2.6	5.7	13.4	17.9	23.1	2.3	-15.4	8.9	12.3	21.6	1.9
H	-7.7	12.9	17.9	23.4	2.4	7.7	12.9	17.9	23.4	2.4	-13.4	10.4	12.3	20.9	1.7
I	-5.7	13.4	17.9	23.1	2.3	9.7	12.2	17.9	23.8	2.6	-11.4	11.5	12.3	20.3	1.6

Table 15. Instrument Port Positions, Intracorporeal Tool Length (IL), and Intracorporeal:Extracorporeal Length Ratio (I/E) for Conventional Laparoscopic Surgery (Patient 2, 10cm between ports)

	Instrument 1 Port					Instrument 2 Port					Instrument 3 Port				
Pos.	**X**	**Y**	**Z**	**I.L.**	**I/E**	**X**	**Y**	**Z**	**I.L.**	**I/E**	**X**	**Y**	**Z**	**I.L.**	**I/E**
A	-11.7	11.4	13.4	21.1	1.8	7.7	12.9	13.4	20.1	1.6	-18.7	4.9	6.3	20.4	1.6
B	-9.7	12.3	13.4	20.6	1.7	9.7	12.3	13.4	20.6	1.7	-16.7	7.7	6.3	19.5	1.4
C	-7.7	12.9	13.4	20.1	1.6	11.7	11.4	13.4	21.1	1.8	-14.7	9.5	6.3	18.6	1.3
D	-11.7	11.4	15.4	22.4	2.1	7.7	12.9	15.4	21.5	1.9	-18.7	4.9	8.3	21.1	1.8
E	-9.7	12.3	15.4	21.9	2.0	9.7	12.3	15.4	21.9	2.0	-16.7	7.7	8.3	20.2	1.6
F	-7.7	12.9	15.4	21.5	1.9	11.7	11.4	15.4	22.4	2.1	-14.7	9.5	8.3	19.4	1.4
G	-11.7	11.4	17.4	23.8	2.6	7.7	12.9	17.4	23.0	2.3	-18.7	4.9	10.3	22.0	2.0
H	-9.7	12.3	17.4	23.4	2.4	9.7	12.3	17.4	23.4	2.4	-16.7	7.7	10.3	21.1	1.8
I	-7.7	12.9	17.4	23.0	2.3	11.7	11.4	17.4	23.8	2.6	-14.7	9.5	10.3	20.3	1.6

Table 16. Instrument Port Positions, Intracorporeal Tool Length (IL), and Intracorporeal:Extracorporeal Length Ratio (I/E) for Robot-Assisted Laparoscopic Surgery (Patient 1, 8cm between ports)

	Instrument 1 Port					Instrument 2 Port					Instrument 3 Port				
Pos.	**X**	**Y**	**Z**	**I.L.**	**I/E**	**X**	**Y**	**Z**	**I.L.**	**I/E**	**X**	**Y**	**Z**	**I.L.**	**I/E**
A	-8.9	8.8	12.0	17.4	1.1	4.9	10.4	12.0	16.6	1.0	-15.0	0.0	14.1	20.6	1.7
B	-6.9	9.8	12.0	16.9	1.1	6.9	9.8	12.0	16.9	1.1	-14.7	2.3	14.1	20.5	1.6
C	-4.9	10.4	12.0	16.6	1.0	8.9	8.8	12.0	17.4	1.1	-12.7	5.9	14.1	19.8	1.5
D	-8.9	8.8	14.0	18.8	1.3	4.9	10.4	14.0	18.1	1.2	-15.0	0.0	16.1	22.0	2.0
E	-6.9	9.8	14.0	18.4	1.3	6.9	9.8	14.0	18.4	1.3	-14.7	2.3	16.1	21.9	2.0
F	-4.9	10.4	14.0	18.1	1.2	8.9	8.8	14.0	18.8	1.3	-12.7	5.9	16.1	21.3	1.8
G	-8.9	8.8	16.0	20.3	1.6	4.9	10.4	16.0	19.7	1.5	-15.0	0.0	18.1	23.5	2.5
H	-6.9	9.8	16.0	20.0	1.5	6.9	9.8	16.0	20.0	1.5	-14.7	2.3	18.1	23.4	2.4
I	-4.9	10.4	16.0	19.7	1.5	8.9	8.8	16.0	20.3	1.6	-12.7	5.9	18.1	22.8	2.2

Table 17. Instrument Port Positions, Intracorporeal Tool Length (IL), and Intracorporeal:Extracorporeal Length Ratio (I/E) for Robot-Assisted Laparoscopic Surgery (Patient 2, 8cm between ports)

	Instrument 1 Port					Instrument 2 Port					Instrument 3 Port				
Pos.	**X**	**Y**	**Z**	**I.L.**	**I/E**	**X**	**Y**	**Z**	**I.L.**	**I/E**	**X**	**Y**	**Z**	**I.L.**	**I/E**
A	-8.9	12.5	12.0	19.5	1.4	4.9	13.6	12.0	18.8	1.3	-16.7	7.8	14.1	23.1	2.3
B	-6.9	13.1	12.0	19.1	1.4	6.9	13.1	12.0	19.1	1.4	-14.7	9.5	14.1	22.4	2.1
C	-4.9	13.6	12.0	18.8	1.3	8.9	12.5	12.0	19.5	1.4	-12.7	10.8	14.1	21.8	1.9
D	-8.9	12.5	14.0	20.8	1.7	4.9	13.6	14.0	20.1	1.6	-16.7	7.8	16.1	24.4	2.8
E	-6.9	13.1	14.0	20.4	1.6	6.9	13.1	14.0	20.4	1.6	-14.7	9.5	16.1	23.7	2.6
F	-4.9	13.6	14.0	20.1	1.6	8.9	12.5	14.0	20.8	1.7	-12.7	10.8	16.1	23.2	2.4
G	-8.9	12.5	16.0	22.2	2.1	4.9	13.6	16.0	21.5	1.9	-16.7	7.8	18.1	25.8	3.6
H	-6.9	13.1	16.0	21.8	2.0	6.9	13.1	16.0	21.8	2.0	-14.7	9.5	18.1	25.1	3.2
I	-4.9	13.6	16.0	21.5	1.9	8.9	12.5	16.0	22.2	2.1	-12.7	10.8	18.1	24.6	2.9

Table 18. Instrument Port Positions, Intracorporeal Tool Length (IL), and Intracorporeal:Extracorporeal Length Ratio (I/E) for Robot-Assisted Laparoscopic Surgery (Patient 2, 10cm between ports)

	Instrument 1 Port					Instrument 2 Port					Instrument 3 Port				
Pos.	**X**	**Y**	**Z**	**I.L.**	**I/E**	**X**	**Y**	**Z**	**I.L.**	**I/E**	**X**	**Y**	**Z**	**I.L.**	**I/E**
A	-10.7	11.8	11.0	19.4	1.4	6.7	13.2	11.0	18.4	1.3	-20.0	0.0	13.6	24.2	2.7
B	-8.7	12.6	11.0	18.8	1.3	8.7	12.6	11.0	18.8	1.3	-18.3	5.6	13.6	23.5	2.5
C	-6.7	13.2	11.0	18.4	1.3	10.7	11.8	11.0	19.4	1.4	-16.3	8.1	13.6	22.7	2.2
D	-10.7	11.8	13.0	20.6	1.7	6.7	13.2	13.0	19.7	1.5	-20.0	0.0	15.6	25.4	3.3
E	-8.7	12.6	13.0	20.1	1.6	8.7	12.6	13.0	20.1	1.6	-18.3	5.6	15.6	24.7	3.0
F	-6.7	13.2	13.0	19.7	1.5	10.7	11.8	13.0	20.6	1.7	-16.3	8.1	15.6	24.0	2.7
G	-10.7	11.8	15.0	21.9	2.0	6.7	13.2	15.0	21.1	1.8	-20.0	0.0	17.6	26.6	4.2
H	-8.7	12.6	15.0	21.4	1.9	8.7	12.6	15.0	21.4	1.9	-18.3	5.6	17.6	26.0	3.7
I	-6.7	13.2	15.0	21.1	1.8	10.7	11.8	15.0	21.9	2.0	-16.3	8.1	17.6	25.3	3.3

6.6.2 Reachability

All port position combinations were able to reach the target region 100% of the time. Thus no comparison could be made between the different combinations of port positions based on reachability.

6.6.3 General Interference

The volume common between two instruments was compared to the total

volume of the region of analysis for each combination of two instruments as well as for all three instruments. For each set of port placement combinations for both conventional and robot-assisted laparoscopic surgery, a summary of the statistics of the results was calculated (Table 19, Table 21, and Table 23). The summary was used to extract port positions that were in the first quartile for the four different combinations of instrument volumes. The result was then sorted first by the fourth column followed by the first, second, and third in that order. This produced the port positions with the lowest volume of overlap between the three instruments followed by the lowest volume of overlap between instruments 1 and 2. The five port positions with the lowest values using the above sort order are shown along with the values for the base port configuration with ports at position E in Table 20, Table 22, and Table 24. The percent difference between the values for the base port configuration and the first port combination, highlighted in yellow, was also calculated for comparison. The percent difference in total volume for each set of ports was compared between patient 1, 8cm separation between ports, and patient 2, 8 and 10 cm separation between ports. The results are shown in Table 25. The results of the corresponding analysis for the port placement pattern for robot-assisted laparoscopic surgery are shown in Table 26 to Table 32.

Port Placement Based on Conventional Laparoscopic Surgery

Table 19. Summary of Percent of Total Volume of Analysis Common Between Instruments (Patient 1, 8cm between ports, Port Placement for Conventional Laparoscopic Surgery)

	% Total Volume Occupied By Common Volume Between Sets of Instruments 1, 2, & 3			
	Instruments 1 and 2	**Instrument 1 and 3**	**Instrument 2 and 3**	**Instrument 1, 2, and 3**
Minimum	0.18	0.14	0.09	0.09
1st Quartile	0.22	0.20	0.14	0.12
Median	0.25	0.24	0.16	0.15
Mean	0.26	0.25	0.17	0.15
3rd Quartile	0.30	0.30	0.19	0.17
Maximum	0.41	0.43	0.25	0.23

Table 20. Percent of Total Volume of Analysis of Base Port Configuration, the Five Lowest Volume Port Positions, and the Percent Difference between the Base and the Lowest Volume (Patient 1, 8cm between ports, Port Placement for Conventional Laparoscopic Surgery)

% Total Volume Occupied By Common Volume Between Sets of Instruments 1, 2, & 3						
Instruments 1 and 2	**Instrument 1 and 3**	**Instrument 2 and 3**	**Instrument 1, 2, and 3**	**Port Positions**		
Base Port Position				Port 1	Port 2	Port 3
0.26	0.25	0.16	0.15	E	E	E
% Diff. between Base Value and Corresponding Values in First Row Below						
27.05	39.65	44.16	44.11			
Lowest Volume						
0.19	0.15	0.09	0.09	C	A	C
0.18	0.15	0.09	0.09	C	B	C
0.18	0.18	0.09	0.09	B	A	C
0.18	0.15	0.10	0.09	C	C	C
0.18	0.18	0.09	0.09	B	B	C

Table 21. Summary of Percent of Total Volume of Analysis Common Between Instruments (Patient 2, 8cm between ports, Port Placement for Conventional Laparoscopic Surgery)

	% Total Volume Occupied By Common Volume Between Sets of Instruments 1, 2, & 3			
	Instruments 1 and 2	**Instrument 1 and 3**	**Instrument 2 and 3**	**Instrument 1, 2, and 3**
Minimum	0.29	0.29	0.19	0.18
1st Quartile	0.34	0.36	0.23	0.22
Median	0.38	0.41	0.26	0.25
Mean	0.39	0.43	0.27	0.26
3rd Quartile	0.43	0.48	0.29	0.28
Maximum	0.55	0.65	0.36	0.35

Table 22. Percent of Total Volume of Analysis of Base Port Configuration, the Five Lowest Volume Port Positions, and the Percent Difference between the Base and the Lowest Volume (Patient 2, 8cm between ports, Port Placement for Conventional Laparoscopic Surgery)

% Total Volume Occupied By Common Volume Between Sets of Instruments 1, 2, & 3						
Instruments 1 and 2	**Instrument 1 and 3**	**Instrument 2 and 3**	**Instrument 1, 2, and 3**	**Port Positions**		
Base Port Position				Port 1	Port 2	Port 3
0.39	0.42	0.26	0.26	E	E	E
% Diff. between Base Value and Corresponding Values in First Row Below						
22.07	29.88	27.91	28.51			
Lowest Volume						
0.30	0.30	0.19	0.18	C	B	C
0.29	0.30	0.19	0.18	C	C	C
0.33	0.34	0.19	0.19	E	B	C
0.29	0.34	0.19	0.19	B	B	C
0.32	0.30	0.19	0.19	C	A	C

Table 23. Summary of Percent of Total Volume of Analysis Common Between Instruments (Patient 2, 10cm between ports, Port Placement for Conventional Laparoscopic Surgery)

	% Total Volume Occupied By Common Volume Between Sets of Instruments 1, 2, & 3			
	Instruments 1 and 2	**Instrument 1 and 3**	**Instrument 2 and 3**	**Instrument 1, 2, and 3**
Minimum	0.27	0.27	0.19	0.18
1st Quartile	0.31	0.34	0.25	0.22
Median	0.34	0.38	0.27	0.24
Mean	0.35	0.39	0.27	0.24
3rd Quartile	0.39	0.43	0.30	0.26
Maximum	0.47	0.54	0.36	0.33

Table 24. Percent of Total Volume of Analysis of Base Port Configuration, the Five Lowest Volume Port Positions, and the Percent Difference between the Base and the Lowest Volume (Patient 2, 10cm between ports, Port Placement for Conventional Laparoscopic Surgery)

% Total Volume Occupied By Common Volume Between Sets of Instruments 1, 2, & 3						
Instruments 1 and 2	**Instrument 1 and 3**	**Instrument 2 and 3**	**Instrument 1, 2, and 3**	**Port Positions**		
Base Port Position				Port 1	Port 2	Port 3
0.35	0.38	0.27	0.25	E	E	E
% Diff. between Base Value and Corresponding Values in First Row Below						
22.82	29.04	28.61	28.30			
Lowest Volume						
0.27	0.27	0.19	0.18	C	A	C
0.27	0.27	0.20	0.18	C	B	C
0.27	0.31	0.19	0.18	B	A	C
0.27	0.27	0.21	0.18	C	C	C
0.27	0.31	0.20	0.18	B	B	C

Table 25. Pct. Difference between Base Port Position Values Patient 1 and Patient 2 (8 and 10cm distance between ports), Robot-Assisted Laparoscopic Surgery

	% Total Volume Occupied By Common Volume Between Sets of Instruments 1, 2, & 3			
	Instruments 1 and 2	**Instrument 1 and 3**	**Instrument 2 and 3**	**Instrument 1, 2, and 3**
Patient 2, 8cm	46.31	67.77	62.04	67.71
Patient 2, 10cm	32.69	52.80	66.49	60.48

Port Placement Based on Robot-Assisted Laparoscopic Surgery

Table 26. Summary of Percent of Total Volume of Analysis Common Between Instruments, Results for Base Port Position, and Port Positions with the Lowest Values (Patient 1, 8cm between ports, Port Placement for Robot-Assisted Laparoscopic Surgery)

	% Total Volume Occupied By Common Volume Between Sets of Instruments 1, 2, & 3			
	Instruments 1 and 2	**Instrument 1 and 3**	**Instrument 2 and 3**	**Instrument 1, 2, and 3**
Minimum	0.11	0.16	0.14	0.10
1st Quartile	0.15	0.25	0.18	0.13
Median	0.18	0.30	0.21	0.15
Mean	0.19	0.32	0.22	0.16
3rd Quartile	0.22	0.38	0.25	0.19
Maximum	0.31	0.60	0.30	0.26

Table 27. Percent of Total Volume of Analysis of Base Port Configuration, the Five Lowest Volume Port Positions, and the Percent Difference between the Base and the Lowest Volume (Patient 1, 8cm between ports, Port Placement for Robot-Assisted Laparoscopic Surgery)

% Total Volume Occupied By Common Volume Between Sets of Instruments 1, 2, & 3						
Instruments 1 and 2	**Instrument 1 and 3**	**Instrument 2 and 3**	**Instrument 1, 2, and 3**	**Port Positions**		
Base Port Position				Port 1	Port 2	Port 3
0.18	0.30	0.21	0.16	E	E	E
% Diff. between Base Value and Corresponding Values in First Row Below						
36.22	45.54	28.97	41.21			
Lowest Volume Overlap						
0.12	0.16	0.15	0.10	C	B	A
0.11	0.16	0.17	0.10	C	C	A
0.12	0.18	0.15	0.10	C	B	B
0.11	0.18	0.16	0.10	C	C	B
0.13	0.16	0.14	0.10	C	A	A

Table 28. Summary of Percent of Total Volume of Analysis Common Between Instruments, Results for Base Port Position, and Port Positions with the Lowest Values (Patient 2, 8cm between ports, Port Placement for Robot-Assisted Laparoscopic Surgery)

	% Total Volume Occupied By Common Volume Between Sets of Instruments 1, 2, & 3			
	Instruments 1 and 2	**Instrument 1 and 3**	**Instrument 2 and 3**	**Instrument 1, 2, and 3**
Minimum	0.22	0.31	0.24	0.19
1st Quartile	0.26	0.43	0.29	0.24
Median	0.29	0.50	0.32	0.26
Mean	0.30	0.51	0.33	0.27
3rd Quartile	0.34	0.58	0.36	0.30
Maximum	0.45	0.84	0.42	0.39

Table 29. Percent of Total Volume of Analysis of Base Port Configuration, the Five Lowest Volume Port Positions, and the Percent Difference between the Base and the Lowest Volume (Patient 2, 8cm between ports, Port Placement for Robot-Assisted Laparoscopic Surgery)

% Total Volume Occupied By Common Volume Between Sets of Instruments 1, 2, & 3				**Port Positions**		
Instruments 1 and 2	**Instrument 1 and 3**	**Instrument 2 and 3**	**Instrument 1, 2, and 3**	Port 1	Port 2	Port 3
Base Port Position						
0.30	0.51	0.32	0.27	E	E	E
% Diff. between Base Value and Corresponding Values in First Row Below						
26.38	37.91	16.98	29.53			
Lowest Volume Overlap						
0.22	0.31	0.27	0.19	C	C	A
0.23	0.31	0.25	0.20	C	B	A
0.22	0.34	0.26	0.20	C	C	B
0.22	0.36	0.27	0.20	B	C	A
0.22	0.36	0.25	0.20	B	B	A

Table 30. Summary of Percent of Total Volume of Analysis Common Between Instruments, Results for Base Port Position, and Port Positions with the Lowest Values (Patient 2, 10cm between ports, Port Placement for Robot-Assisted Laparoscopic Surgery)

	% Total Volume Occupied By Common Volume Between Sets of Instruments 1, 2, & 3			
	Instruments 1 and 2	**Instrument 1 and 3**	**Instrument 2 and 3**	**Instrument 1, 2, and 3**
Minimum	0.19	0.26	0.23	0.16
1st Quartile	0.22	0.36	0.27	0.20
Median	0.25	0.43	0.31	0.23
Mean	0.25	0.44	0.31	0.23
3rd Quartile	0.29	0.49	0.35	0.26
Maximum	0.35	0.72	0.40	0.32

Table 31. Percent of Total Volume of Analysis of Base Port Configuration, the Five Lowest Volume Port Positions, and the Percent Difference between the Base and the Lowest Volume (Patient 2, 10cm between ports, Port Placement for Robot-Assisted Laparoscopic Surgery)

% Total Volume Occupied By Common Volume Between Sets of Instruments 1, 2, & 3						
Instruments 1 and 2	**Instrument 1 and 3**	**Instrument 2 and 3**	**Instrument 1, 2, and 3**	**Port Positions**		
Base Port Position				Port 1	Port 2	Port 3
0.25	0.44	0.31	0.23	E	E	E
% Diff. between Base Value and Corresponding Values in First Row Below						
24.56	39.46	21.50	29.43			
Lowest Volume Overlap						
0.19	0.26	0.24	0.16	C	A	A
0.19	0.26	0.26	0.16	C	B	A
0.19	0.30	0.24	0.17	B	A	A
0.19	0.29	0.25	0.17	C	B	B
0.19	0.28	0.27	0.17	C	B	D

Table 32. Pct. Difference between Base Port Position Values Patient 1 and Patient 2 (8 and 10cm distance between ports), Robot-Assisted Laparoscopic Surgery

	% Total. Vol. Occupied By Common Vol. Between Sets of Instruments 1, 2, & 3			
	Instruments 1 and 2	**Instrument 1 and 3**	**Instrument 2 and 3**	**Instrument 1, 2, and 3**
Patient 2, 8cm	63.62	67.07	50.29	67.37
Patient 2, 10cm	36.28	43.85	43.95	42.22

6.6.4 Interference with Unequal Instrument Priority

For each instrument pair, the volume common between them was calculated as a percentage of the total volume of what was designated as the primary instrument. Instrument 1 and 2 are usually the primary instruments but the calculations were also performed with instrument 3 as the primary and

secondary instruments. For each set of port placement combinations for both conventional and robot-assisted laparoscopic surgery, a summary of the statistics of the results was calculated and shown in Table 33, Table 35, and Table 37. The values for the base port configuration and the five port positions with the lowest common volume between the primary and secondary instruments for both instruments 1 and 2 are listed in Table 34, Table 36, and Table 38. The results of the corresponding analysis for the port placement pattern for robot-assisted laparoscopic surgery are shown in Table 39 - Table 44.

Port Placement Based on Conventional Laparoscopic Surgery

Table 33. Summary of Percent of Work Volume of Primary Instrument In Common with A Secondary Instrument (Patient 1, 8cm between ports, Port Placement for Conventional Laparoscopic Surgery)

	% of Total Volume of One Instrument Overlapped by A Second Instrument						
	1 by 2	**2 by 1**	**1 by 3**	**3 by 1**	**2 by 3**	**3 by 2**	**All by All**
Minimum	19.76	19.76	15.75	22.73	10.67	18.79	5.33
1st Quartile	24.57	24.57	21.38	32.05	15.14	22.60	7.59
Median	28.17	28.17	25.71	36.91	17.80	25.32	8.82
Mean	28.18	28.18	26.97	38.08	17.71	25.03	8.78
3rd Quartile	31.94	31.94	31.11	43.38	20.66	27.95	9.90
Maximum	37.89	37.89	54.02	60.14	24.31	29.98	13.11

Table 34. Results for Base Port Position, and Port Positions with the Lowest Common Volumes between the Primary and Secondary Instrument (Patient 2, 8cm between ports, Port Placement for Conventional Laparoscopic Surgery)

% of Total Volume of One Instrument Overlapped by A Second Instrument									
1 by 2	**2 by 1**	**1 by 3**	**3 by 1**	**2 by 3**	**3 by 2**	**All by All**	**Port Positions**		
Base Port Position							Port 1	Port 2	Port 3
28.52	28.52	27.08	38.67	17.65	25.21	9.26	E	E	E
Lowest Volume Overlap of Instrument 1 by Instrument 2									
21.45	28.17	20.35	32.92	18.34	22.60	7.51	D	B	A
23.22	27.13	19.14	29.35	18.36	24.10	7.59	E	C	A
23.22	27.13	20.15	38.42	12.68	20.69	6.36	E	C	C
23.22	27.13	20.46	34.70	15.51	22.50	7.19	E	C	B
23.94	22.48	20.81	25.65	18.36	24.10	7.58	B	C	A
Lowest Volume Overlap of Instrument 2 by Instrument 1									
28.17	21.45	24.25	37.16	11.82	23.78	7.13	B	F	C
27.11	21.99	26.93	43.95	11.82	23.78	7.31	A	F	C
23.94	22.48	24.25	37.16	12.68	20.69	6.91	B	C	C
25.23	22.53	21.38	31.17	12.68	20.69	6.68	C	C	C
23.02	23.02	26.93	43.95	12.68	20.69	7.05	A	C	C

Table 35. Summary of Percent of Work Volume of Primary Instrument In Common with A Secondary Instrument (Patient 1, 8cm between ports, Port Placement for Conventional Laparoscopic Surgery)

	% of Total Volume of One Instrument Overlapped by A Second Instrument						
	1 by 2	**2 by 1**	**1 by 3**	**3 by 1**	**2 by 3**	**3 by 2**	**All by All**
Minimum	24.01	24.01	22.98	33.06	15.55	23.87	8.55
1st Quartile	29.13	29.13	30.58	41.77	20.26	27.18	10.75
Median	32.47	32.47	35.66	45.83	22.73	29.55	11.72
Mean	32.56	32.56	36.13	46.84	22.58	29.43	11.80
3rd Quartile	35.63	35.63	40.89	51.45	24.92	31.66	12.74
Maximum	42.15	42.15	62.10	67.41	28.87	34.38	16.18

Table 36. Results for Base Port Position, and Port Positions with the Lowest Common Volumes between the Primary and Secondary Instrument (Patient 2, 8cm between ports, Port Placement for Conventional Laparoscopic Surgery)

% of Total Volume of One Instrument Overlapped by A Second Instrument							**Port Positions**		
1 by 2	**2 by 1**	**1 by 3**	**3 by 1**	**2 by 3**	**3 by 2**	**All by All**	Port 1	Port 2	Port 3
Base Port Position									
32.75	32.75	35.66	46.94	22.45	29.55	12.12	E	E	E
Lowest Volume Overlap of Instrument 1 by Instrument 2									
26.15	31.18	29.62	51.82	18.66	27.38	9.51	D	C	C
26.15	31.18	30.58	48.42	20.55	27.29	10.12	D	C	B
27.82	31.55	28.54	47.49	18.66	27.38	9.68	E	C	C
27.82	31.55	29.01	43.69	20.55	27.29	10.18	E	C	B
27.82	31.55	29.42	39.80	22.75	27.14	10.50	E	C	A
Lowest Volume Overlap of Instrument 2 by Instrument 1									
34.38	24.19	36.30	53.26	15.55	32.44	10.32	A	I	C
34.38	24.19	36.36	48.28	17.11	32.29	10.73	A	I	B
35.03	25.76	36.30	53.26	16.27	32.46	10.72	A	H	C
32.83	26.03	34.14	47.35	17.18	30.06	10.53	B	F	C
32.83	26.03	33.64	42.22	18.90	29.93	10.75	B	F	B

Table 37. Summary of Percent of Work Volume of Primary Instrument In Common with A Secondary Instrument (Patient 2, 10cm between ports, Port Placement for Conventional Laparoscopic Surgery)

	% of Total Volume of One Instrument Overlapped by A Second Instrument						
	1 by 2	**2 by 1**	**1 by 3**	**3 by 1**	**2 by 3**	**3 by 2**	**All by All**
Minimum	21.89	21.89	22.22	28.27	16.44	22.83	8.50
1st Quartile	26.73	26.73	28.45	36.11	20.83	26.70	10.12
Median	29.68	29.68	32.37	40.08	22.97	28.73	10.65
Mean	29.45	29.45	32.56	40.47	22.97	28.52	10.71
3rd Quartile	32.09	32.09	35.77	44.53	25.12	30.54	11.30
Maximum	36.43	36.43	50.38	55.71	28.89	32.37	13.31

Table 38. Results for Base Port Position, and Port Positions with the Lowest Common Volumes between the Primary and Secondary Instrument (Patient 2, 10cm between ports, Port Placement for Conventional Laparoscopic Surgery)

% of Total Volume of One Instrument Overlapped by A Second Instrument									
1 by 2	**2 by 1**	**1 by 3**	**3 by 1**	**2 by 3**	**3 by 2**	**All by All**	**Port Positions**		
Base Port Position							Port 1	Port 2	Port 3
29.63	29.63	32.40	40.56	23.01	28.80	11.03	E	E	E
Lowest Volume Overlap of Instrument 1 by Instrument 2									
23.71	31.82	27.60	45.86	20.74	25.68	9.39	D	A	C
24.15	30.60	27.60	45.86	20.43	26.78	9.48	D	B	C
25.06	29.63	27.60	45.86	20.02	28.13	9.58	D	C	C
25.42	32.09	26.68	41.70	20.74	25.68	9.55	E	A	C
25.42	32.09	27.71	38.40	23.32	25.60	9.99	E	A	B
Lowest Volume Overlap of Instrument 2 by Instrument 1									
31.82	23.71	29.03	35.94	18.27	30.35	9.63	C	F	C
31.82	23.71	29.43	32.31	20.54	30.25	9.81	C	F	B
30.60	24.15	31.00	40.65	18.27	30.35	9.94	B	F	C
28.62	25.22	29.03	35.94	20.02	28.13	9.75	C	C	C
32.09	25.42	29.03	35.94	18.75	29.31	9.89	C	E	C

The results for conventional laparoscopic surgery show that moving instrument 2 closer to the target in the z-axis direction while moving it away from the patient centerline in the x-axis direction would help minimize the risk of collisions between instrument 1 and instrument 2. The corresponding position for instrument 1 is at position D, away from the patient centerline. Instrument port 3 will also move closer to the target in both the x and z-axis. If the additional condition that the overlap of instrument 1 by instrument 3 be minimized, the port for instrument 1 can stay at the original location, position E, while the port for instrument 3 can move lower from the original position or lower and away from the patient centerline.

If a higher priority was given to minimizing the overlap of instrument 2 by instrument 1 and instrument 3 separately, instrument port 2 should be moved to position F or I. These positions are both away from the patient centerline. The corresponding location for instrument port 1 would be closer to the target at positions A, B, or C. Instrument port 3 in all instances was calculated to be best at position C.

Port Placement Based on Robot-Assisted Laparoscopic Surgery

Table 39. Summary of Percent of Work Volume of Primary Instrument In Common with A Secondary Instrument (Patient 1, 8cm between ports, Port Placement for Robot-Assisted Laparoscopic Surgery)

	% of Total Volume of One Instrument Overlapped by A Second Instrument						
	1 by 2	**2 by 1**	**1 by 3**	**3 by 1**	**2 by 3**	**3 by 2**	**All by All**
Minimum	16.84	16.84	29.57	14.00	24.11	11.75	5.51
1st Quartile	20.33	20.33	37.08	21.47	26.35	15.37	7.68
Median	24.61	24.61	41.19	27.00	28.86	18.80	8.77
Mean	24.77	24.77	42.24	27.82	28.71	18.73	8.94
3rd Quartile	28.57	28.57	46.09	32.91	30.80	21.90	10.06
Maximum	35.40	35.40	62.31	51.44	33.72	25.89	14.03

Table 40. Results for Base Port Position, and Port Positions with the Lowest Common Volumes between the Primary and Secondary Instrument (Patient 1, 8cm between ports, Port Placement for Robot-Assisted Laparoscopic Surgery)

% of Total Volume of One Instrument Overlapped by A Second Instrument							Port Positions		
1 by 2	**2 by 1**	**1 by 3**	**3 by 1**	**2 by 3**	**3 by 2**	**All by All**			
Base Port Position							Port 1	Port 2	Port 3
25.11	25.11	41.19	25.75	29.23	18.27	9.14	E	E	E
Lowest Volume Overlap of Instrument 1 by Instrument 2									
17.94	19.16	36.38	23.00	25.98	15.37	6.90	A	B	A
18.52	18.52	36.38	23.00	26.65	16.85	7.10	A	C	A
19.16	17.94	32.52	19.25	26.65	16.85	6.65	B	C	A
19.16	17.94	35.71	21.47	26.17	16.81	6.90	B	C	B
19.16	17.94	36.03	17.76	28.90	15.22	6.20	B	C	D
Lowest Volume Overlap of Instrument 2 by Instrument 1									
19.16	17.94	35.71	21.47	26.17	16.81	6.90	B	C	B
18.52	18.52	40.82	26.22	26.17	16.81	7.41	A	C	B
17.94	19.16	40.82	26.22	25.57	15.37	7.22	A	B	B
17.94	19.16	36.38	23.00	25.98	15.37	6.90	A	B	A
19.23	19.23	35.71	21.47	25.57	15.37	6.89	B	B	B

Table 41. Summary of Percent of Work Volume of Primary Instrument In Common with A Secondary Instrument (Patient 2, 8cm between ports, Port Placement for Robot-Assisted Laparoscopic Surgery)

	% of Total Volume of One Instrument Overlapped by A Second Instrument						
	1 by 2	**2 by 1**	**1 by 3**	**3 by 1**	**2 by 3**	**3 by 2**	**All by All**
Minimum	22.42	22.42	39.48	19.18	27.78	15.08	8.188
1st Quartile	27.34	27.34	46.82	28.55	31.25	19.35	10.641
Median	31.03	31.03	50.87	33.73	33.13	21.91	11.727
Mean	30.93	30.93	51.86	35.01	33.09	22.11	11.863
3rd Quartile	34.14	34.14	55.93	40.53	34.75	25.10	12.941
Maximum	41.25	41.25	69.07	58.69	37.68	29.59	16.869

Table 42. Results for Base Port Position, and Port Positions with the Lowest Common Volumes between the Primary and Secondary Instrument (Patient 2, 8cm between ports, Port Placement for Robot-Assisted Laparoscopic Surgery)

% of Total Volume of One Instrument Overlapped by A Second Instrument							**Port Positions**		
1 by 2	**2 by 1**	**1 by 3**	**3 by 1**	**2 by 3**	**3 by 2**	**All by All**			
Base Port Position							Port 1	Port 2	Port 3
31.08	31.08	52.05	34.32	33.23	21.91	12.21	E	E	E
Lowest Volume Overlap of Instrument 1 by Instrument 2									
24.19	32.91	46.80	34.40	33.12	17.89	10.38	H	C	D
24.35	35.11	42.54	36.23	31.45	18.57	10.61	H	B	A
24.35	35.11	46.80	34.40	33.45	17.04	10.37	H	B	D
25.13	37.92	46.80	34.40	34.00	16.55	10.52	H	A	D
25.90	29.30	44.11	31.23	31.21	19.53	10.36	E	C	A
Lowest Volume Overlap of Instrument 2 by Instrument 1									
30.49	24.13	44.37	26.20	30.72	22.92	10.04	B	F	A
28.88	24.23	49.19	30.79	30.72	22.92	10.54	A	F	A
26.76	25.25	48.43	31.13	30.22	20.59	10.33	B	C	B
26.76	25.25	44.37	26.20	31.21	19.53	9.51	B	C	A
25.26	25.26	49.19	30.79	31.21	19.53	9.89	A	C	A

Table 43. Summary of Percent of Work Volume of Primary Instrument In Common with A Secondary Instrument (Patient 2, 10cm between ports, Port Placement for Robot-Assisted Laparoscopic Surgery)

	% of Total Volume of One Instrument Overlapped by A Second Instrument						
	1 by 2	**2 by 1**	**1 by 3**	**3 by 1**	**2 by 3**	**3 by 2**	**All by All**
Minimum	19.78	19.78	35.81	14.46	28.93	12.93	6.414
1st Quartile	23.96	23.96	41.15	21.84	31.87	16.72	8.392
Median	27.25	27.25	45.93	25.86	33.22	18.91	9.294
Mean	26.95	26.95	46.10	26.91	33.08	19.07	9.387
3rd Quartile	29.68	29.68	50.48	31.34	34.53	21.42	10.29
Maximum	34.01	34.01	61.02	46.59	35.91	26.08	13.215

Table 44. Results for Base Port Position, and Port Positions with the Lowest Common Volumes between the Primary and Secondary Instrument (Patient 2, 10cm between ports, Port Placement for Robot-Assisted Laparoscopic Surgery)

% of Total Volume of One Instrument Overlapped by A Second Instrument							**Port Positions**		
1 by 2	**2 by 1**	**1 by 3**	**3 by 1**	**2 by 3**	**3 by 2**	**All by All**	Port 1	Port 2	Port 3
Base Port Position							E	E	E
27.06	27.06	46.85	26.49	33.27	18.81	9.61			
Lowest Volume Overlap of Instrument 1 by Instrument 2							A	A	A
22.11	25.29	40.19	21.84	32.97	15.67	7.79	A	B	A
22.61	24.32	40.19	21.84	33.09	16.72	7.89	A	C	A
23.63	23.63	40.19	21.84	32.94	17.90	8.07	E	C	D
23.69	26.14	40.60	21.34	34.40	16.38	8.01	B	A	A
23.70	25.19	37.76	19.08	32.97	15.67	7.61			
Lowest Volume Overlap of Instrument 2 by Instrument 1							C	I	A
31.62	19.78	35.81	17.02	30.87	23.44	7.92	B	I	A
30.47	20.27	37.76	19.08	30.87	23.44	8.29	C	H	A
32.26	21.37	35.81	17.02	31.44	22.55	8.11	C	B	B
25.19	23.70	39.97	20.58	31.79	17.39	8.09	B	B	B
23.75	23.75	43.58	23.85	31.79	17.39	8.37			

The results for robot-assisted laparoscopic surgery show that moving instrument 2 closer to the target in the z-axis direction while moving it away from the patient centerline in the x-axis direction, position C, would help minimize the risk of collisions between instrument 1 and instrument 2. The corresponding position for instrument 1 can be at A, B, or E. Instrument port 3 moves away from the centerline to the edge of the patient torso at position A.

If a higher priority was given to minimizing the overlap of instrument 2 by instrument 1 and instrument 3 separately, instrument port 2 should be moved to position C, F or I, away from its original position. Instrument port 1 should be moved down or down and to the right at positions B or C and instrument port 3

should be moved down or down and to the left at positions B or A.

6.6.5 Interference with Unequal Instrument Priority (Constrained)

A secondary analysis of the results was performed based on the results of the analysis of instrument work volumes when one instrument was assigned a higher priority. In this instance, port combinations for instruments 1 and 2 were constrained to only allow offsets in the z-axis of 0 or +2cm such that port positions A, B, and C were removed from consideration. In this iteration, the values of volume overlap were selected from values that were less than the median because using the more stringent criterion of values in the first quartile did not produce any results. The best port position was determined as the one with the lowest volume overlap between instruments 1 and 2, and instruments 1 and 3, columns 1, 2, and 3 in Table 45 for conventional laparoscopic surgery and Table 46 for robot-assisted laparoscopic surgery. The values in each column for these ports were then compared with the values corresponding to the base port position to determine the percent difference and also included in Table 45 and Table 46. For each of these six select ports (highlighted) and base ports, the intracorporeal tool lengths and intracorporeal:extracorporeal ratios, and manipulation angles were also calculated and compared. The results are shown in Table 47 and Table 48.

Table 45. Results of Selection of Port Positions with Lowest Volume Overlap of One Instrument Work Volume by Another Instrument or Instruments with Additional Constraints (Conventional Laparoscopic Surgery)

% of Total Volume of One Instrument Overlapped by A Second Instrument							**Port Positions**		
1 by 2	**2 by 1**	**1 by 3**	**3 by 1**	**2 by 3**	**3 by 2**	**All by All**	Port 1	Port 2	Port 3
Patient 1, 8cm between ports									
26.60	28.07	22.21	39.72	14.33	24.30	7.59	D	E	B
26.60	28.07	21.58	43.40	12.05	22.97	6.69	D	E	C
26.67	26.67	22.21	39.72	14.21	25.42	7.59	D	F	B
26.67	26.67	21.58	43.40	11.82	23.78	6.68	D	F	C
28.07	26.60	20.46	34.70	14.21	25.42	7.49	E	F	B
28.07	26.60	20.15	38.42	11.82	23.78	6.72	E	F	C
Base Port Position, Patient 1, 8cm between ports									
28.5	28.5	27.1	38.7	17.7	25.2	9.26	E	E	E
% Difference between Base and New Port									
6.47	6.47	20.3	-12.2	33	5.67	27.9			
Patient 2, 8cm between ports									
30.45	32.02	30.58	48.42	19.55	29.44	10.56	D	E	B
30.45	32.02	29.62	51.82	17.94	29.85	9.99	D	E	C
30.19	30.19	30.58	48.42	18.90	29.93	10.35	D	F	B
30.19	30.19	29.62	51.82	17.18	30.06	9.73	D	F	C
32.02	30.45	29.42	39.80	20.92	29.75	10.70	E	F	A
32.02	30.45	29.01	43.69	18.90	29.93	10.36	E	F	B
32.02	30.45	28.54	47.49	17.18	30.06	9.89	E	F	C
Base Port Position, Patient 2, 8cm between ports									
32.8	32.8	35.7	46.9	22.5	29.6	12.1	E	E	E
% Difference between Base and New Port									
7.84	7.84	16.9	-10.4	23.5	-1.73	19.7			
Patient 2, 10cm between ports									
28.53	28.53	27.60	45.86	18.27	30.35	9.64	D	F	C
29.63	29.63	26.68	41.70	18.75	29.31	9.74	E	E	C
Base Port Position, Patient 2, 10cm between ports									
29.6	29.6	32.4	40.6	23	28.8	11	E	E	E
% Difference between Base and New Port									
3.7	3.7	14.8	-13.1	20.6	-5.35	12.5			

Table 46. Results of Selection of Port Positions with Lowest Volume Overlap of One Instrument Work Volume by Another Instrument or Instruments with Additional Constraints (Robot-Assisted Laparoscopic Surgery)

% of Total Volume of One Instrument Overlapped by A Second Instrument							**Port Positions**		
1 by 2	**2 by 1**	**1 by 3**	**3 by 1**	**2 by 3**	**3 by 2**	**All by All**			
Patient 1, 8cm between ports							Port 1	Port 1	Port 1
23.3	23.3	37.1	29.1	26.7	21	9.34	D	F	A
Base Port Position, Patient 1, 8cm between ports									
25.1	25.1	41.2	25.8	29.2	18.3	9.14	E	E	E
% Difference between Base and New Port									
7.05	7.05	9.72	4.48	-8.66	5.41	8.83			
Patient 2, 8cm between ports									
28.7	30.2	48.5	36.2	31.3	22.1	11.8	D	E	A
28.4	28.4	48.5	36.2	30.7	22.9	11.6	D	F	A
30.2	28.7	44.1	31.2	30.7	22.9	11.3	E	F	A
30.2	28.7	47.9	36.9	29.7	24.2	12.2	E	F	B
30.2	28.7	47.7	29.1	32.9	21.2	10.9	E	F	D
30.2	28.7	50.8	26.7	35	19.4	10.2	E	F	G
28.7	30.2	48.5	36.2	31.3	22.1	11.8	D	E	A
Base Port Position, Patient 2, 8cm between ports									
31.1	31.1	52.1	34.3	33.2	21.9	12.2	E	E	E
% Difference between Base and New Port									
8.74	8.74	6.79	-5.45	7.54	-4.6	4.66			
Patient 2, 10cm between ports									
26.2	26.2	40.2	25.8	32.1	20.6	9.45	D	F	A
26.2	26.2	42.9	24.1	33.7	18.9	8.98	D	F	D
26.2	26.2	45.4	22.2	35.3	17.3	8.39	D	F	G
27.1	27.1	38.1	22.8	32.5	19.5	9.14	E	E	A
27.1	27.1	43.7	28.4	31.5	20.5	10.1	E	E	B
27.1	27.1	40.6	21.3	34.1	17.9	8.7	E	E	D
27.1	27.1	42.9	19.7	35.6	16.3	8.15	E	E	G
Base Port Position, Patient 2, 10cm between ports									
27.1	27.1	46.8	26.5	33.3	18.8	9.61	E	E	E
% Difference between Base and New Port									
3.35	3.35	14.11	2.71	3.51	-9.30	1.63			

Table 47. Comparison of Port Placement Intracorporeal Tool Length, Intracorporeal:Extracorporeal Ratio, and Manipulation Angle between New and Base Port Positions for Conventional Laparoscopic Surgery)

Port 1	**I.L. (cm)**	**I/E Ratio***	**Port 2**	**I.L. (cm)**	**I/E Ratio***	**Manip. Angle 1 & 2**	**Port 3**	**I.L. (cm)**	**I/E Ratio***	**Manip. Angle 1 & 3**
Patient 1, 8cm between ports										
D	20.46	1.63	F	20.46	1.63	56.78	C	15.79	0.92	20.54
E	20.06	1.55	E	20.06	1.55	45.32	E	17.59	1.14	27.16
Percent Difference between Base and New Port Position										
		5.22			5.22	25.30		10.22	19.59	24.38
Patient 2, 8cm between ports										
D	22.32	2.09	F	22.32	2.09	51.68	C	18.18	1.23	19.13
E	21.91	1.98	E	21.91	1.98	41.30	E	19.82	1.50	22.46
Percent Difference between Base and New Port Position										
		5.67			5.67	25.15		8.28	18.43	14.86
Patient 2, 10cm between ports										
D	22.42	2.12	F	22.42	2.12	62.66	C	18.62	1.30	25.43
E	21.93	1.98	E	21.93	1.98	52.26	E	20.21	1.58	29.91
Percent Difference between Base and New Port Position										
		6.97			6.97	19.90		7.83	17.98	14.99

*Standard laparoscopic tool length defined as 33cm for this calculation.

Table 48. Comparison of Port Placement Intracorporeal Tool Length, Intracorporeal:Extracorporeal Ratio, and Manipulation Angle between New and Base Port Positions for Robot-Assisted Laparoscopic Surgery)

Port 1	**I.L. (cm)**	**I/E Ratio***	**Port 2**	**I.L. (cm)**	**I/E Ratio***	**Manip. Angle 1 & 2**	**Port 3**	**I.L. (cm)**	**I/E Ratio***	**Manip. Angle 1 & 3**
Patient 1, 8cm between ports										
D	18.81	1.33	F	18.81	1.33	56.67	A	23.48	2.47	28.86
E	18.42	1.26	E	18.42	1.26	44.20	E	21.88	1.97	29.86
Percent Difference between Base and New Port Position										
		4.97			4.97	28.23		7.36	25.52	3.36
Patient 2, 8cm between ports										
D	20.80	1.70	F	20.80	1.70	50.84	A	25.77	3.56	21.47
E	20.41	1.62	E	20.41	1.62	39.69	E	23.74	2.57	21.25
Percent Difference between Base and New Port Position										
		5.20			5.20	28.08		8.52	38.90	1.07
Patient 2, 10cm between ports										
D	20.57	1.65	F	20.57	1.65	62.44	A	24.18	2.74	38.37
E	20.08	1.55	E	20.08	1.55	51.10	E	24.70	2.98	29.39
Percent Difference between Base and New Port Position										
		6.41			6.41	22.21		2.11	7.90	30.56

*Standard laparoscopic tool length defined as 33cm for this calculation. Endo-Wrist® instruments used with the da Vinci Surgical System have a tool length of about 50cm.

For the conventional laparoscopic surgery port placement pattern, shifting instrument ports 1 and 2 from the base position away from the patient centerline to positions D and F, respectively, reduced the portion of each instrument's work volume where collisions could occur by 3 – 9% (Table 45). For instruments 1 and 2, this shift also resulted in an increase of intracorporeal:extracorporeal tool length ratio by 5 to 7% and an increase in manipulation angle by 20 – 25%, closer to the recommended sixty-degree angle (Ferzli & Fingerhut, 2004).

The corresponding position of instrument port 3 was at position C, a shift in both the x and z-axis of 2 cm. This had the undesirable effect of a reduction in intracorporeal:extracorporeal tool length ratio by 18 to 20%. For patient 1, the ratio was 0.9, less than the minimum of 1.0 recommended for optimal ergonomics (Ferzli & Fingerhut, 2004). Likewise, manipulation angle was reduced by 15 – 24%.

The results of the analysis for the robot-assisted laparoscopic surgery port placement arrangement showed similar results as for conventional laparoscopic surgery. Moving both instrument ports 1 and 2 away from the patient centerline to positions D and F, respectively, reduced the instrument work volume overlap where collisions could occur by 7 – 15%. This shift also resulted in an increase of intracorporeal:extracorporeal tool length ratio by 5 – 6% and an increase in manipulation angle by 22 – 28% (Table 48).

For instrument port 3 the calculations recommended that the port be located at position A. At this position, the volume of the overlap of instrument 1

by instrument 3 decreased by 7 – 14%. In this position, intracorporeal tool length also increases by 7 – 9% for the pattern with 8cm separation between ports. For the pattern with 10cm separation between ports, this value decreased by 2%. The intracorporeal:extracorporeal tool length ratio increased 26 – 39% for the first two arrangements with ports separated by 8cm and decreased by 8% for the pattern with 10cm between ports. The manipulation angle decreased by 3% for patient 1 and increased by 1 and 31% for patient 2 with 8 and 10cm separation between ports, respectively (Table 48).

6.6.6 More Extreme Port Positions, Unequal Instrument Priority

The previous results were based on combinations of port positions offset from the original position by 2cm, positive or negative, in the x and z-axis direction. What effect would changing the port position by another 2cm have on the volume overlap of the primary instrument by secondary instruments? The Octave program was run with the new set of combinations shown in Figure 52 for both patient 1 and 2 with 8cm distance between ports and for patient 2 with 10cm distance between ports. For this computation, the position of instrument port 3 was fixed at $\begin{bmatrix} -13.4 \\ 5.0 \\ 10.3 \end{bmatrix}$ for patient 1 and $\begin{bmatrix} -13.4 \\ 10.40 \\ 10.3 \end{bmatrix}$ for patient 2. The location of the endoscope port remained unchanged. For patient 1, the endoscope port was located at $\begin{bmatrix} 0 \\ 11 \\ 18 \end{bmatrix}$. For patient 2, it was located at $\begin{bmatrix} 0 \\ 14 \\ 18 \end{bmatrix}$.

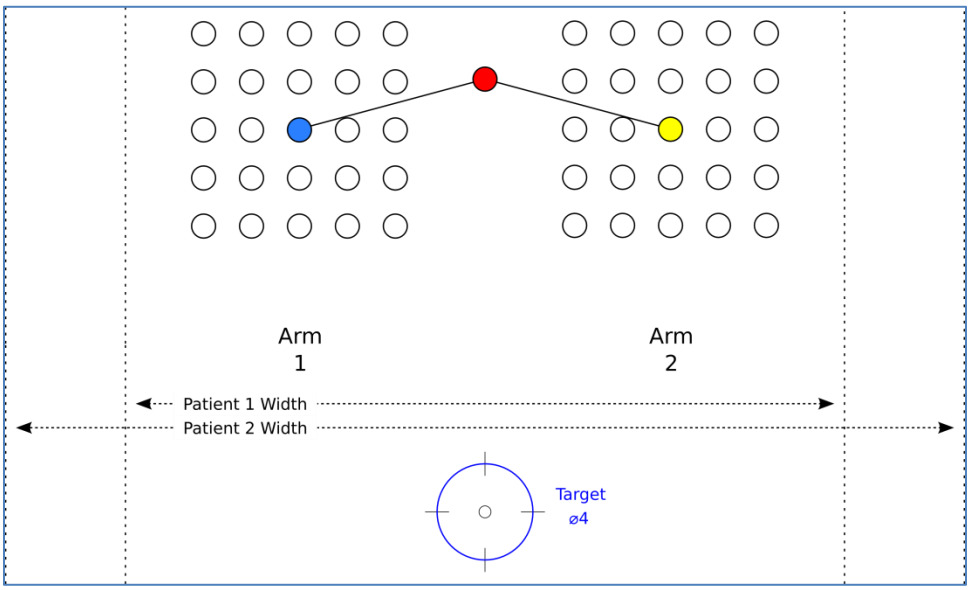

Figure 52. Port Position Locations for with -4, -2, 0, 2, and 4cm offset from the original position for Instrument Port 1 and 2 shown in Blue and Yellow, respectively (Conventional Laparoscopic Surgery)

The results of the work volume calculations were analyzed and shown using scatter plots to illustrate the interaction between changes in X and Z axis positions and the corresponding changes in percent volume overlap of one instrument's work volume by another. The data set was filtered to remove those port combinations that resulted in manipulation angles between instrument 1 and 2 and instrument 1 and 3 below the first quartile. These values were much smaller than the manipulation angle at the base position and may cause difficulties in tool manipulation. The data set was not filtered for an upper limit of manipulation angles. Constraining the position of instrument port 3 served a similar function.

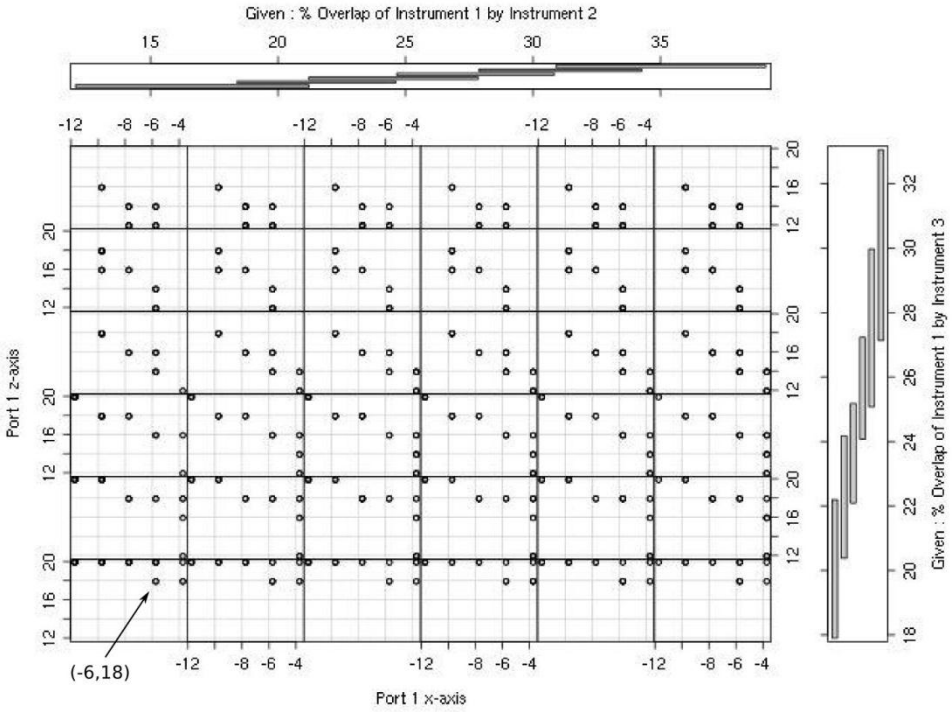

Figure 53. Interaction between x-axis and z-axis position of Instrument 1 and the % overlap of instrument 1 work volume by instruments 2 and 3 (Conventional Laparoscopic Surgery Patient 1, 8cm separation between ports).

In Figure 53, the scatter plot is showing the volume overlap of the work volume of instrument 1 by instruments 2 (top) and 3 (right) separately based on x-axis position (horizontal) and z-axis position (vertical). The lower left section shows what values correspond to the lowest of x and z-axis positions that would result in the lowest volume overlap. In this case, the z-axis position must be at 18cm or 2cm above the base position for the entire range of x-axis positions. To be at the base z-axis position, the x-axis position has to be at the at least at -6cm position or 2cm closer to the patient centerline from the base position.

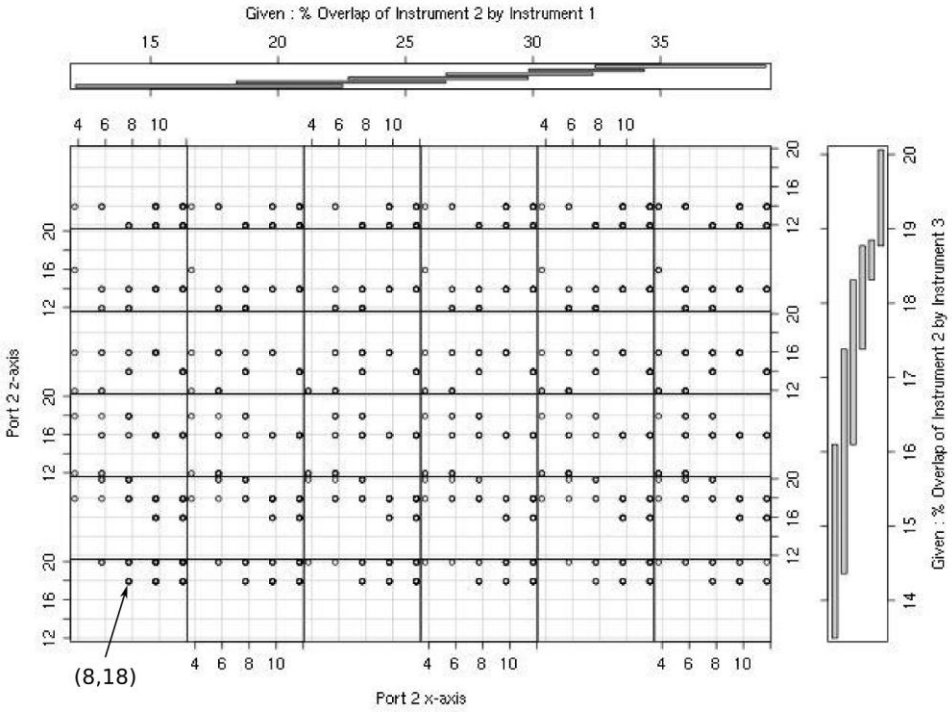

Figure 54. Interaction between x-axis and z-axis position of Instrument 2 and the % overlap of instrument 2 work volume by instruments 1 and 3.

In Figure 54, the scatter plot is showing the volume overlap of the work volume of instrument 2 by instruments 1 (top) and 3 (right) separately based on x-axis position (horizontal) and z-axis position (vertical). The lower left section shows what values correspond to the lowest of x and z-axis positions that would result in the lowest volume overlap. In this case, the z-axis position must be at 18cm or 2cm above the base position. The x-axis position can be at about 6cm or 2cm closer to the patient centerline than the base position. This is symmetrical to the results shown in Figure 53 across the patient centerline.

Finally, in Figure 55, the interaction between the x-axis positions of instruments 1 and 2 and the resulting volume overlap of instrument 1 by

instrument 2 and of instrument 2 by instrument 3 is shown. This scatterplot shows that the lowest distance separation between instrument 1 and 2 is 16cm though the separation that has the lowest values for percent volume overlap for instrument 1 by instrument 2 and instrument 2 by instrument 3 is when port 1 is at -8cm and port 2 is at 10cm, an 18cm separation. The calculations were also performed for patient 2 with both 8 and 10cm distance between ports that showed similar results.

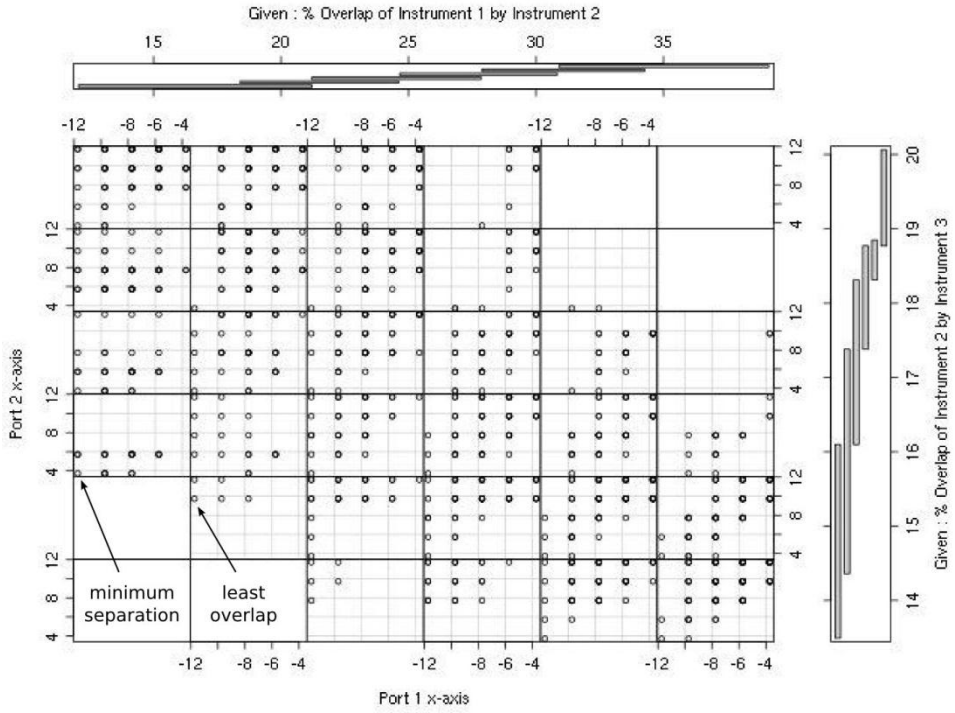

Figure 55. Interaction between x-axis positions of Instrument 1 and 2 and the % overlap of instrument 1 work volume by instrument 2 and of instrument 2 by instrument 3.

6.6.7 Accuracy

The software program also calculated the accuracy of the estimate of the volume for the target sphere and the endoscope and instrument cones. The error

in estimating the volume of the sphere was 1.48% in all cases. The error in estimating the volume of the instrument cones varied from a minimum of 1.07% to a maximum of 1.22%.

7. Discussion

7.1. Field Study

The early cases of surgery with the robot at the hospital in France showed that the surgical team experienced a lot of difficulty even with experts brought in to assist. As summarized by the surgeon, the main problem was that the experts and the procedure cards provided by Intuitive Surgical did not account for variations in patient characteristics (J.M. Classe, personal communication, 2011). This supported the early goal of helping surgeons with the complex task of accounting for all the variables to consider in port placement, especially with the changes resulting from insufflation.

However, the effects of insufflation, while significant with regards to the sagittal thickness of the patient torso, does not significantly affect the width of the torso. Thus the positions of the markings of port placements made before insufflation are not significantly different in the horizontal plane. In addition, it is not always possible for ports to penetrate the skin exactly where they were intended. Experienced surgeons are able to adjust the pose plan during the docking process accordingly (P. Hendessi, personal communication, 2012). A hypothesis was proposed that the problem couldn't be solved by addressing the cognitive task of considering all the patient variables but by focusing on the

docking process, when the robot arms have to be connected to the ports that have been placed.

7.2. Patient Model

The measurements collected from patients at Cambridge Health Alliance were useful in showing that the simplified method, after some initial adjustments, could be used to collect patient measurements on the operating table. The dimensions were used to create the 3D model of the abdominal area. However they were undergoing laparoscopic procedures not commonly performed with robot assistance. The data collection protocol was designed to have minimal impact on the patient. Measuring the position of organs that were not the target of planned surgical procedure was deemed as exceeding minimal impact.

7.3. Robot Model

The robot model, combined with the torso model, could be used to calculate the optimal port placement. This could be done by solving the inverse kinematics (IK) equations to compute the angle of each of the joints knowing the desired position of the end effectors. The intersection of the links of the instrument arms and the torso model would represent the optimal port placement. However, the author was unsuccessful in using Symoro+ to calculate the IK equations.

7.4. Comparison of Port Locations Based On Instrument Work Volumes

The results showed that if the objective was simply reducing the volume

where possible collisions might occur, all that would be necessary would be to move the ports closer to the target. However, there are other factors that have to be considered, principally the manipulation angle which is an issue for both conventional and robot-assisted laparoscopic surgery. In conventional laparoscopic surgery, studies have shown that the optimal manipulation angle for knot-tying is 60 degrees. Deviation from this value could adversely affect the surgeon's ability to perform the surgery. In robot-assisted laparoscopic surgery, manipulation angle can have an effect on the risk of collisions between instrument arms external of the patient. Another issue that can arise from bringing ports too close is the reduction of the intracorporeal:extracorporeal tool length ratio which in conventional laparoscopic surgery can affect the dexterity of the surgeon to perform the surgical procedure. There was no study found that indicated the effect an intracorporeal:extracorporeal tool length ratio below 1.0 would have in robot-assisted laparoscopic surgery.

By assigning different priorities to each instrument and comparing collision volumes based on the priority of each instrument, a more realistic result was obtained. The results recommended in some cases that ports be moved away from the target region. However, the best results came about by removing positions A, B, and C from consideration for instrument ports 1 and 2, thus constraining the alternative locations allowed in the calculation. For conventional laparoscopic surgery, the best combination of ports was obtained by moving instrument port 1 to position D, moving instrument port 2 to position F, and

moving instrument port 3 to C. For robot-assisted laparoscopic surgery, the analysis showed similar results for instruments 1 and 2. For instrument port 3, the best position was to move it to position A. These results were applicable to both patient 1 and patient 2, with both 8 and 10cm distance between ports.

Analysis of more extreme port placement combinations for conventional laparoscopic surgery showed the interaction between the x-axis and z-axis positions of each port and between each port. The results obtained showed that for patient 1 and 2 with both 8cm and 10cm separation between ports, there is a minimum separation distance between ports 1 and 2, regardless of patient size, of 16 – 18cm. In this configuration, the minimum distance away from the target sphere was also shown to be about 16-18cm to minimize collisions, the values recommended in literature. The results also showed that changes in port position in the z-axis had more effect on volume of possible collision than changes in the x-axis.

7.4.1 Reachability

The port locations analyzed did not have a reachability score less than 1 (100%). However, this analysis was focused on work volumes. There was no distinction made with regards to whether or not the procedure required access to the outside surface or the inside surface of the organ represented by the sphere. In addition, the location of the endoscope port was not analyzed to determine if it provided an optimal view angle. For some procedures the location of the port that

provides an optimal view angle is not necessarily direct but off to the side.

7.4.2 Patient Body Mass Index

This analysis did not show significant difference between a patient with average BMI and a patient classified as obese. However, this analysis was performed with an idealized patient model that did not consider thickness of the abdominal wall, the shift of the umbilicus to a lower position, and co-morbidities associated with above average patient BMI.

7.5. Decision Aid Design

The decision aid was implemented as a software prototype to serve as a proof-of-concept for what could be done to address some of the issues encountered in pre-operative planning. However, it was designed to be fully-realizable with mobile or desktop computers already in some operating rooms. For instance, the patient modeling as implemented in the current design could be adjusted to take in more parameters. It could also use inexpensive digital cameras and computer vision software such as OpenCV to create 3D models of the torso on the operating table.

In the concept design, the port placement phase was intended to be iterative. Surgeons may not be able to place the ports exactly where the calculations recommended they be placed for whatever reason. Using the same cameras and computer vision software to create the 3D model of the torso, the actual port placements could be captured into the system to adjust the robot pose

plan accordingly. In actual practice, experienced surgeons are able to adjust the patient cart pose based on the actual port placement instead of what was originally planned. In that case the decision aid might be used as a verification tool for both the port placement and the pose planning (P. Hendessi, personal communication, 2012).

8. Decision Aid

Following requirements definition, concept generation, and focused research on the areas of patient measurement and robot modeling, a brief literature review was conducted on the subject of procedural instructions to guide how the software tool would be implemented. The structure of the planning aid would be based on the pre-operative planning workflow shown in Figure 38 and repeated in Figure 56 below:

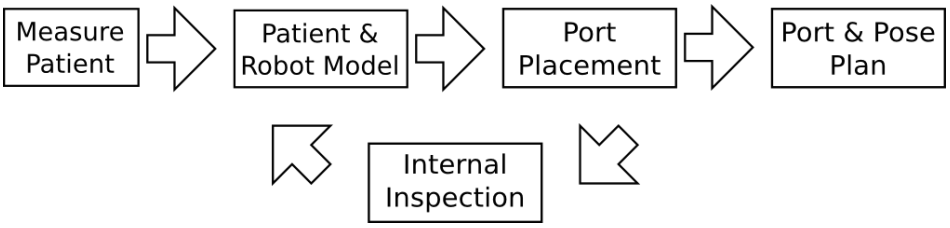

Figure 56. Pre-operative Planning Process

8.1. Procedural Instruction

There have been previous studies that proposed solutions in port placement and robot pose planning but none have addressed how to effectively present the information to a surgical team in an operating room. There are several ways to provide instruction for the surgical team that conveys the recommended port placement and robot position and pose. It can be done in text, graphics,

video, voice, haptics, or some combination. Graphics can be still or animated, and two or three dimensional. One of the oldest published studies in comparing methods to present information is by King (1975). He tested forty-five students randomly assigned to one of three instruction methods: text with animated graphics, text with still graphics, or text only. While he did not find the differences between the groups statistically significant, the group provided text with animated graphics exhibited the highest mean performance. Carney & Levin (2002) found that in the correct context with the correct kind of imagery, from the five functions that Levin defined in an earlier study, images can be effective. One guideline they provide is that the more complex the text, the more pictures can be helpful. Both studies focused on effectively conveying complex concepts to support learning instead of merely understanding a complex instruction. However, the research indicates that providing graphics may be better than text alone.

A study by Taylor and Rapp (2004) describes three different reference frames relevant to providing instruction for docking the robot: the speaker's (the one providing the instruction), the listener's (the one receiving the instruction), and the object's (the about which the instruction is being provided) point of view. The different points of view can lead to incorrect interpretation of the instruction. There are two models for how the brain processes spatial information defined by Milner and Goodale as cited by Krull, D'Souza, Roy, and Sharp (2004): egocentric and allocentric processing. In egocentric processing, people view

objects in 3D space relative to their body, a body centered point of view. In allocentric processing, people view objects relative to each other. Their point of view is that a spectator on the outside looking in. The researchers state that the most effective procedural illustrations may be those based on body centered or object centered tasks. The researchers also found that test subjects had difficulty making judgments on differences when objects were rotated about the vertical axis of the display plane (parallel to the display plane) and were more effective when the axis of rotation was across the display plane (normal to the display plane). These factors will be considered in the design of the decision aid.

8.2. Implementation

Based on research on providing procedural instructions, it was decided that decision aid would be primarily graphical and minimal text. The graphics will show the recommended port placement and pose of the robot from positions that would be realistic from the perspective of the surgical staff to minimize the effect on the cognitive load on the surgical team. The same pose plan will be shown from different points of view to benefit from object-centered and body-centered processing as described in Krull, et al (2004).

While not specifically tied to the requirements defined in Table 6 or the design concepts developed, two additional design goals were added. These goals were what may be characterized as “nice to have” as compared to the requirements which were critical. The first was that the decision aid must be deployable on computers that already exist or are readily available in the

operating room. During field observations, almost every operating room in hospitals in Boston, USA had a workstation that circulating nurses used for recording information related to surgery. This was not the case in the hospital in France. Designing a system that required specialized computers with expensive graphic cards would have a negative impact on the system's usability.

Based on the first design goal, the second goal was to make it usable on a tablet computer either as a web-based application or an application installed on the tablet itself. Tablets designed for use in the medical field are commonly available. The first goal dictated that the decision aid not be compute or graphically intensive to require specialized computers. The second goal defined the look and feel of the decision aid. Creating a tablet based application was also suggested by an expert surgeon when reviewing early design concepts for the decision aid (P. Hendessi, personal communication, 2012).

The planning aid was designed as a step-by-step guide for users to follow through port placement, patient cart positioning, and docking process. In the first part, patient modeling, users are prompted to provide specific measurements necessary to create the 3D model of the abdominal area. Following the patient modeling, the software would request additional information about the procedure. Based on this information, a recommendation for port placement would be shown to the user. After the ports are placed, the software would remind the user of important steps to perform in driving the patient cart to the patient. Finally, the user is shown the recommended pose plan. The process flow is shown in Figure

57

Figure 57. Planning Aid Process Flow

8.3. Patient Modeling

In the patient modeling part, users are first asked the gender of the patient before they enter the dimensions used for modeling the patient. The dimensions are width at subcostal plane, width at transtubercular plane, distance between the umbilicus and the subcostal plane, distance between the umbilicus and the transtubercular plane, distance between the subcostal and transtubercular planes, and, finally, the sagittal thickness after insufflation. An interface was designed to accept patient measurements using a touch screen interface. A sample screen for entering the width of a male patient at the subcostal plane is shown in Figure 58.

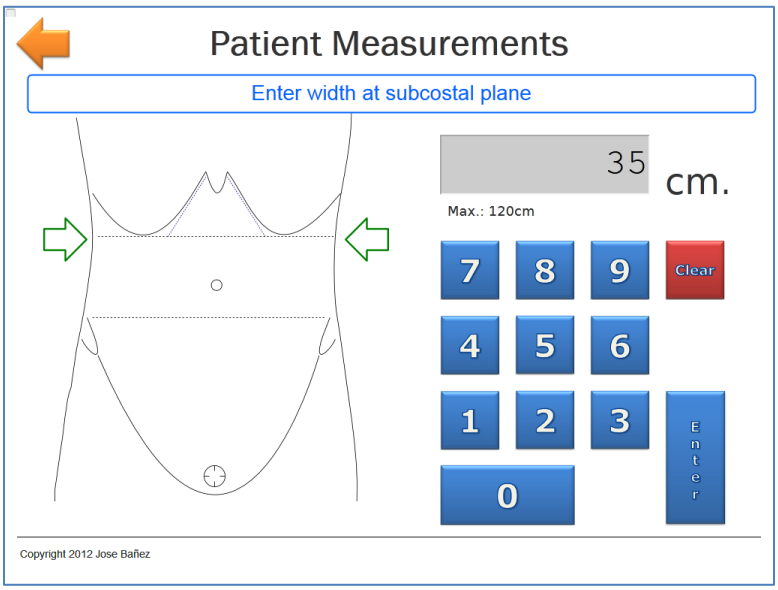

Figure 58. Patient Modeling Interface

The green arrows highlight the dimension to measure that is also indicated by the text instruction in blue near the top of the screen. The on-screen numeric keypad was sized to the same approximate size as the numeric keypad on an actual keyboard when the decision aid is deployed on a tablet with a 10 to 12" screen with a resolution of 72dpi.

8.4. Procedure Information

Following the patient modeling, the software would request additional information such as what is the planned intervention (Figure 59), whether or not the surgeon would use instrument arm 3 (Figure 60), and if so, which position it would be: patient left or right (Figure 61).

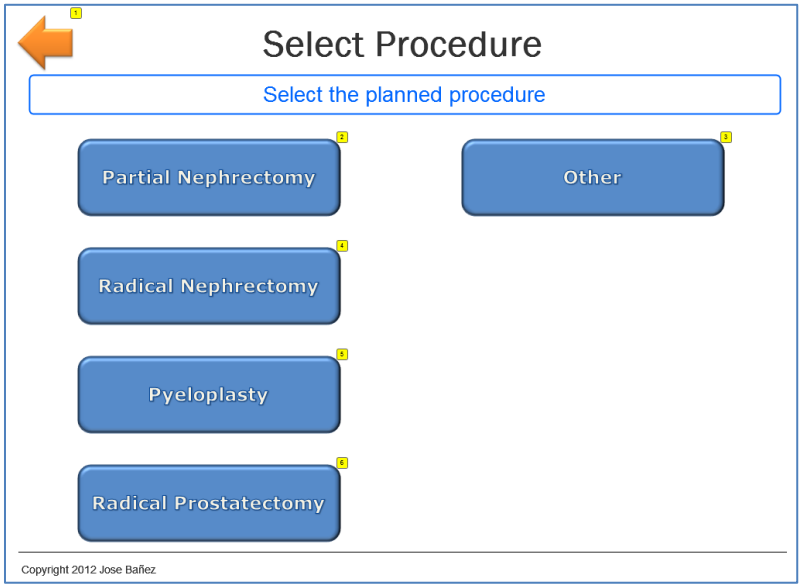

Figure 59. Planned Intervention

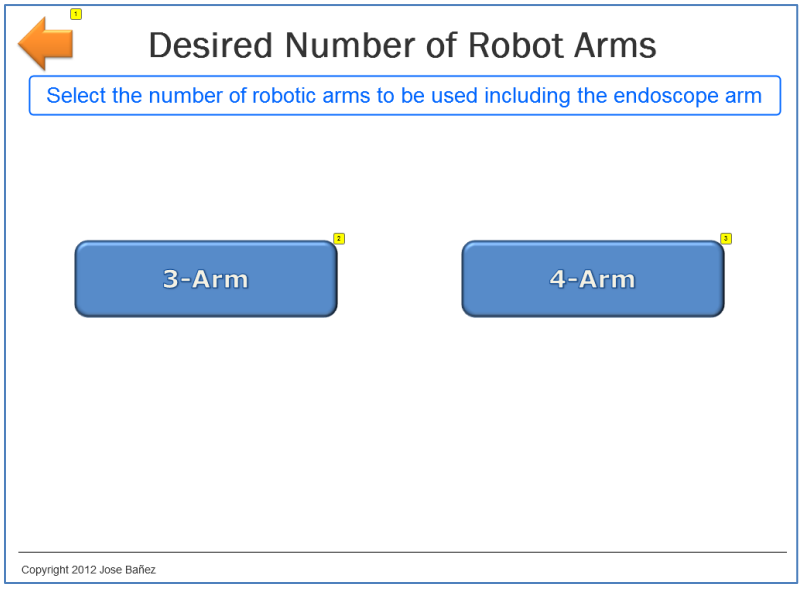

Figure 60. Select Number of Robot Arms

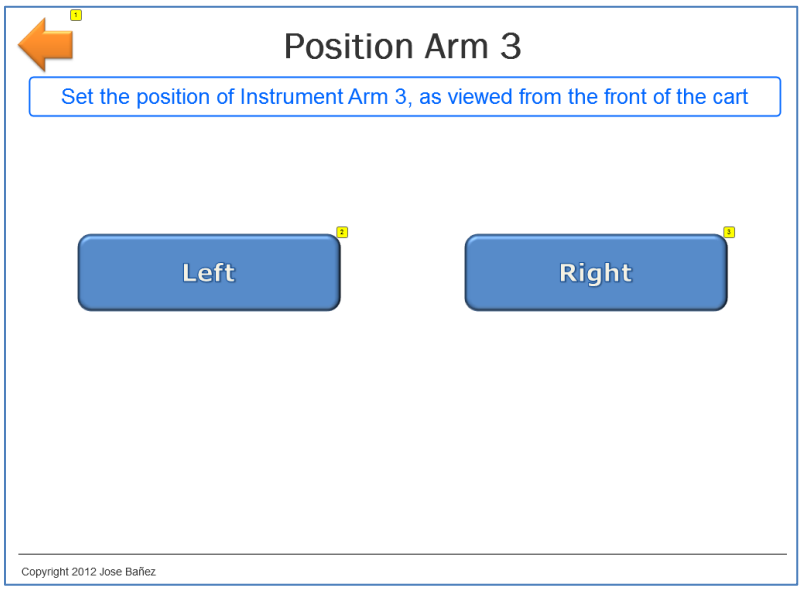

Figure 61. Position of Arm 3

8.5. Port Placement

The actual calculation of port placement recommendations was not implemented in the decision aid wireframe but done externally of the software. To develop the software to perform the calculations and integrate it in the user interface is beyond the scope of this research. As implemented, subjects were shown the recommended port placement aligned the same way they would view the patient when standing at the patient's left or right side. The lines showing the distance between ports were cyan colored to stand out against the gray background of the torso. The port markers were colored in the same manner as in the procedure card for a prostatectomy that is provided by Intuitive Surgical and shown in Figure 62.

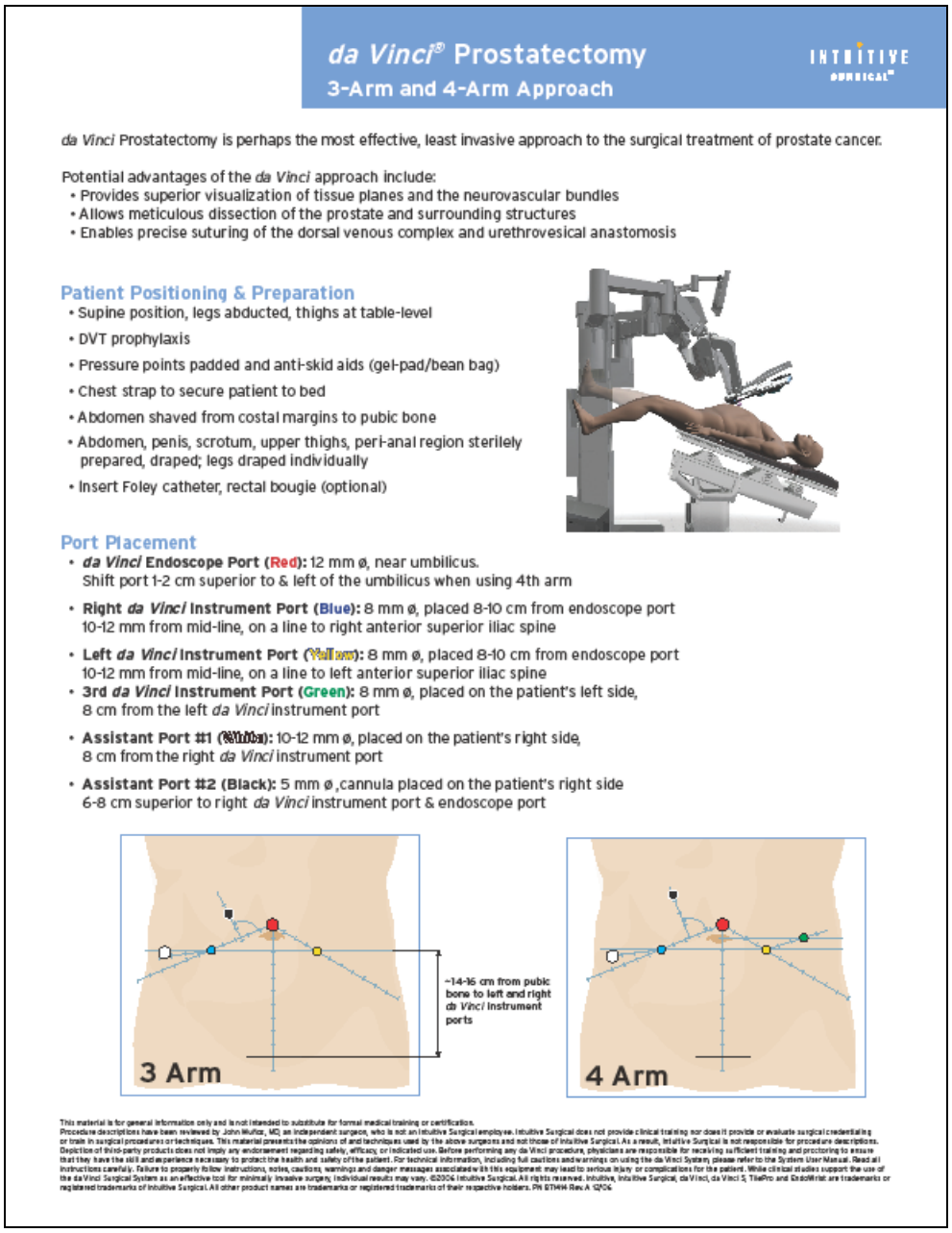

da Vinci® Prostatectomy
3-Arm and 4-Arm Approach

INTUITIVE SURGICAL

da Vinci Prostatectomy is perhaps the most effective, least invasive approach to the surgical treatment of prostate cancer.

Potential advantages of the *da Vinci* approach include:
- Provides superior visualization of tissue planes and the neurovascular bundles
- Allows meticulous dissection of the prostate and surrounding structures
- Enables precise suturing of the dorsal venous complex and urethrovesical anastomosis

Patient Positioning & Preparation
- Supine position, legs abducted, thighs at table-level
- DVT prophylaxis
- Pressure points padded and anti-skid aids (gel-pad/bean bag)
- Chest strap to secure patient to bed
- Abdomen shaved from costal margins to pubic bone
- Abdomen, penis, scrotum, upper thighs, peri-anal region sterilely prepared, draped; legs draped individually
- Insert Foley catheter, rectal bougie (optional)

Port Placement
- ***da Vinci* Endoscope Port (Red):** 12 mm ø, near umbilicus.
  Shift port 1-2 cm superior to & left of the umbilicus when using 4th arm
- **Right *da Vinci* Instrument Port (Blue):** 8 mm ø, placed 8-10 cm from endoscope port
  10-12 mm from mid-line, on a line to right anterior superior iliac spine
- **Left *da Vinci* Instrument Port (Yellow):** 8 mm ø, placed 8-10 cm from endoscope port
  10-12 mm from mid-line, on a line to left anterior superior iliac spine
- **3rd *da Vinci* Instrument Port (Green):** 8 mm ø, placed on the patient's left side,
  8 cm from the left *da Vinci* instrument port
- **Assistant Port #1 (White):** 10-12 mm ø, placed on the patient's right side,
  8 cm from the right *da Vinci* instrument port
- **Assistant Port #2 (Black):** 5 mm ø ,cannula placed on the patient's right side
  6-8 cm superior to right *da Vinci* instrument port & endoscope port

~14-16 cm from pubic bone to left and right *da Vinci* instrument ports

3 Arm

4 Arm

This material is for general information only and is not intended to substitute for formal medical training or certification.
Procedure descriptions have been reviewed by John Mufor, MD, an independent surgeon, who is not an Intuitive Surgical employee. Intuitive Surgical does not provide clinical training nor does it provide or evaluate surgical credentialing or train in surgical procedures or techniques. This material presents the opinions of and techniques used by the above surgeons and not those of Intuitive Surgical. As a result, Intuitive Surgical is not responsible for procedure descriptions. Depiction of third-party products does not imply any endorsement regarding safety, efficacy, or indicated use. Before performing any da Vinci procedure, physicians are responsible for receiving sufficient training and proctoring to ensure that they have the skill and experience necessary to protect the health and safety of the patient. For technical information, including full cautions and warnings on using the da Vinci System, please refer to the System User Manual. Read all instructions carefully. Failure to properly follow instructions, notes, cautions, warnings and danger messages associated with this equipment may lead to serious injury or complications for the patient. While clinical studies support the use of the da Vinci Surgical System as an effective tool for minimally invasive surgery, individual results may vary. ©2006 Intuitive Surgical. All rights reserved. Intuitive, Intuitive Surgical, da Vinci, da Vinci S, TilePro and EndoWrist are trademarks or registered trademarks of Intuitive Surgical. All other product names are trademarks or registered trademarks of their respective holders. PN 87494 Rev A 12/06

Figure 62. Procedure Card Prostatectomy

An example port placement recommendation for a prostatectomy is shown in Figure 63 below:

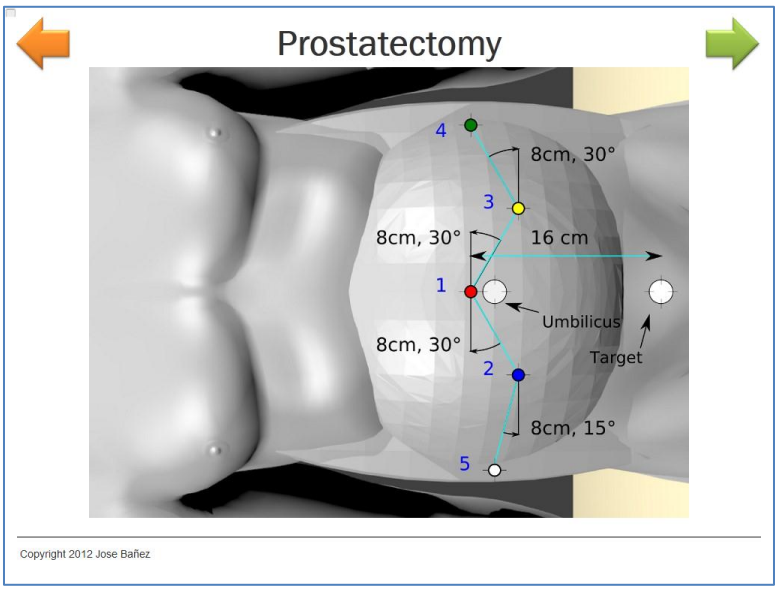

Figure 63. Sample Screen from Planning Aid Showing Recommended Port Placement for a Prostatectomy

8.6. Patient Cart Positioning

After ports have been placed, the next step is to bring the patient cart into position for docking. This step is called patient cart positioning. The patient cart positioning part of the decision aid was designed to be an informal checklist for the surgical team. Its purpose was to remind them of important steps they have to perform when they bring the patient cart to the patient. It was not one of the requirements defined or developed as a design concept. However, these steps are important in achieving proper alignment between the patient cart and the ports that have been placed.

This screens in this section show in graphical form the steps defined in the user manual da Vinci Si User Manual (Intuitive Surgical, 2009). The steps are setting the sweet spot, aligning the patient with the patient cart, and setting the

shift switch to drive. The term “sweet spot” as used in the da Vinci Si User Manual refers to setting the angle of joint R3 on the endoscope arm to a range specified by a blue band on link 2. The screen corresponding to the step for setting the “sweet spot” is shown in Figure 64. Notice the green arrows calling attention to the blue band.

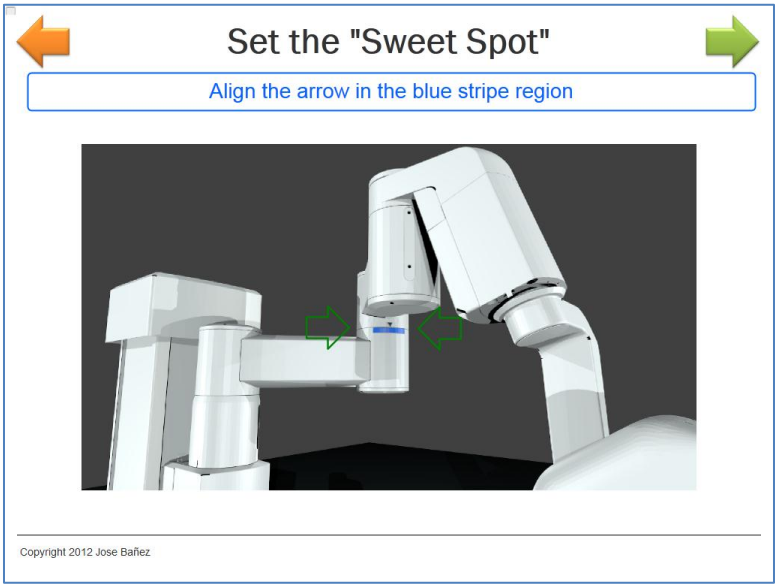

Figure 64. Positioning the Patient Cart

In the following screen, shown in Figure 65, users are asked which position the cart would be in relation to the patient. The purpose of this screen is two-fold: First, to help both the person driving the cart and the person providing guidance confirm that they are both trying to drive the cart to the same place. Secondly, it controls which alignment views are shown in the screens that follow.

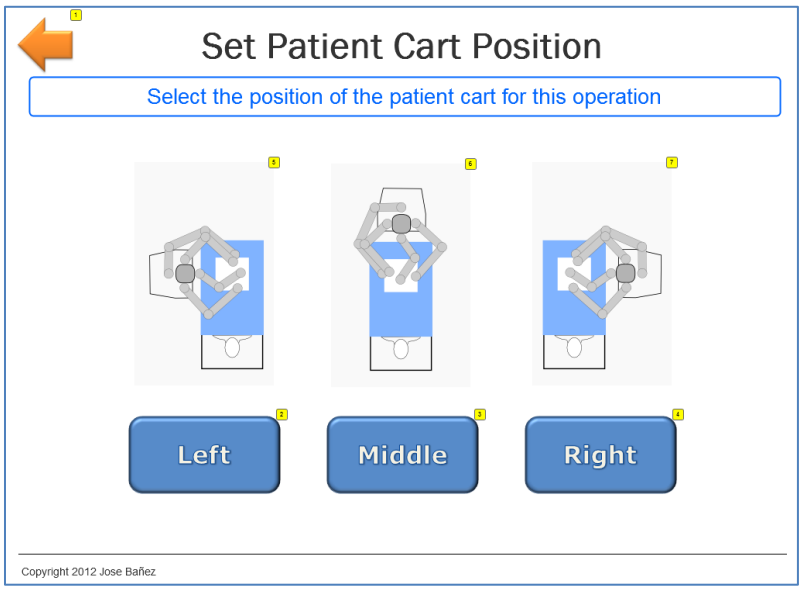

Figure 65. Set Patient Cart Position

Figure 66 shows the initial alignment of the patient cart tower, with the cannula mount, and the cannula. The green arrow with a dashed line shows the path of travel. Figure 67 shows the alignment after the patient cart has been driven to the patient. In this case, the cannula and the cannula mount have been connected. Having the patient cart aligned properly to the patient would help in being able to pose the robot arms correctly.

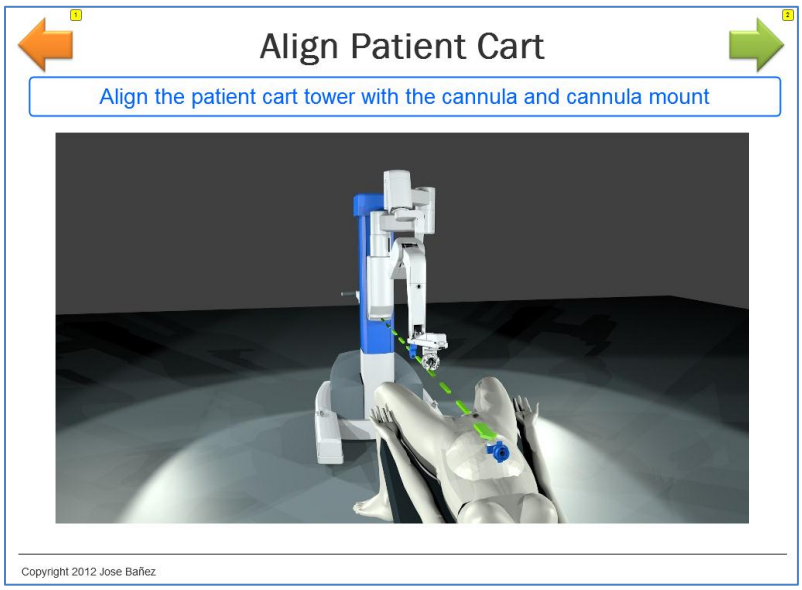

Figure 66. Align Patient Cart Middle Position (Initial)

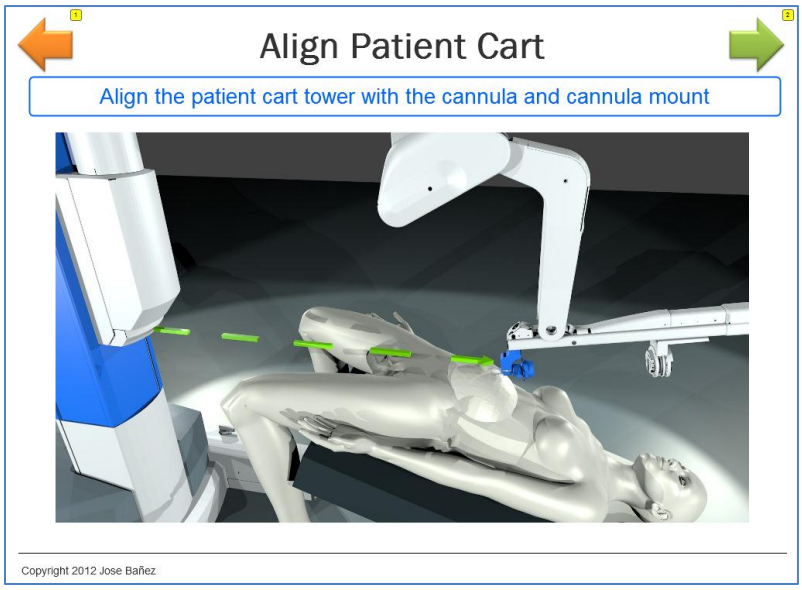

Figure 67. Align Patient Cart Middle Position (Final)

Finally, Figure 68 shows the step of setting the shift switches to drive. The patient cart can be moved in drive wherein the motors are used to position the cart or in neutral wherein the motors are not assisting in positioning the cart. After the cart

is in the desired position, it is important to set the shift switches to drive to keep the cart from moving when attached to the patient as this can cause serious injury.

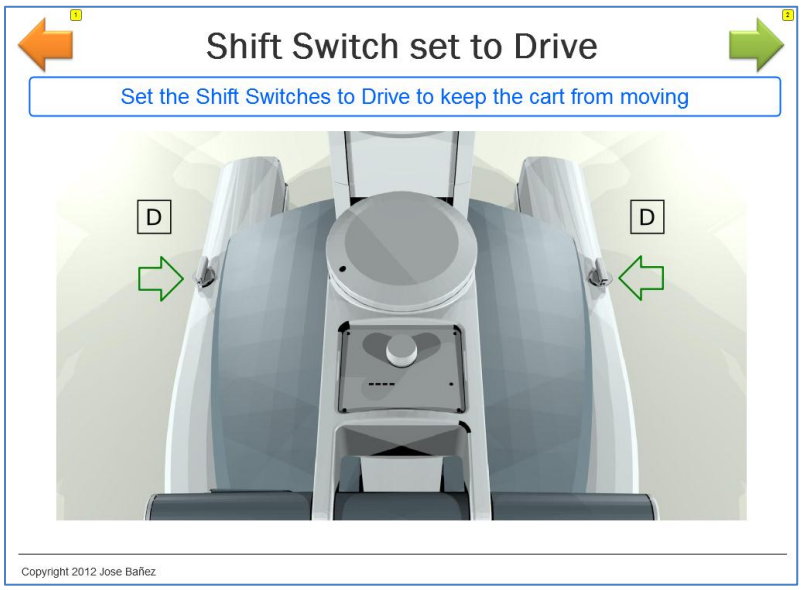

Figure 68. Shift Switch set to Drive

8.7. Posing the Patient Cart

To satisfy the requirement of showing the recommended arrangement of the instrument arms, a 1:6 scale model in a SolidWorks part file of the da Vinci Si Surgical System patient side cart was converted for use in a Blender, three-dimensional (3D) visualization environment. The environment was configured to provide views of the cart from approximately 1.5m, about the average eye-level at approximately the distance a person might stand to view the whole cart while assessing its pose. The view provided was perspective versus orthographic and the lighting in the 3D environment was designed to provide shadows to give the viewer depth cues.

Each arm was colored differently to help users distinguish between them.

The arms of the actual cart are colored uniformly. The two (left and right) arrows at the bottom of the screen allowed the user to toggle between showing all the arms and showing each of them individually. The two middle arrows allowed the user to rotate the patient cart about an imaginary vertical axis through the center of the patient cart tower.

An example screen showing all the arms at eye-level from a 30° rotation is shown in Figure 69. The same configuration from a 60°rotation is shown in Figure 71. The views of only instrument arm 2 from the same 30° and 60°rotation positions are shown in Figure 58 and Figure 59.

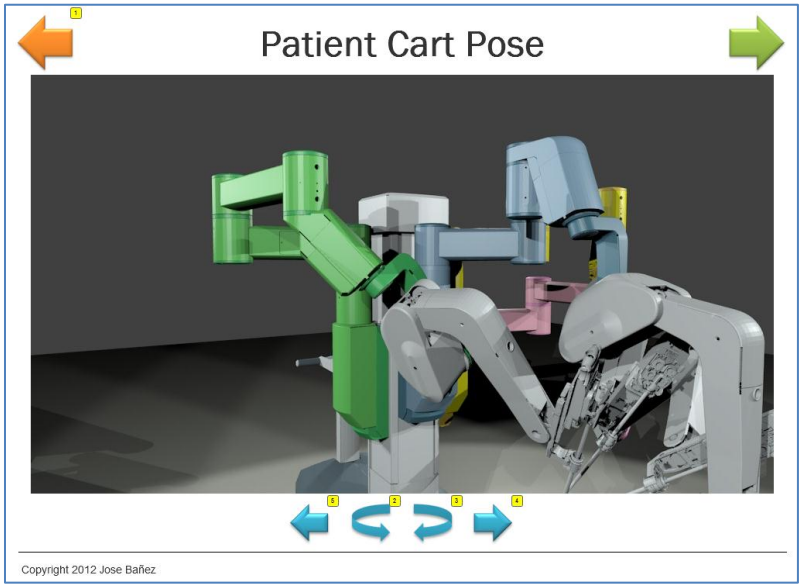

Figure 69. Posing the Patient Cart - Eye Level (30°rotation)

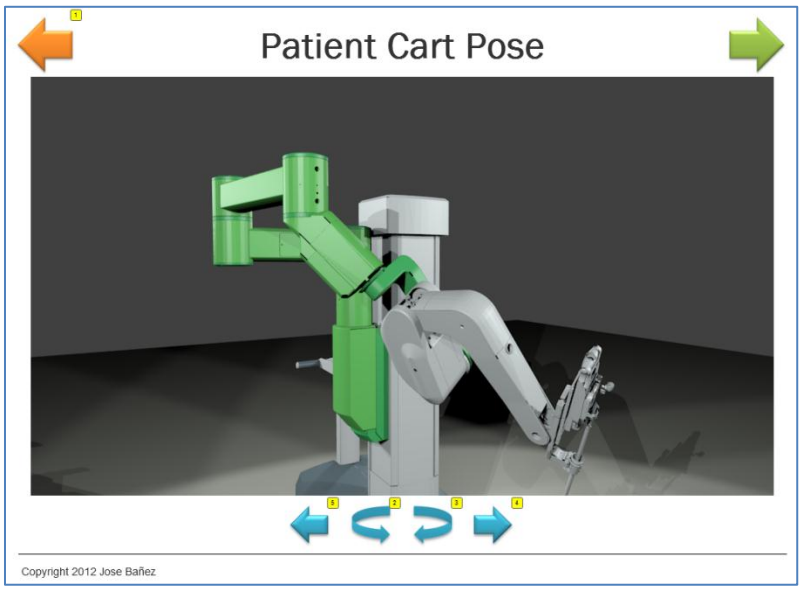

Figure 70. Posing the Patient Cart - Eye Level – Instrument Arm 2 Only (30°rotation)

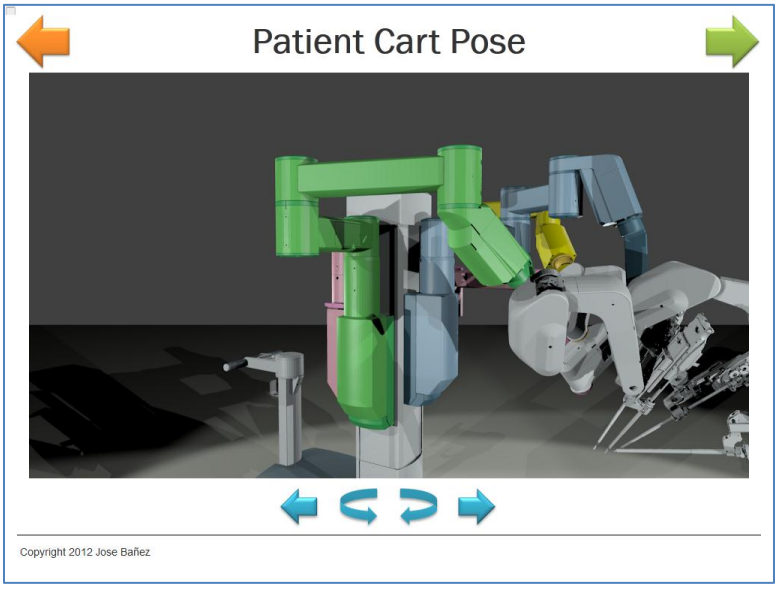

Figure 71. Posing the Patient Cart - Eye Level (60°rotation)

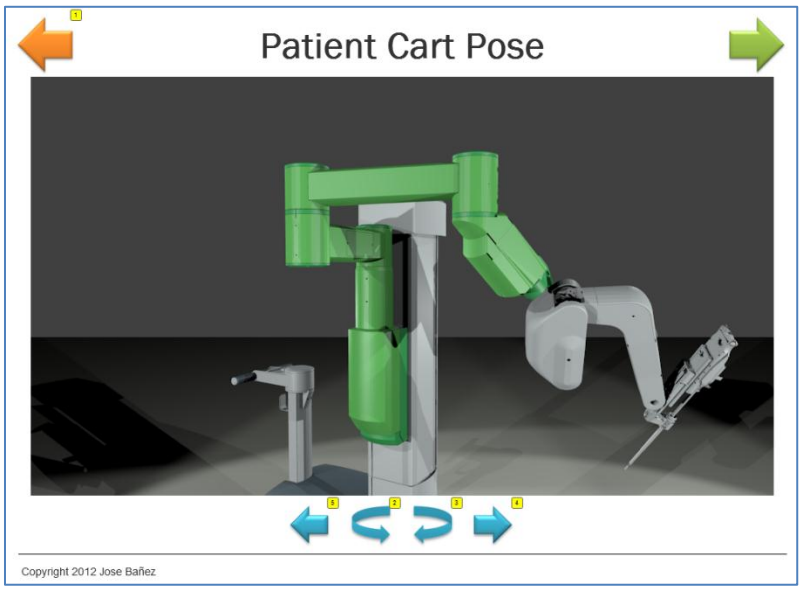

Figure 72. Posing the Patient Cart - Eye Level – Instrument Arm 2 Only (60°rotation)

An early prototype of the decision aid showed the simulated view of the patient cart relative to the patient on the operating table from the front left, front right, rear left, and rear right. These four positions were based on where a person docking the cart might be standing if the cart would be positioned between the patient's legs. One can't actually be in front of the cart if it were between the patient's legs because that would be where the patient would be. During pilot testing of this prototype, it was deemed insufficient to satisfy the requirement of displaying the pose plan. The follow-up prototype showed the patient cart from every 30°. In addition, a second simulated view of the patient cart was produced from approximately 3m from the floor (Figure 73).

In the usability testing that followed the design process the effectiveness of both views were compared. Subjects were assigned to one of two groups. One

group was shown the simulated views from 1.5 meters first followed by the views from 3 meters. The other group was shown the views from 3 meters first followed by the view from 1.5 meters. This was done to determine which method was more effective while counteracting any possible learning effects.

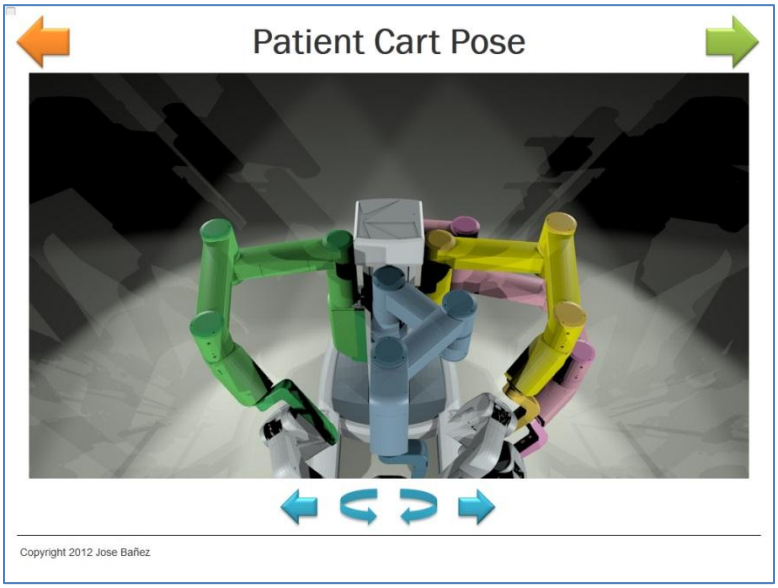

Figure 73. Posing the Patient Cart - Ceiling Level

9. Usability Testing

A testing protocol was designed to determine the usability of the different parts of the decision aid as they relate to phases of pre-operative planning in robot-assisted laparoscopic surgery, namely, patient modeling, port placement, patient cart positioning, and patient cart pose. This protocol was approved by the Tufts Institutional Review Board (IRB). In order to conduct the usability test, a test environment was set up at the Tufts Ergonomics in Remote Environments Lab (EREL) at 200 Boston Avenue.

9.1.1 Test Environment

The overall test setup is shown in Figure 74. On the left is the patient cart model built using a TETRIX® Building System. In the middle is the decision aid deployed on a tablet. On the right is the port placement test. Not visible are the computers which were used for capturing images from the web camera above the patient cart model and for administering the subject demographic questionnaires and patient cart positioning tests.

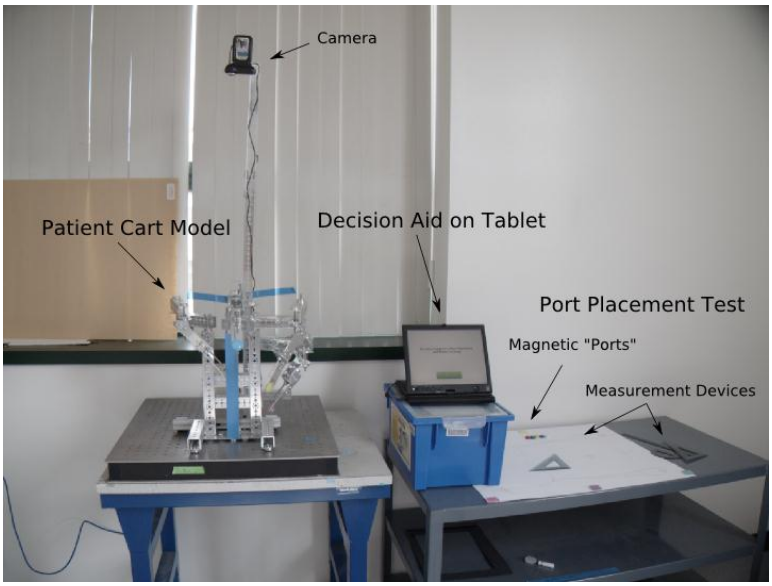

Figure 74. Usability Test Setup

9.1.2 Decision Aid

The decision aid was deployed on a Lenovo Thinkpad X60-6364 Tablet equipped with an Intel Core Duo L2400 @1.66GHz and 2GB RAM. The tablet platform was chosen because it would be similar to tablets that are now being used in some operating rooms. The tablet was not touch-screen enabled and

required participants to use a stylus to interact with the user interface. While there is a keyboard, the screen was rotated to prevent participants from using the keyboard which is not supported by the software.

The operating system selected was Gentoo Linux 3.2.1-R2 32-bit because this allowed for the installation of a system optimized specifically for the purpose of hosting the decision aid application. Only components necessary to the correct functioning of the decision aid were installed to maximize system responsiveness. The web browser chosen was Mozilla Firefox ESR 10.0.3, the latest version available at the time of the start of usability testing, because it was compatible with the decision aid without the need for additional software unlike web browsers such as Google Chrome.

9.1.3 Port Placement

For the port placement phase of the usability test, an outline of a patient torso, based on Patient 1 shown in Figure 42 and Figure 43, was printed in black and white on plain 18x24" paper at 1:1 scale.

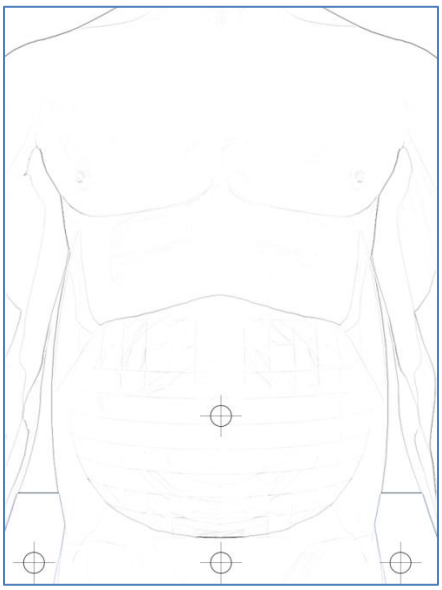

Figure 75. Patient Torso Outline

This was affixed by magnets to a cart that is 76.2cm (30.0in.) tall. Five colored magnets (red, blue, yellow, green, and white) with a 2cm diameter at the base tapering to 1.7cm at the top were provided for use to designate port placement. Four measurement devices consisting of a ruler, a protractor, a 45-45-90, and 30-60-90 triangle were also provided for participants to use. The port placement testing equipment can be seen in Figure 76.

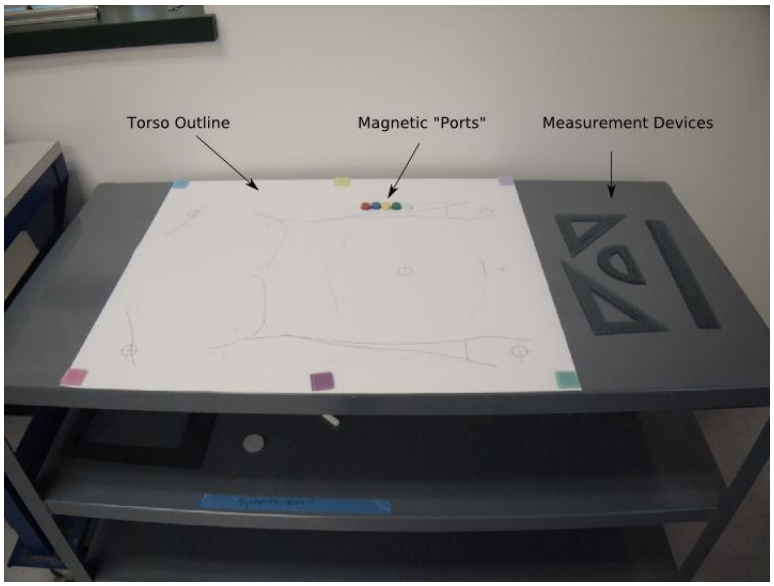

Figure 76. Port Placement Test

This task is similar to what a surgeon might do in planning port placement as can be seen in Figure 77 with the port placements marked on the patient torso.

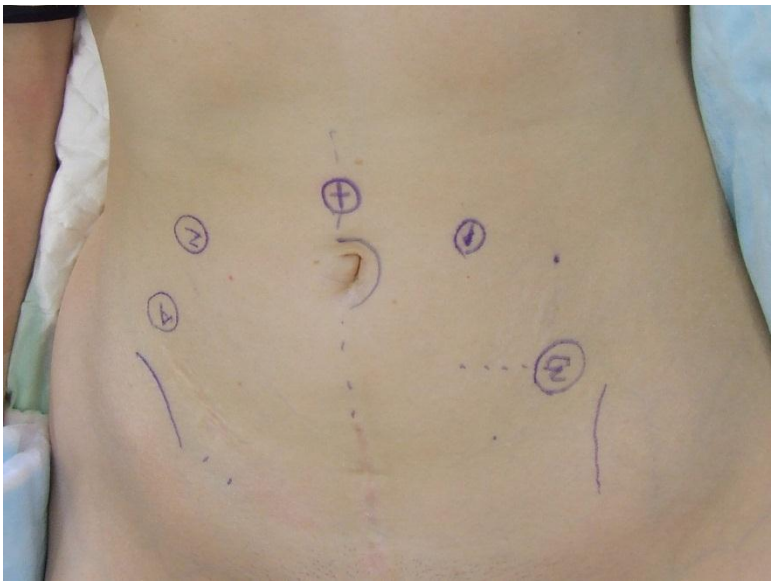

Figure 77. Patient Torso Marked for Port Placement

9.1.4 Patient Cart Pose

A model of the da Vinci Si Surgical System was built using TETRIX® Robotics components as shown in Figure 78. The model represents the unpowered revolute joints R2 and R3 for the endoscope arm, R2 – R4 for instrument arms 1 and 2, and R2-R5 for instrument arm 3. The link between R2 and R3 for instrument arm 3 is shorter than the corresponding link on the da Vinci Si Surgical System patient side cart. This was due to the length of the standard components of the TETRIX® Building System used to build the model which were not modified. This is fact was made known to the study participants because it affected the position of arm 3 relative to the other arms in the 3D visualization.

The model is 44.5 cm (17.5") tall and was mounted on a platform the top of which was 94cm (37") above the floor. This put the model at approximately average eye-level. A Logitech Webcam Pro 9000 was mounted 101cm above the platform to capture images of the model after completion of patient cart posing tasks. These images will be used to evaluate the accuracy of the model as described in a later section.

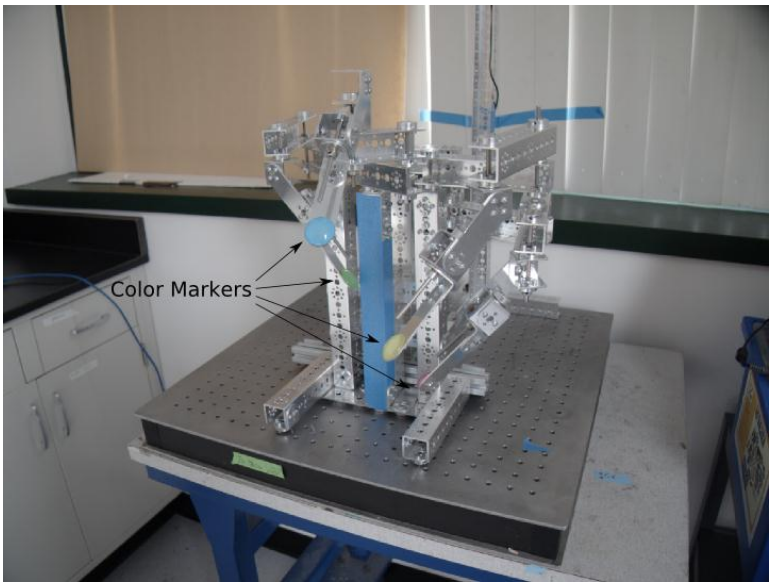

Figure 78. Patient Cart Model

9.1.5 Study Participants

Participants were recruited from Tufts University students and Boston area residents between the ages of 18 and 59, without any known disabilities, and not pregnant. These criteria were intended to avoid participation by anyone considered as vulnerable by Federal regulations which would require additional review and approval from the Tufts IRB. A total of 21 subjects participated in the usability test with 11 female and 10 male between the ages of 20 and 37 with a median age of 24. All subjects had at least some college education.

Before testing began, subjects were asked to review and sign a written consent form. The consent form provided background information on robot-assisted laparoscopic surgery and the motivation of the project as well as detailed information about the steps of the usability test.

To capture subject demographics, a short questionnaire was administered to each subject. It asked each subject their gender and age and to self-report their comfort level with computers, video game use, and frequency of use of each. The text of the questionnaire is shown below:

Subject Demographic and Computer and Video Game Use Questionnaire

This questionnaire collects your basic demographic information and presents several statements about your computer and video game use. After each statement, you should circle a number to indicate your level of agreement with the statement.

Sex: F M Today's Date: _____
Age: _____

Computer and Video Game Use Self-Assessment

For questions 1 and 3, circle "1" if you strongly agree that the statement applies to you, "7" if you strongly disagree, or some number in between if your agreement is intermediate. Circle "4" if you neither agree nor disagree.

1. I am comfortable using a computer.

   strongly agree 1 2 3 4 5 6 7 strongly disagree

2. On average, how many days a week do you use a computer?

   less than one day per week 1 2 3 4 5 6 7

3. I enjoy playing video games.

   strongly agree 1 2 3 4 5 6 7 strongly disagree

4. On average, how many days a week do you play video games?

   less than one day per week 1 2 3 4 5 6 7

Following the questionnaire, a pen-and-paper spatial orientation test based

on Thurstone's Cube tests was administered. This test had test subjects compare drawings of two blocks with letters, numbers, or symbols on each face. The subject has to perform a mental rotation to determine if the patterns shown are the same or different. The test is intended to provide a repeatable measure of the subject's spatial ability as compared to other subjects. The scores they received in performing this test were analyzed to see if there was any correlation between the subject's spatial ability and the performance in some tasks performed in this usability test.

9.1.6 Training

After the questionnaire and spatial orientation test were administered, subjects were provided a training session on the use of the software to familiarize them with the user interface and with applicable concepts in robot assisted laparoscopic surgery. This training session was designed to provide a common baseline for all participants regardless of prior knowledge of the subject.

For each of the four tasks of the decision aid, subjects were asked to read the onscreen instructions provided. This was followed by the investigator explaining what task they would be performing, how it was related to the overall purpose of the research, and how they would be evaluated, reiterating the information provided in the instructions. The instructor would then perform the task with the subject using the decision aid, further reinforcing the actions and underlying concepts. This method was designed to promote better learning,

retention, and performance as described in the study by Kieras & Bovair (1984).

For the first phase, the patient modeling phase, the primary investigator provided participants with patient information from Patient 2 shown Figure 44 and Figure 45. Participants entered measurements in the user interface and the investigator noted any difficulties or errors as well as discrepancies from the Use Case shown at the summary screen after completing the task.

This was followed by a port placement task wherein subjects were presented with an example port placement for a sacrocolpopexy (Figure 79).

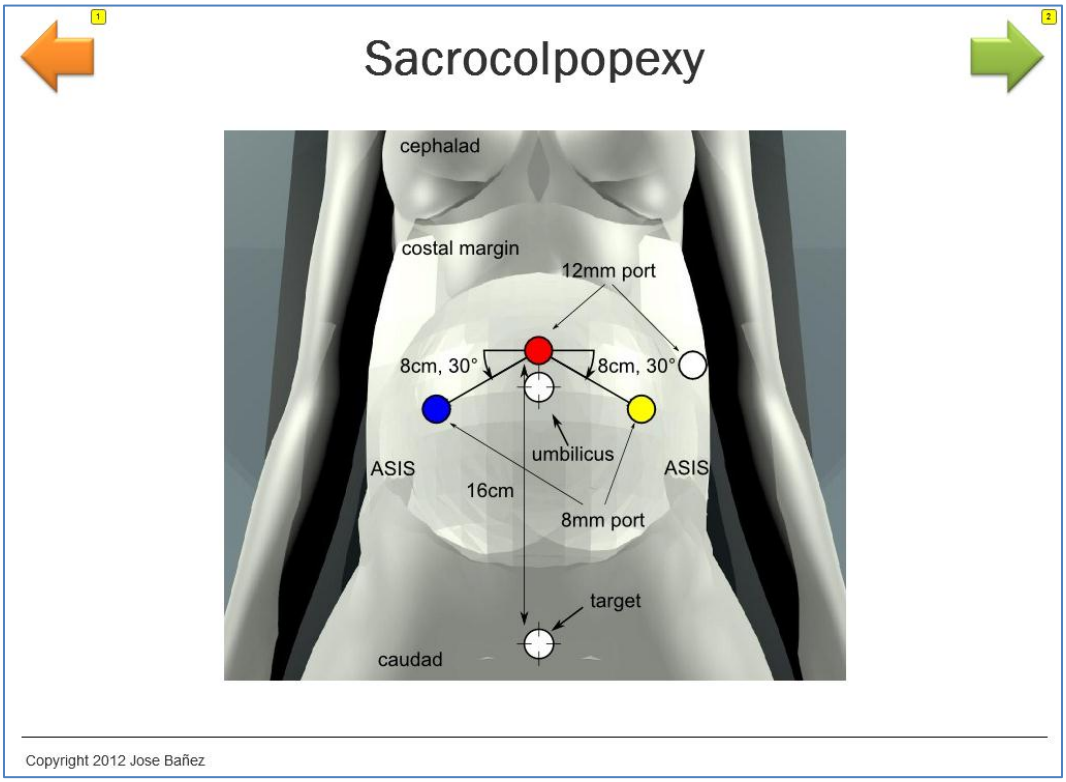

Figure 79. Port Placement for a Sacrocolpopexy

The primary investigator explained the process of port placement and provided a demonstration of how to use the triangles, ruler, and protractor. The subjects were

then asked to replicate the port placement recommendation shown on the screen on the torso outline on the cart. They started by placing the port at the umbilicus at a specified distance from the target region along the patient midline. The subjects then placed the additional instrument ports relative to the initial port and finally the assistant port was placed relative to the other ports.

The primary investigator explained that in the operating room the port placement task would be followed by positioning the patient side cart according to the steps recommended by Intuitive. The key steps, shown graphically, were as follows: set the sweet spot, coordinate the patient cart position with the primary surgeon, align the patient cart tower with the cannula mount and the cannula and keep it aligned while driving the cart to the operating table, and finally, set the shift switches to drive if not already in drive. To assess the effectiveness of the patient cart positioning section of the software for which there was no physical task to perform during the usability test, a short test of the subject's understanding is administered. This test was delivered using a Google Docs form accessed via Google Chrome browser. The page with the online form was hidden by a tab. The contents of the form are shown below:

Positioning the Patient Cart

Please answer the following questions regarding what you have learned about positioning the patient cart. You may refer to the decision aid to check your answers. You will be evaluated based on the accuracy of your answers and the time you take to perform this test.

What is the first step?

- [ ] Select the desired cart position
- [ ] Set the shift switch to neutral
- [ ] Align the patient cart tower, cannula, and cannula mount
- [ ] Set the shift switch to drive
- [ ] Drive the patient cart into position
- [ ] Set the sweet spot

What is the second step?

- [ ] Select the desired cart position
- [ ] Set the shift switch to neutral
- [ ] Align the patient cart tower, cannula, and cannula mount
- [ ] Set the shift switch to drive
- [ ] Drive the patient cart into position
- [ ] Set the sweet spot

What is the third step?

- [ ] Select the desired cart position
- [ ] Set the shift switch to neutral
- [ ] Align the patient cart tower, cannula, and cannula mount
- [ ] Set the shift switch to drive
- [ ] Drive the patient cart into position
- [ ] Set the sweet spot

What is the fourth step?

- [ ] Select the desired cart position
- [ ] Set the shift switch to neutral
- [ ] Align the patient cart tower, cannula, and cannula mount

- [ ] Set the shift switch to drive
- [ ] Drive the patient cart into position
- [ ] Set the sweet spot

Subjects were instructed to base their responses only on what was shown on the screen and to make inferences based on prior knowledge or other parts of the test. Subjects were given 3 minutes to complete this test and the time and accuracy of subject answers were recorded with timing starting from the time the subject switched tabs.

Finally, the subject was shown a demonstration of the patient cart posing task that showed views of the patient cart from four corners of the simulated operating room environment. The subjects familiarized themselves with the controls of the interface and the primary investigator explained how they would attempt to recreate the pose shown in the decision aid using the physical patient cart model. The colors at the end of each arm on the model were also explained as well as how they would be evaluated, the difference between orthographic and perspective views, and how they should approach the task as explained in the instructions they read. Once they were satisfied with their understanding of the tasks the actual usability test was started.

9.1.7 Actual Usability Test

The actual usability test was very similar to the training session. For each

of the four tasks: patient modeling, port placement, patient cart positioning, and docking, subjects were asked if they would like to read the on-screen instructions before beginning the task. As during the training, the investigator reiterated to the subject objective of each task. They were again told what actions they were expected to perform. If the task was timed and there was a time limit, they were told of the amount of time they had to perform the task. Finally, how they would be evaluated was explained. The specific details of each task and how performance was measured are discussed in the sections that follow.

9.1.8 Patient Modeling Task

Participants entered the six (6) measurements provided by the investigator using the on-screen interface using Patient 1 patient measurements shown in Figure 42 and Figure 43 and the scenario below:

Gender	Age	Height	Weight	Procedure	Number of Arms	Position of Arm 3	Position of Patient Cart
M	48	5’3”	137lbs	Prostatectomy	4	Left	Middle

The information entered was summarized and shown in a separate screen at the end of task. The investigator compared the data entered with patient information from the use case for any errors. Use of the clear button or any other action that would indicate difficulty with using the interface was noted. Hesitations and questions were noted but only incorrect entry of patient measurement was considered an error.

9.1.9 Port Placement Task

Subjects were asked to reproduce the port placement plan shown in Figure 63 on the torso outline on the cart with the magnets using the measurement tools provided, as shown in Figure 76. Subjects were given 20 minutes to perform this task. This was a change from the original study protocol where subjects were given 3 minutes to perform this task based on pilot testing. After the subject had completed the port placement task, a digital image was captured of the torso outline and port placement for evaluation as shown Figure 80.

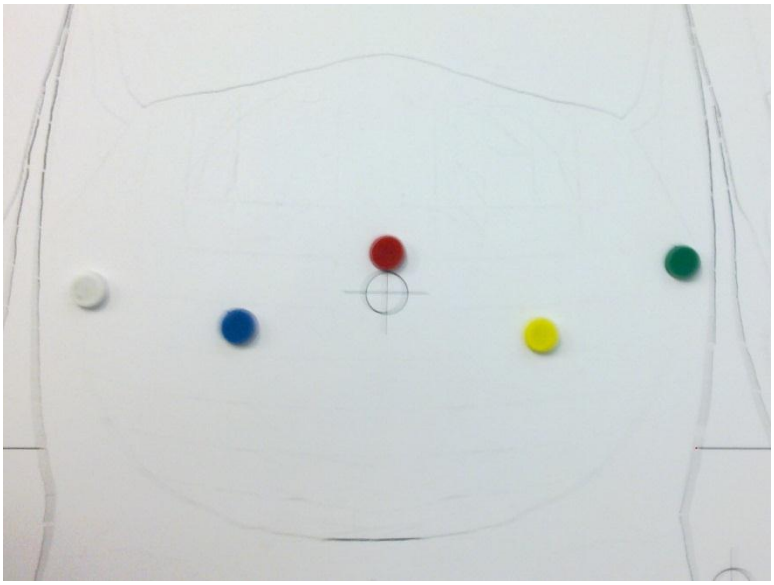

Figure 80. Port Placement Task Example

To evaluate the subject's performance, the digital images were processed and analyzed using GIMP. The exact procedure used is as follows:

1. Rotate the image to align it horizontally and vertically using the center of the umbilicus in the image as the center of rotation.

2. Using the Measure tool, measure the pixels between the horizontal alignment reference lines in the torso image just above the trans-tubercular plane as shown in Figure 81. Compare this with the known measurement, 30.8cm, to determine the horizontal scale, the equivalent length per pixel.

3. Measure the length in pixels of the perpendicular line from the horizontal line measured in step 2 to the center of the umbilicus. Compare with the known quantity, 7.3cm, to obtain the vertical scale.

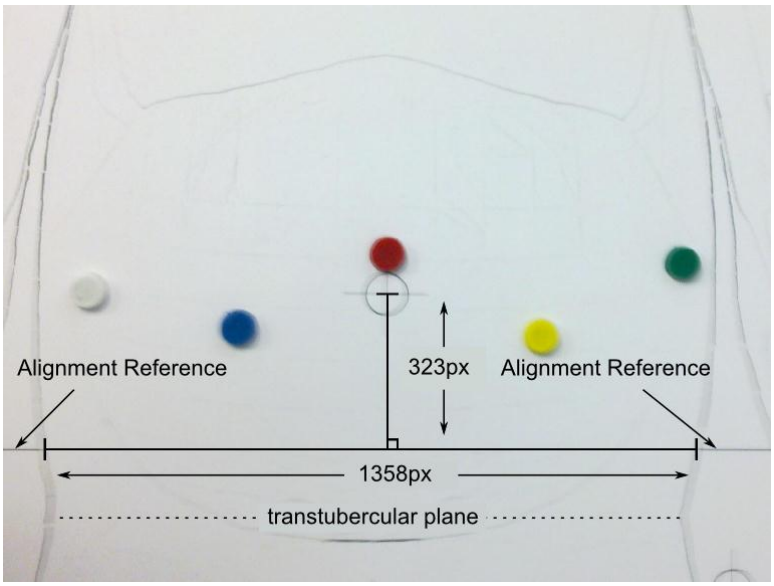

Figure 81. Determining Image Scale

4. Add horizontal guides to align with the bottoms of the magnetic markers in the image. Add vertical guides to the approximate vertical center of the magnetic markers.

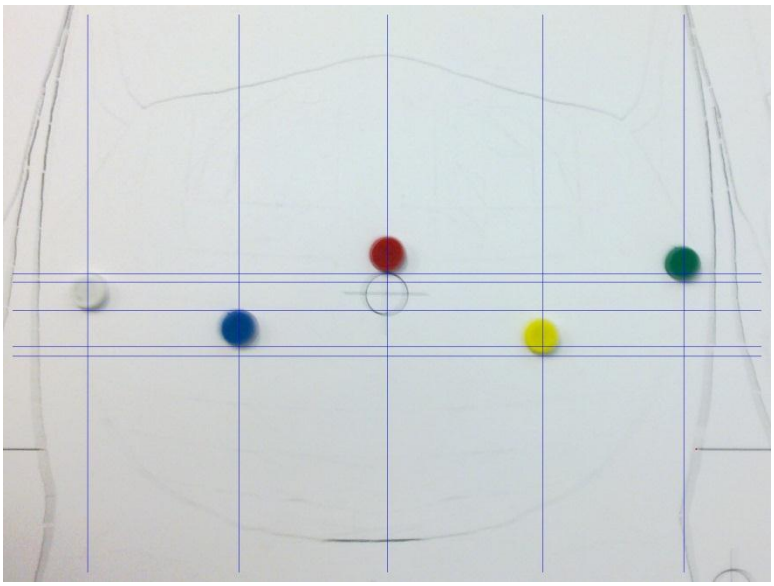

Figure 82. Measurement Guides

5. Measure the vertical and horizontal distances in pixels between the bottom of marker 1 (Red) and bottom of marker 2 (Blue). This is equivalent to measuring the vertical and horizontal distances between the centers of the two markers. Measuring the pixels of the diagonal distance will produce incorrect results if there are differences between the horizontal and vertical scales. Repeat for marker 3 (Yellow).

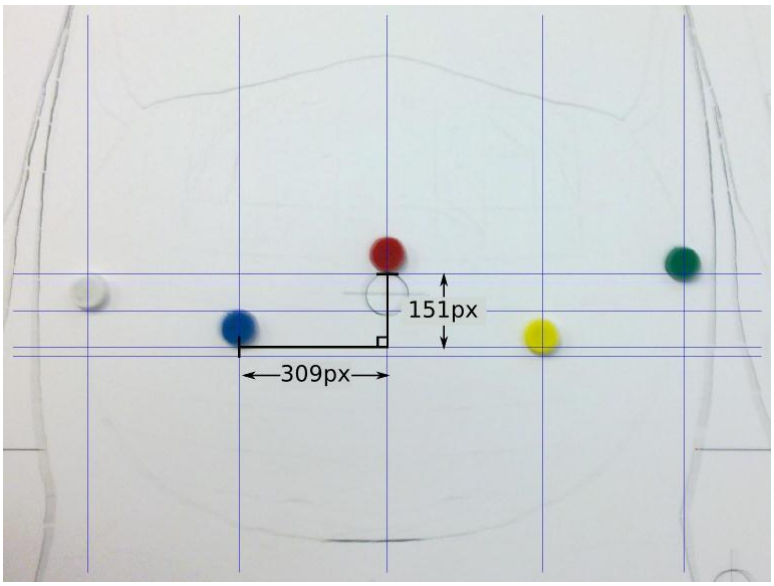

Figure 83. Measuring Distance between Ports 1 & 2

6. Measure the vertical and horizontal distances in pixels between the bottom of marker 2 (Blue) and marker 5 (white). Repeat for the vertical and horizontal distances between marker 3 (Yellow) and marker 4 (Green).

7. Convert the vertical and horizontal measurements in pixels to centimeters using the scales calculated in Step 2 and 3.

8. Calculate the effective distance between each marker and the angle from the horizontal and compare with the port placement reference shown in Figure 84.

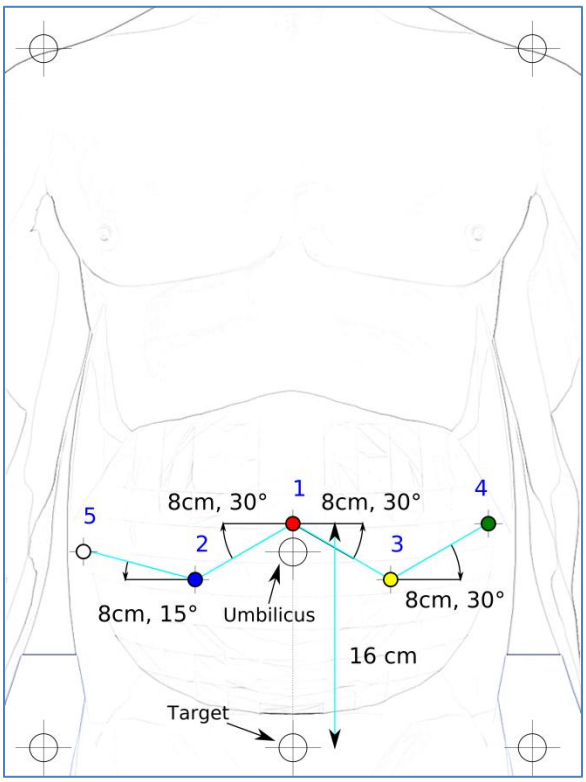

Figure 84. Port Placement Test Reference

9.1.10 Patient Cart Positioning

As in the training session, subjects viewed the screens presenting the key steps in patient cart positioning and then they were given 3 minutes to complete a post-test to see how well they understood the concepts. The score they received based on number of correct answers and the time they took to complete the test were compared with their pre-test scores and test completion time.

9.1.11 Posing the Patient Cart

Subjects were given 20 minutes to replicate the pose shown in a 3D simulation on the TETRIX® model. After they were satisfied with the model pose, a digital image of the model was taken from above and the elapsed time was

recorded.

To evaluate the subject's performance, the digital images were processed and analyzed using GIMP. The exact procedure used is as follows:

1. Rotate the image to align it horizontally and vertically using the center of the axis corresponding to the endoscope on the model as the center of rotation as shown in red in Figure 85.

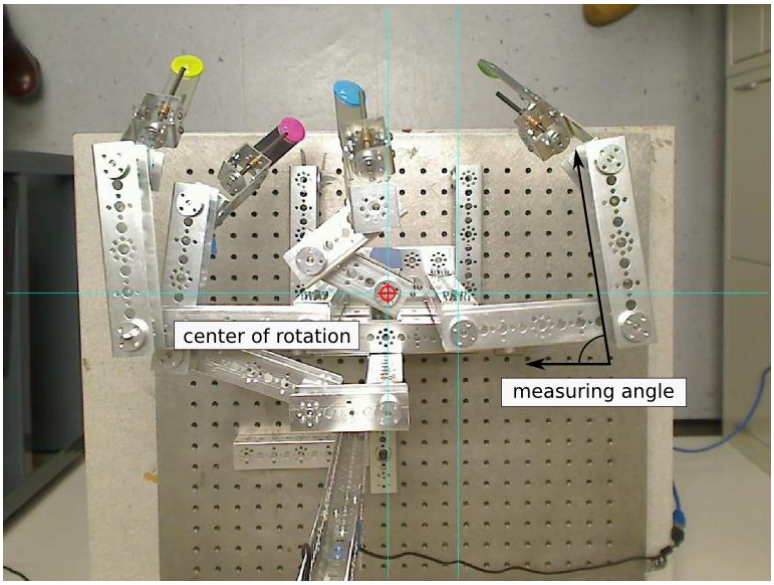

Figure 85. Aligning the picture of the model

2. Using the Measure tool, measure the angles of each of the links of each of the arms in the model from the horizontal, shown in Figure 85 and Figure 86.

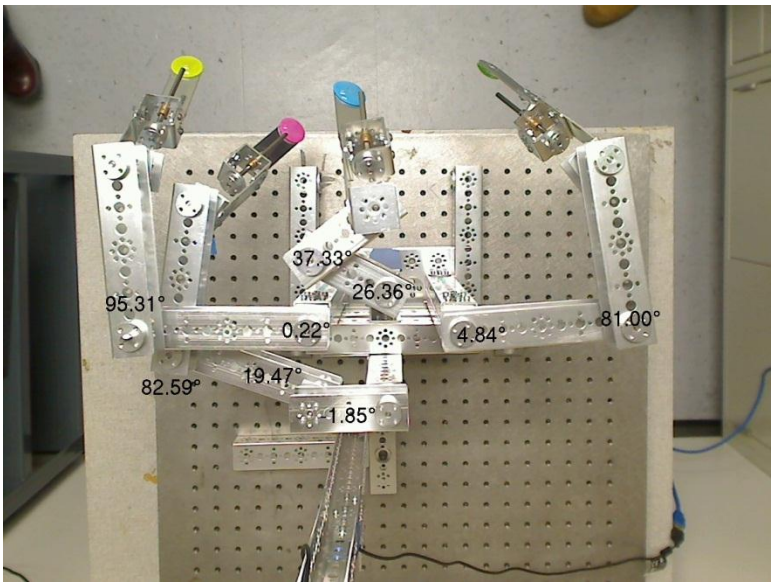

Figure 86. Example Patient Cart Model Angle Measurements

3. Compare the results with the reference angles shown in Figure 87.

4. For each of the nine revolute joints (R2 – R4 for instrument arms 1 and 2 and endoscope arm, R2- R5 for instrument arm 3), if the absolute value of the difference between the angles is less than or equal to 9° (5% error margin), they are given a score of 1. Otherwise, they receive a score of 0. The highest possible score is 9 for each view.

Figure 87. Robot Arm Angles (From Horizontal)

This part of the usability test was designed as a split-plot factorial design. The between-blocks treatment corresponds to the order that the subjects are shown the two views, eye-level (1.5m) or ceiling-level (3.0m). The within-blocks treatment corresponds to their scores for how closely the physical model they posed replicated the model shown on screen. The purpose of this split-plot

factorial design was to remove possible learning effects.

9.1.12 Subjective Feedback

At the conclusion of the usability test, subjects were given the opportunity to provide verbal feedback about the effectiveness, clarity, and possible improvements in the design of the decision aid. The primary investigator discussed each of the four tasks separately while asking the subjects for issues and difficulties they may have experienced while using the interface in performing the task. Their feedback were recorded, summarized, and discussed in the sections that follow.

9.2. Results and Analysis

9.2.1 Demographics

Most subjects, 19 of 21, strongly agreed with the statement that indicated they were comfortable using a computer and all subjects used a computer at least six days a week. The population was distributed across the 7-point Likert scale in their agreement with the statement that they enjoy playing video games (Shapiro-Wilk normality test W = 0.8817, p-value = 0.01570) with most (13 of 21) indicating that they play video games less than one day per week.

The spatial abilities tests were scored and converted to a percent value. The scores were normally distributed (Shapiro-Wilk normality test W = 0.9577, p-value = 0.4718). The minimum score was 64% and the maximum score was 100% with a median score of 83%. This is shown in the boxplot and strip chart in

Figure 88. A correlation analysis was performed between each subject's spatial ability score and other performance measures in the usability test

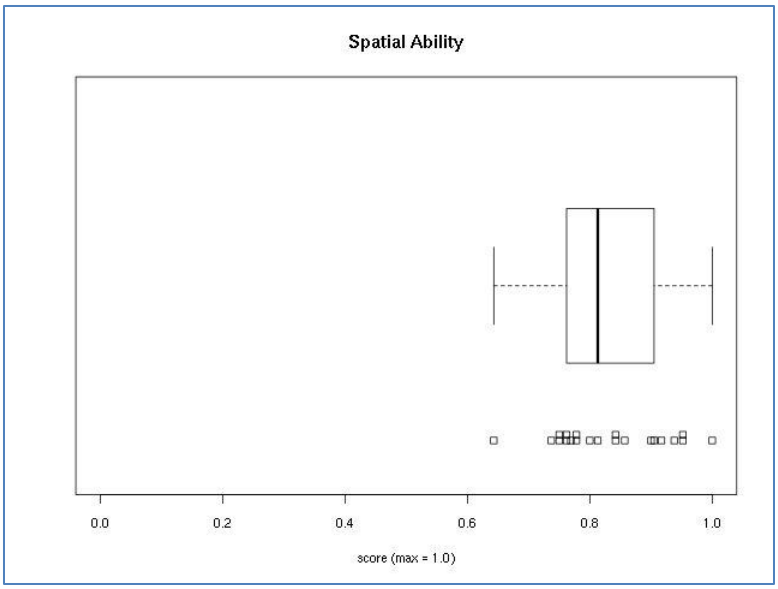

Figure 88. Spatial Abilities of Study Participants

9.2.2 Patient Modeling

There were no errors committed by subjects in entering the patient data. Only one subject had to use the clear button and that was only once. This was the result of the subject entering the number faster than the interface could register it.

9.2.3 Port Placement

The results of the port placement test using the method specified in 9.2.3 are shown in Table 49. For each subject in column 1, the elapsed time t to complete the task in seconds is listed in column 2. For each pair of ports listed in the top row, two values are listed. The first is the difference from the desired distance between ports (dL). The second is the difference from the desired angle

between ports from the horizontal (dA). The numbers that follow each designation dL or dA indicate the port pair. For example, the values in column dL12 list the difference from the reference distance that the subject's port placements achieved. Timing data was missing for subjects 1, 3, 5, and 6.

Table 49. Results of Port Placement Difference Distance and Angle from Target

		Port 1 to 2		**Port 1 to 3**		**Port 3 to 4**		**Port 2 to 5**	
Subj	**t (s)**	**dL12**	**dA12**	**dL13**	**dA13**	**dL34**	**dA34**	**dL25**	**dA25**
1		-0.28	1.89	0.22	4.09	0.44	2.42	0.7	1.53
2	140	0.42	-6.42	-0.92	-7.26	0.3	5.43	0.94	-0.61
3		-0.18	-2.52	0.22	2.45	0.66	5.88	0.48	1.15
4	210	0.84	5.22	1.29	3.43	0.71	3.08	0.79	-4.44
5		0.83	-0.14	1.55	-10.6	1.56	-6.16	-0.52	-7.05
6		0.58	2.74	0.49	3.09	1.21	16.37	0.43	2.8
7	255	0.87	-4.14	0.2	-0.84	0.71	-3.25	1.15	-8.2
8	147	1.06	-11.5	1.11	-9.7	0.58	15.96	0.5	-1.26
9	175	0.67	4.13	0.22	2.45	1.6	3.03	1.21	1.37
10	206	-0.28	1.89	-0.36	3.74	0.89	2.35	0.53	2.64
11	287	0.93	1.26	1.09	-1.39	1.07	12.35	1.13	-1.06
12	115	1.04	-2.09	0.95	-1.66	1.37	-3.93	0.57	-4.65
13	145	0.31	-2.24	1.25	4.57	0.93	1.26	0.89	-12.65
14	155	0.81	-1.92	0.47	-0.31	1	-0.96	0.6	-3.92
15	272	0.89	2.35	0.87	-1.24	1.06	1.59	1.01	-1.62
16	284	0.88	0.55	1.36	-0.82	1.19	0.05	1.01	-1.62
17	297	0.28	-6.57	0.82	-4.8	1.29	-3.45	1.38	0.12
18	131	0.97	0.15	1.16	3.06	1.15	1.19	1.23	-1.29
19	274	0.54	-2.41	0.64	-1.1	-0.68	1.07	-0.78	0.49
20	279	1.23	-4.16	1.28	-6.53	1.34	-2.74	1.36	-3.43
21	211	1.2	3.81	0.25	6.41	0.24	8.06	1.2	-9.3

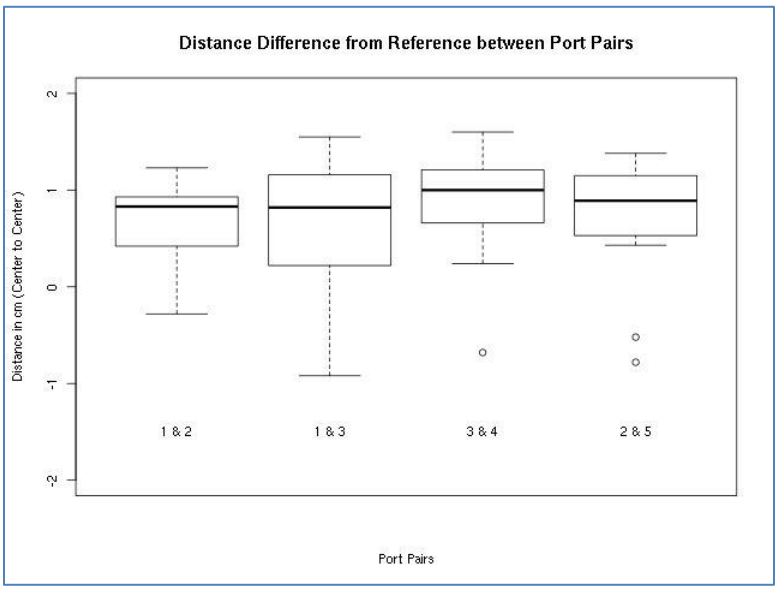

Figure 89. Port Placement Test Performance, Distance Difference from Reference between Ports

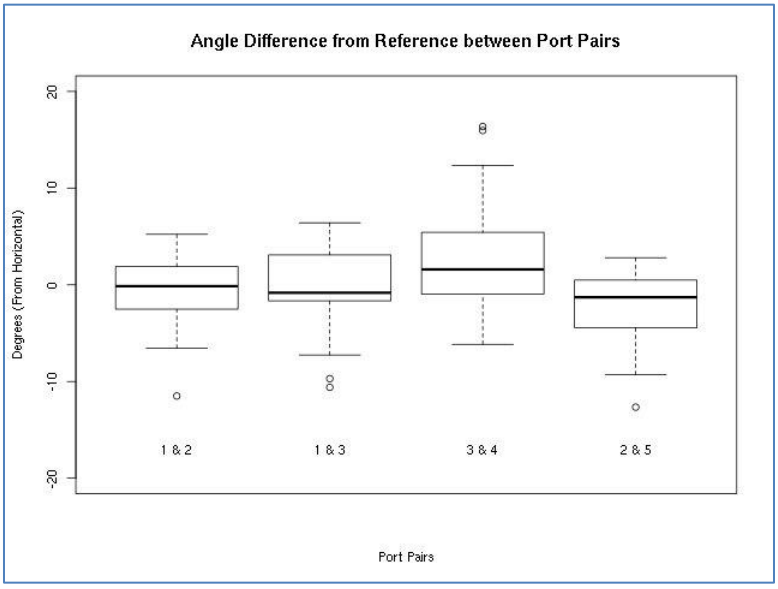

Figure 90. Port Placement Test Performance, Angle Difference from Reference between Ports

The Spearman's Rank correlation was calculated to find any relationship

between the subject's spatial ability (SA), time to perform the port placement test (t), the difference between the distance between any two ports x and y and the reference distance (dL_{xy}), and the difference between the angle between any two ports x and y and the reference angle (dA_{xy}) using R. The hypothesis is that there is some correlation, positive or negative, between these variables. The results are shown in Table 50. The data from subjects 1, 3, 5, and 6 were excluded from this analysis because of missing timing data. Replacing the missing timing data using means or other methods might produce unreliable results.

The critical value for the Spearman's Rank Correlation Coefficient r_s (two-tailed test) at n = 17 and $\alpha = 0.05$ is 0.485 (Zar, 1972). For the port placement test, there is a statistically significant correlation between the difference in angle from the reference for ports 1 and 2 and for ports 1 and 3 ($r_{s(obs)} = 0.696$) and between the difference from the reference for the distance between ports 3 and 4 and between ports 2 and 5 ($r_{s(obs)} = 0.497$). There is no statistically significant correlation between the subject's spatial ability or time to complete the port placement task and the performance in the test.

Table 50. Spearman's Rank Correlation Port Placement Test

	SA	**t**	**dL_{12}**	**dA_{12}**	**dL_{13}**	**dA_{13}**	**dL_{34}**	**dA_{34}**	**dL_{25}**	**dA_{25}**
SA	1	-0.26	-0.05	-0.37	0.05	-0.002	-0.23	-0.33	-0.119	-0.14
t	-0.258	1	0.01	-0.03	-0.15	0.152	-0.09	0.12	-0.357	-0.19
dL_{12}	-0.054	0.01	1	0.04	0.41	-0.221	0.14	0.09	0.21	-0.42
dA_{12}	-0.372	-0.03	0.04	1	0.04	**0.696**	0.11	0.33	0.045	-0.06
dL_{13}	0.048	-0.15	0.41	0.04	1	-0.02	0.32	-0.08	0.069	-0.34
dA_{13}	-0.002	0.15	-0.22	**0.696**	-0.02	1	-0.146	0.13	0.001	-0.29
dL_{34}	-0.229	-0.09	0.14	0.11	0.32	-0.146	1	-0.47	**0.497**	0.08
dA_{34}	-0.333	0.12	0.09	0.33	-0.08	0.125	-0.47	1	-0.186	0.21
dL_{25}	-0.119	-0.36	0.21	0.05	0.07	0.001	**0.497**	-0.19	1	-0.06
dA_{25}	-0.143	-0.19	-0.42	-0.06	-0.34	-0.286	0.08	0.21	-0.055	1

9.2.4 Patient Cart Positioning

The results of the patient cart positioning test, both the elapsed time and the total score (max = 4), are shown in Table 51. The data from subject 5 was excluded from this analysis because of missing timing data. Also included in the table are the scores from the spatial ability test. These scores were ranked in ascending order and time elapsed in descending order.

The Spearman's Rank correlation was calculated using R and the results shown in Table 52. For simplicity of input into R, the columns were encoded as x1, x1r, etc. Regarding the pre-test and post-test scores, the hypothesis was that there would be a positive correlation. The critical value for the Spearman's Rank Correlation Coefficient r_s (one-tailed test) at n = 20 and $\alpha = 0.05$ is 0.380 (Zar, 1972). A statistically significant correlation between the pre-test and post-test scores ($r_{s(obs)} = 0.659$) was found.

Table 51. Results of Patient Cart Positioning Pre and Post Test

	Spatial		**Pre-Test**				**Post-Test**			
Subj	Score (%)	Rank	Time (s)	Rank	Score	Rank	Time (s)	Rank	Score	Rank
code	x1	x1r	y1	y1r	y2	y2r	y3	y3r	y4	y4r
1	0.762	16.5	120	19	2	14	60	17	4	6
2	0.952	2.5	46	5.5	3	9.5	20	5	4	6
3	1	1	45	4	1	18	30	9	1	19.5
4	0.8	12	120	19	4	4	60	17	4	6
6	0.842	9.5	120	19	2	14	180	20	4	6
7	0.778	13.5	46	5.5	4	4	10	1	4	6
8	0.762	16.5	34	1	3	9.5	30	9	2	16
9	0.9	7	55	8	2	14	32	11	2	16
10	0.857	8	43	3	4	4	19	3.5	4	6
11	0.952	2.5	63	10.5	1	18	40	13	1	19.5
12	0.905	6	48	7	3	9.5	21	6	3	12.5
13	0.813	11	85	14	1	18	60	17	2	16
14	0.643	20	63	10.5	4	4	15	2	4	6
15	0.938	4	83	13	4	4	30	9	4	6
16	0.842	9.5	62	9	0	20	25	7	3	12.5
17	0.75	18.5	105	16	3	9.5	34	12	2	16
18	0.917	5	89	15	4	4	19	3.5	4	6
19	0.75	18.5	35	2	2	14	42	14	2	16
20	0.769	15	114	17	4	4	48	15	4	6
21	0.778	13.5	67	12	2	14	143	19	4	6
5	0.737	#N/A		#N/A	1			#N/A	2	

For the relationship between the timing, score, and spatial ability, the hypothesis was that there would be some difference. A critical value of 0.447 for the Spearman's Rank Correlation Coefficient r_s (two-tailed test) at n = 20 and $\alpha = 0.05$ was used (Zar, 1972). A statistically significant correlation between the time it took to complete the tests ($r_{s(obs)} = 0.560$) was found, as shown in Table 52. There was no significant correlation between the subject's spatial ability test score and time it took to complete the test or the outcome of the tests.

Table 52. Spearman's Rank Correlation Patient Cart Positioning

	x1r	**y1r**	**y2r**	**y3r**	**y4r**
x1r	1	0.151378	-0.18841	0.205594	-0.13659
y1r	0.151378	1	-0.09326	**0.560303**	-0.39201
y2r	-0.18841	-0.09326	1	0.435985	**0.659052**
y3r	0.205594	**0.560303**	0.435985	1	0.110939
y4r	-0.13659	-0.39201	**0.659052**	0.110939	1

Using a matched-T test on the pre-test and post-test scores for each subject, the calculated t = 2.118, df = 20, p-value = 0.0235. The level of significance for a one-tailed test at the $\alpha = 0.05$ level is 1.725. There is a statistically significant difference between the pre-test and post-test scores. The difference between the pre-test and post-test scores is also shown graphically in Figure 91. The box plots show the distribution of scores and the corresponding strip charts the actual scores, at the top for the pre-test and at the bottom for the post-test. The median score from the pre-test has improved in the post-test.

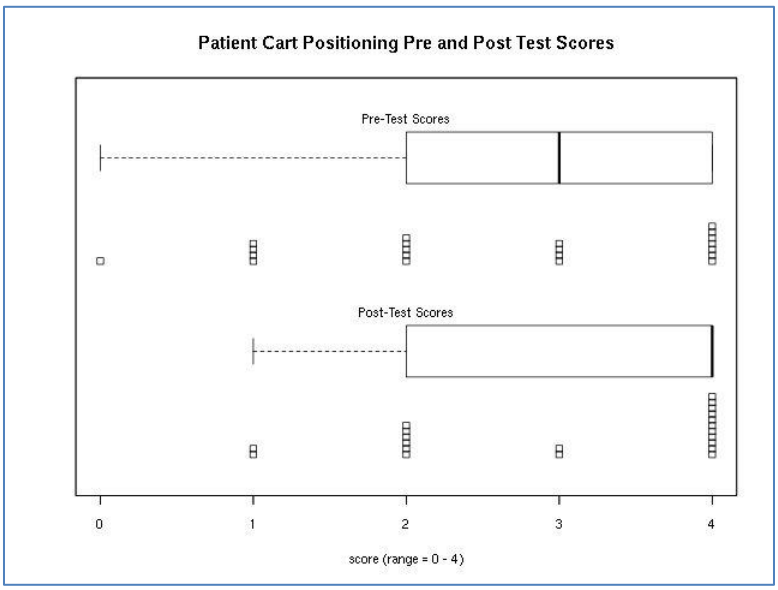

Figure 91. Comparison of Pre-test and Post-test Scores

9.3. Posing the Robot Model

A Spearman's Rank Correlation was performed for the The scores achieved for posing the robot model to find any correlation between the subject's spatial ability (SA.R), the time it took to complete the task (Time1.R or Time2.R for view 1 or view 2, respectively), and the score achieved for that view (Score1.R or Score2.R for view 1 or view 2, respectively). Data from subject 5 was again excluded due to missing data.

For all scores, regardless of the order the views were shown, the results are shown in Table 53. The critical value for the Spearman's Rank Correlation Coefficient r_s (two-tailed test) at n = 20 and $\alpha = 0.05$ is 0.447 (Zar, 1972). The results of the analysis shows that there a statistically significant positive correlation between the time it took to complete the task in both view 1 and view

2 ($r_{s(obs)}$ = 0.528). It also found a negative correlation between the time it took to complete view 2 and the score in view 1 ($r_{s(obs)}$ = -0.533). No statistically significant correlation was found for spatial ability and the time it took to complete the task or the score received.

Table 53. Spearman's Rank Correlation Posing the Robot Model (All Subjects)

	Subj	**SA.R**	**Time1.R**	**Score1.R**	**Time2.R**	**Score2.R**
Subj	1	0.286	0.56	-0.438	0.405	-0.115
SA.R	0.286	1	0.168	0.079	0.161	0.275
Time1.R	0.56	0.168	1	-0.243	**0.528**	-0.209
Score1.R	-0.438	0.079	-0.243	1	**-0.533**	0.293
Time2.R	0.405	0.161	**0.528**	**-0.533**	1	-0.164
Score2.R	-0.115	0.275	-0.209	0.293	-0.164	1

In Table 54 and Table 54, the scores of all subjects who were shown view 1 first were analyzed separately from those subjects shown view 2 first. The critical value for the Spearman's Rank Correlation Coefficient r_s (two-tailed test) at n = 10 and $\alpha = 0.05$ is 0.648 (Zar, 1972). The analysis found a statistically significant correlation between the time it took to complete view 1 and the time it took to complete view 2 ($r_{s(obs)}$ = 0.794). The analysis also found a statistically significant negative correlation between the score in view 1 and the time it took to perform view 2 ($r_{s(obs)}$ = -0.654). It found no statistically significant relationship between any of the scores and the time it took to perform the task for subjects shown view 2 first as shown in Table 55. It found no statistically significant relationship between the subject's spatial ability and their performance in both groups.

Table 54. Spearman's Rank Correlation Posing the Robot Model (View1 First)

	Subj	**SA.R**	**Time1.R**	**Score1.R**	**Time2.R**	**Score2.R**
Subj	1	0.372	0.576	-0.247	0.479	0.378
SA.R	0.372	1	-0.012	0.109	0.177	0.249
Time1.R	0.576	-0.012	1	-0.617	**0.794**	0.124
Score1.R	-0.247	0.109	-0.617	1	**-0.654**	0.29
Time2.R	0.479	0.177	**0.794**	**-0.654**	1	-0.186
Score2.R	0.378	0.249	0.124	0.29	-0.186	1

Table 55. Spearman's Rank Correlation Posing the Robot Model (View2 First)

	Subj	**SA.R**	**Time1.R**	**Score1.R**	**Time2.R**	**Score2.R**
Subj	1	0.182	0.539	-0.823	0.358	-0.59
SA.R	0.182	1	0.419	-0.019	0.523	0.293
Time1.R	0.539	0.419	1	-0.231	0.261	-0.242
Score1.R	-0.823	-0.019	-0.231	1	-0.287	0.543
Time2.R	0.358	0.523	0.261	-0.287	1	-0.292
Score2.R	-0.59	0.293	-0.242	0.543	-0.292	1

The scores for subject 5 were removed due to a missing score for one view. The analysis was performed with n = 20. A boxplot showing the summary of the scores by the order that views were shown (Figure 92), by the view (Figure 93), and by the order with the view (Figure 94) are shown below:

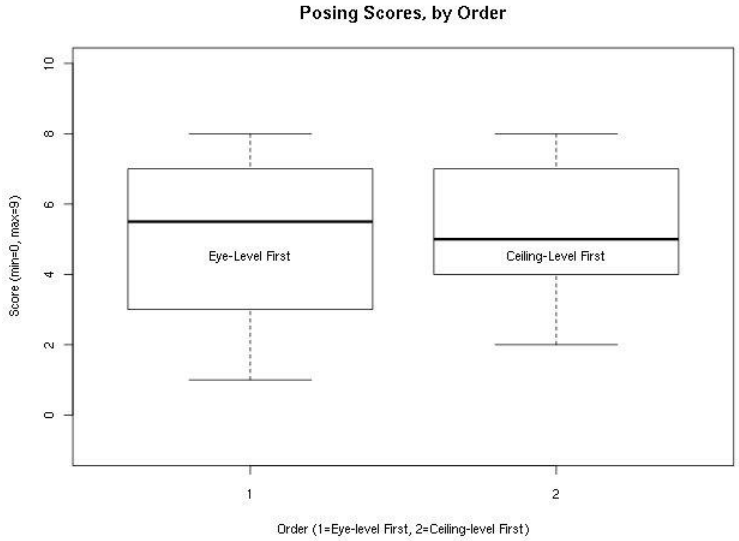

Figure 92. Comparison of Posing Scores, By Order

Figure 92 shows a narrower range of scores for both tests when subjects were shown the ceiling view first.

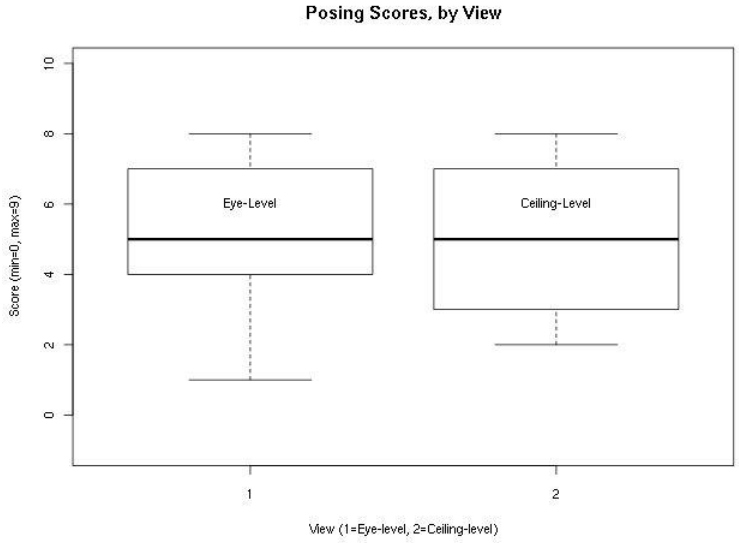

Figure 93. Comparison of Posing Scores, By View

Figure 93 shows that the median performance for either view was about the same. Performance when given the ceiling view varied more though the eye-level view

had more outliers.

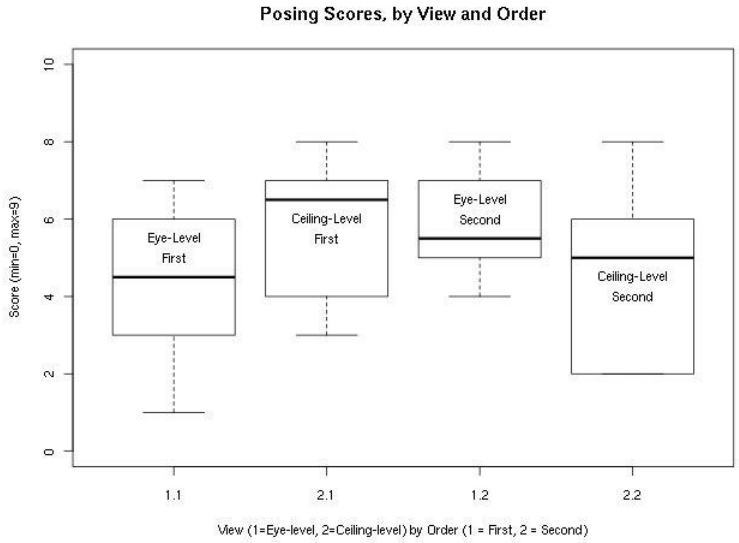

Figure 94. Comparison of Posing Scores, By View and Order

Figure 94 shows that subjects performed best with view 1 when they were shown the ceiling view first when the range of scores are compared. When the medians are compared, subjects seemed to be able perform best when shown view 2 first. The scores of the posing task were analyzed as an SPF p.q ANOVA in R. The model used and the output from R are shown in Figure 95.

```
> fit <- aov(score ~ (order*view) +
Error(subj/(view)) + (order), data=spf.pq)
> summary (fit)

Error: subj
      Df Sum Sq Mean Sq
order  1 8.7969  8.7969

Error: subj:view
     Df  Sum Sq Mean Sq
view  1 0.70359 0.70359

Error: Within
           Df  Sum Sq Mean Sq F value  Pr(>F)
order       1   0.093  0.0934  0.0262 0.87230
view        1   1.517  1.5168  0.4262 0.51827
order:view  1  16.251 16.2511  4.5659 0.03989 *
Residuals  34 121.013  3.5592
```

Figure 95. ANOVA of Posing Scores (SPF-p.q) using R

The only statistically significant effect found was the interaction between the two orders that subjects were shown the two views.

9.4. Subjective Feedback

At the conclusion of the usability testing, study participants were given the opportunity to provide feedback regarding specific portions of the test as well as the overall test. The results are summarized below:

9.4.1 Patient Modeling

- Study participants found the interface for entering the patient measurements to be simple and intuitive.
- Left-handed users did not experience any difficulty with the layout.

- Some participants commented that their understanding of the task was enhanced by having the specific source of the measurements shown on the screen even though they were only entering measurements. It helped with their mental model.
- One subject recommended devising a method to ensure that the measurements entered are for the correct part of the torso.

9.4.2 Port Placement

- Study participants did not state that they experienced any difficulties with regards to the port placement task.
- Most did not notice that the use case used in the training session was in portrait orientation with the head at the top of the screen while the use case used in the actual test was in landscape orientation, aligned with their view of the patient torso
- Some participants wished that the angle for port 5, the assistant port, which was different than all the other angles be highlighted.
- Some participants recommended that it be made clearer in the diagram that the distance measurement corresponded to the distance between the ports because they initially confused the horizontal base of the angle measurement as the distance corresponding to the measurement.
- Most study participants commented that they wished they could mark the

torso outline with measurements instead of just placing the magnetic markers.

- Most study participants expressed frustration with the use of the protractors and triangles which they had forgotten how to use.

9.4.3 Positioning the Patient Cart

- Some study participants stated that they were confused by the test and made inferences in their responses.
- Some study participants commented on the use of the term sweet spot and said that it confused them because it was not in agreement with their understanding of the term's meaning.
- Some study participants noted that they would be better able to understand and retain the concepts if they had to actually perform a physical task.
- Several study participants commented that setting the shift switch to drive to keep the cart from moving was counterintuitive. Two suggested having a park setting in addition to drive and neutral.

9.4.4 Posing the Robot Model

- All participants expressed preference for the ceiling view.
- Several subjects recommended installing cameras above the patient cart in the operating room to provide a top view.

- Two subjects recommended that arms of the robot model and actual robot be colored in similar manner as they are in the decision aid to make them easier to visualize than the uniform color.
- One subject noted that she had to think about how the view rotation controls worked when she used them. She expected that the directions of the arrows indicated which way the viewer moved instead of the robot.

9.4.5 Overall Feedback

- Subjects found the interface intuitive and easy to use.
- Subject participants found that the training session helped with understanding the concepts.

9.5. Discussion

9.5.1 Usability Test

This usability test was conducted as a formative test of a product that is in current development. The goal of the test was to see if users would find it easy to use, that the controls would be intuitive or at least not confusing, and that it be effective in conveying the information it need to present. Each part of the usability test will be discussed separately.

9.5.2 Demographics

However, the test was conducted with study population that was not

representative of the target audience for which the decision aid was designed. Thus any conclusions drawn or inferences made from the study results in the sections that follow would not necessarily be transferrable to the target population of surgical team members in the target environment of an operating room.

The questionnaire administered to subjects at the beginning of the test was intended to provide another method to analyze the subject's scores in performing the tasks as well as ability to use the planning aid in general. However, the subject population was almost entirely uniform in how they responded to the questions regarding computer and video game use and comfort level so no analysis could be performed.

9.5.3 Patient Modeling

Subjects did not experience any difficulty in interacting with the interface and did not commit any errors in entry of patient torso measurements. The only difficulty subjects experienced was with pronouncing the medical terms used to refer to the specific dimensions such as the transtubercular plane. It is expected that a subject from the target population of surgeons and nurses would not experience the same difficulty pronouncing medical terms. However the target population may experience difficulty interacting with the user interface compared with the test subject population. The test subjects were almost uniform in their comfort level and use of video games and computers and committed no errors so no statistical analysis could be performed on the results.

9.5.4 Port Placement

The example task used in training was oriented in portrait mode and was different from the torso outline used for the actual port placement test. To match the example, the subject would have had to stand where the patient legs would be. The image for the actual port placement test, as shown in Figure 63, was aligned horizontally with the head to the left and feet to the right when viewing the image which corresponded to the view from the patient right.

Most subjects were able to accomplish this task with little difficulty. A few subjects did not notice that port 5, the white assistant port, was at 15° from the horizontal instead of 30° from the horizontal as with the other ports. The median deviation from the target distance of 8cm was approximately 1cm, about half the width of each magnetic port marker as shown in Figure 89. The median deviation from the target angle of 15° or 30° was less than 5° as shown in Figure 90. There was no correlation found between spatial ability and the accuracy of the port placement as measured by the deviation from the target distance and angle. This may mean that the only sources error was in the use of the measuring devices and not the presentation of the port placement information. Most subjects expressed frustration with not remembering how to use a protractor or triangle. However, the objective of this part of the usability test was not to test their ability to use protractors, triangles, or rulers. The objective was to determine if the presentation of the port placement recommendations was effective and the results show that it accomplished that.

9.5.5 Positioning the Patient Cart

Subjects were asked to recall the key steps surgical teams would have to perform without the benefit of performing them on an actual da Vinci patient cart. The analysis of the test scores showed no correlation between the subject's spatial ability and their performance. The analysis did show a statistically significant improvement between the pre-test and post-test results. For the purposes of this usability test, this part of the decision aid was effective.

9.5.6 Posing the Robot Model

The subject questionnaire administered at the beginning of the usability test did not capture the subject's height. This was because the usability test was originally intended to be conducted with an actual da Vinci patient side cart instead of a small scale model. Some subjects whose height put them at eye level with the model expressed preference for that view. Subjects who were taller than the model expressed preference for the ceiling-level view. However, subjects did not perform any better with ceiling-level view than with eye-level view, regardless of their expressed preference. The data only showed a statistically significant effect with the interaction between order and view. The hypothesis was that subjects would perform best when shown the ceiling view. However, the results do not show this. Instead, subjects performed best when performing the task from the eye-level view when they were shown the ceiling-view first. This may be because subjects were able to understand angles of the arms shown on the

screen with the ceiling view. They then applied that knowledge when performing the task with the eye-level view.

10. Conclusion

This research was conducted to understand the human factors issues related to port placement in robot-assisted laparoscopic surgery. It focused on the cognitive task of considering the numerous factors in port placement, and, specifically, on manipulating the robot arms of the da Vinci Si Surgical System patient side cart to achieve a pose compatible with an optimal port placement plan. Other researchers have attempted to provide a solution to port placement but none have addressed the problem of transferring the technical solution to the operating room by achieving a suitable robot pose.

This research was a complex undertaking that was divided into four phases. The first phase consisted of a field study with observations and interviews with experts. This helped in understanding the domain and the issues that were not evident in the literature. The second phase focused on understanding the kinematics of the robot. Without a background in robotics, there was a lot of reliance on experts and books to gain the knowledge necessary to create a symbolic model of the da Vinci Si Surgical System.

The third phase involved the design of two different methods to capture dimensions of patient torsos. The methods developed provided a way to create a three-dimensional model of a patient's torso without unnecessary exposure to

radiation from CT scans or an MRI and can be performed while the patient is on the operating table and insufflated. In addition, a computational method was devised and a software program was written to calculate the goodness of port locations based on intracorporeal volume of instrument work envelopes.

The fourth phase combined the knowledge gained in the first three phases to design a decision aid to assist surgeons in pre-operative planning, the ultimate goal of this project. A wireframe of the decision aid was created and a formative usability test was conducted. The technology and methods do exist to make the planning aid a fully functional software tool. However, that would be beyond the scope of this research.

10.1. Recommendations for Future Work

Testing and validation of the computational method devised for comparing port placement locations could refine the algorithm and allow for real-time analysis of possible port locations in the operating room. This algorithm could be combined with a complete model of the robot for a real-time port placement and pose planning aid.

Based on the testing of decision aid, one way to remind surgical team members of the key steps in positioning the patient cart would be to attach or affix a summary sheet or check-list containing the key steps directly on the cart.

Likewise one of the simplest possible solutions to pose the robot based on inverse kinematic calculations would be to provide guides indicating degrees of rotation on each of the revolute robot joints with zero when the links are parallel

and +/- for each direction up to the limit of rotation. In addition, guides indicating the height on each of the prismatic joints from zero at the lowest to the maximum vertical adjustment would be easy to implement.

Based on observations of how the subjects interacted with the image of the robot on screen, the ability to toggle between ceiling and eye-level views might have been a better design. It may be that some angles are easier to understand from the eye-level view than the ceiling level view. Another method may be to give users the ability to freely rotate the model and view it from whatever perspective this preferred. Unfortunately, this method model was too complex for the graphical display to show. This would slow down the user interface to an unacceptable level of responsiveness.

11. References

ACOG Education Pamphlet AP074 -- Uterine Fibroids. (n.d.). . Retrieved April 18, 2011, from http://www.acog.org/publications/patient_education/bp074.cfm

Adhami, L., & Coste-Manière, È. (2003). Optimal planning for minimally invasive surgical robots. *IEEE Transactions on Robotics and Automation*, *19*(5), 854-863. doi:10.1109/TRA.2003.817061

Advincula, A. P., & Wang, K. (2009). Evolving Role and Current State of Robotics in Minimally Invasive Gynecologic Surgery. *Journal of Minimally Invasive Gynecology*, 16(3), 291-301.

Ambardar, S., Cabot, J., Cekic, V., Baxter, K., Arnell, T. D., Forde, K. A., Nihalani, A., et al. (2008). Abdominal wall dimensions and umbilical position vary widely with BMI and should be taken into account when choosing port locations. *Surgical Endoscopy*, *23*(9), 1995-2000. doi:10.1007/s00464-008-9965-1

Balogun, F. A., Brunetti, A., & Cesareo, R. (2000). Volume of intersection of two cones. Radiation Physics and Chemistry, 59(1), 23–30.

Barnum, C. M. (2011), *Usability Testing Essentials: Ready, Set… Test!.* Burlington, MA: Morgan Kaufmann.

Cannon, J. W., Stoll, J. A., Selha, S. D., Dupont, P. E., Howe, R. D., & Torchiana, D. F. (2003). Port placement planning in robot-assisted coronary artery bypass. *IEEE Transactions on Robotics and Automation*, *19*(5), 912-917. doi:10.1109/TRA.2003.817502

Carney, R. N., & Levin, J. R. (2002). Pictorial illustrations still improve students' learning from text. *Educational Psychology Review*, 14(1), 5–26.

Cestari, A., Buffi, N. Ú. M., Scapaticci, E., Lughezzani, G., Salonia, A., Briganti, A., Rigatti, P., et al. (2010). Simplifying Patient Positioning and Port Placement During Robotic-Assisted Laparoscopic Prostatectomy. *European urology*, *57*(3), 530–533.

Coste-Manière, È., Adhami, L., Mourgues, F., & Carpentier, A. (2003). Planning, simulation, and augmented reality for robotic cardiac procedures: The STARS

system of the ChIR team. *Seminars in Thoracic and Cardiovascular Surgery* (Vol. 15, p. 141–156).

Coste-Manière, È., Adhami, Louaï, Mourgues, Fabien, & Bantiche, O. (2004). Optimal Planning of Robotically Assisted Heart Surgery: First Results on the Transfer Precision in the Operating Room. *The International Journal of Robotics Research*, *23*(4), 539-548. doi:10.1177/0278364904042205

Covidien Surgical 173030. (n.d.). Retrieved May 31, 2012, from http://www.autosuture.com/autosuture/pagebuilder.aspx?topicID=13479&breadcrumbs=0:63659,41313:0,31403:0,7478:0

Laparoscopic Instruments - Laparoscopic Instruments : Stryker. (n.d.). Retrieved May 31, 2012, from http://www.stryker.com/en-us/products/Endoscopy/Laparoscopy/LaparoscopicInstruments/LaparoscopicInstruments/index.htm

Dal Moro, F., Secco, S., Valotto, C., Artibani, W., & Zattoni, F. (2011). Specific learning curve for port placement and docking of da Vinci® Surgical System: one surgeon's experience in robotic-assisted radical prostatectomy. *Journal of Robotic Surgery*. doi:10.1007/s11701-011-0315-2

Emam, T. A., Hanna, G. B., Kimber, C., Dunkley, P., & Cuschieri, A. (2000). Effect of intracorporeal-extracorporeal instrument length ratio on endoscopic task performance and surgeon movements. Archives of Surgery, 135(1), 62–66.

Falk, Volkmar, Mourgues, Fabien, Adhami, Louaï, Jacobs, Stefan, Thiele, H., Nitzsche, S., Mohr, Friedrich W, et al. (2005). Cardio Navigation: Planning, Simulation, and Augmented Reality in Robotic Assisted Endoscopic Bypass Grafting. *Ann Thorac Surg*, *79*(6), 2040-2047.

Ferzli, G. S., & Fingerhut, A. (2004). Trocar placement for laparoscopic abdominal procedures: a simple standardized method. *Journal of the American College of Surgeons*, 198(1), 163-173. doi:doi: DOI: 10.1016/j.jamcollsurg.2003.08.010

Feuerstein, M., Wildhirt, S., Bauernschmitt, R., & Navab, N. (2005). Automatic Patient Registration for Port Placement in Minimally Invasive Endoscopic Surgery. *Medical Image Computing and Computer-Assisted Intervention–MICCAI 2005*, 287–294.

Fingerhut, A., Hanna, G. B., Veyrie, N., Ferzli, G., Millat, B., Alexakis, N., & Leandros, E. (2010). Optimal trocar placement for ergonomic intracorporeal sewing and knotting in laparoscopic hiatal surgery. *The American Journal of Surgery*.

Gomes, P. (2011). Surgical robotics: Reviewing the past, analysing the present, imagining the future. *Robotics and Computer-Integrated Manufacturing*, *27*(2), 261–266.

Hanna, G. B., Shimi, S., & Cuschieri, A. (1997). Optimal port locations for endoscopic intracorporeal knotting. Surgical endoscopy, 11(4), 397–401.

Hayashibe, M., Suzuki, N., Hashizume, M., Kakeji, Y., Konishi, K., Suzuki, S., & Hattori, A. (2005). Preoperative planning system for surgical robotics setup with kinematics and haptics. *International Journal of Medical Robotics and Computer Assisted Surgery*, 01(02), 76. doi:10.1581/mrcas.2005.010208

Hijttenlocher, J., & Presson, C. (1973). Mental Rotation and the Perspective Problem1. *Cognitive Psychology*, *4*, 277–299.

Hu, J. C., Wang, Q., Pashos, C. L., Lipsitz, S. R., & Keating, N. L. (2008). Utilization and Outcomes of Minimally Invasive Radical Prostatectomy. Journal of Clinical Oncology, 26(14), 2278–2284. doi:10.1200/JCO.2007.13.4528

Intuitive Surgical., (2009), da Vinci Si Surgical System User Manual P/N 550650-02 Rev. B 2009.09

Intuitive Surgical - Surgical Specialties. (n.d.). . Retrieved March 30, 2011, from http://www.intuitivesurgical.com/specialties/

Intuitive Surgical., (2006), da Vinci® Prostatectomy PN 871414 Rev. A 12/06

Kenngott, H. G., Fischer, L., Nickel, F., Rom, J., Rassweiler, J., & Müller-Stich, B. P. (2011). Status of robotic assistance—a less traumatic and more accurate minimally invasive surgery? *Langenbeck's Archives of Surgery*, *397*(3), 333–341. doi:10.1007/s00423-011-0859-7

Khalil, W., and Lemoine, P., (2003) Symoro+: Symbolic Modeling of Robots User's Guide. [Software]

Kieras, D. E., & Bovair, S. (1984). The role of a mental model in learning to operate a device. Cognitive Science, 8(3), 255–273. doi:10.1016/S0364-0213(84)80003-8

King, W. A. (1975). A Comparison of Three Combinations of Text and Graphics for Concept Learning. (p. 20p). United States.

Krull, R., D'Souza, S. J., Roy, D., & Sharp, D. M. (2004). Designing Procedural Illustrations. *IEEE Transactions on Professional Communication*, 47(1), 27-33. doi:10.1109/TPC.2004.824288

Kumar, S., & Fusai, G. (2007). Laparoscopic cholecystectomy in situs inversus totalis with left-sided gall bladder. *Annals of The Royal College of Surgeons of England*, 89(2), 16-18. doi:10.1308/147870807X160461

Lalchandani, S., & Philips, K.(2008). Laparoscopic Entry Techniques: Consensus. In P. O'Donovan (Ed.), *Complications in Gynecological Surgery* (pp. 20-33) . London: Springer-Verlag.

Matthews, C. A., Schubert, C. M., Woodward, A. P., & Gill, E. J. (2010). Variance in Abdominal Wall Anatomy and Port Placement in Women Undergoing Robotic Gynecologic Surgery. *Journal of Minimally Invasive Gynecology*, 17(5), 583–586.

Moglia, A., Turini, G., Ferrari, V., Ferrari, M., & Mosca, F. (2011). Patient specific surgical simulator for the evaluation of the movability of bimanual robotic arms. *Studies in Health Technology and Informatics* (Vol. 163, pp. 379–385).

Parkin, R. A. (1991). *Applied Robotic Analysis.* Englewood Cliffs, NJ: Prentice-Hall Inc.

Pasic, R. P., & Levine, R. L. (2007). A Practical Manual of Laparoscopy and Minimally Invasive Gynecology: A Clinical Cookbook. Taylor and Francis. Retrieved from http://books.google.com/books?id=L5x1LU8xNCEC

Pasticier, G., Rietbergen, J. B. W., Guillonneau, B., Fromont, G., Menon, M., & Vallancien, G. (2001). Robotically assisted laparoscopic radical prostatectomy: Feasibility study in men. *European Urology*, *40*(1), 70-74.

Patient Information for Laparoscopic Gall Bladder Removal (Cholecystectomy) from SAGES | Society of American Gastrointestinal and Endoscopic Surgeons. (n.d.). . Retrieved April 19, 2011, from http://www.sages.org/publication/id/PI11/

Patle, N. M., Tantia, O., Sasmal, P. K., Khanna, S., & Sen, B. (2010). Laparoscopic Cholecystectomy In Situs Inversus - Our Experience of 6 Cases. *Indian Journal of Surgery*, 72(5), 391-394. doi:10.1007/s12262-010-0159-4

Pick, D. L., Lee, D. I., Skarecky, D. W., & Ahlering, T. E. (2004). Anatomic guide for port placement for daVinci robotic radical prostatectomy. *Journal of endourology*, *18*(6), 572–575.

Rassweiler, J., Hruza, M., Klein, J., Goezen, A. S., & Teber, D. (2010). The role of laparoscopic radical prostatectomy in the era of robotic surgery. *European Urology Supplements*, 9(3), 379–387.

Reynolds Jr, W. (2001). The first laparoscopic cholecystectomy. *JSLS: Journal of the Society of Laparoendoscopic Surgeons*, 5(1), 89.

Schuessler, W. W., Schulam, P. G., Clayman, R. V., & Kavoussi, L. R. (1997). Laparoscopic radical prostatectomy: Initial short-term experience. *Urology*, 50(6), 854-857.

Shafer, D. M., Khajanchee, Y., Wong, J., & Swanström, L. L. (2006). Comparison of five different abdominal access trocar systems: analysis of insertion force, removal force, and defect size. *Surgical Innovation*, *13*(3), 183.

Spong, M.W., Hutchinson, S., Vidyasagar, M. (2006). *Robot Modeling and Control*. Hoboken, NJ : John Wiley & Sons

Sun, L. W., Van Meer, F., Schmid, J., Bailly, Y., Thakre, A. A., & Yeung, C. K. (2007). Advanced da Vinci surgical system simulator for surgeon training and operation planning. The International Journal of Medical Robotics and Computer Assisted Surgery, 3(3), 245–251. doi:10.1002/rcs.139

Sun, L. W., & Yeung, C. K. (2007). Port placement and pose selection of the da Vinci surgical system for collision-free intervention based on performance optimization. *Intelligent Robots and Systems*, 2007. IROS 2007. IEEE/RSJ International Conference on (pp. 1951–1956).

Tabaie, H. A., Reinbolt, J. A., Graper, W. P., Kelly, T. F., & Connor, M. A. (1999). Endoscopic coronary artery bypass graft (ECABG) procedure with robotic assistance. *Heart Surg Forum* (Vol. 2, p. 310–317).

Taylor, H., & Rapp, D. (2004). Where is the donut? Factors influencing spatial reference frame use. *Cognitive Processing*, 5(3). doi:10.1007/s10339-004-0022-2

Trejos, A. L., Patel, R. V., Ross, I., & Kiaii, B. (2007). Optimizing port placement for robot-assisted minimally invasive cardiac surgery. *The International Journal of Medical Robotics and Computer Assisted Surgery*, *3*(4), 355-364. doi:10.1002/rcs.158

Zar, J. H. (1972). Significance Testing of the Spearman Rank Correlation Coefficient. Journal of the American Statistical Association, 67(339), 578–580. doi:10.1080/01621459.1972.10481251

Zorn, K. C., Gofrit, O. N., Orvieto, M. A., Mikhail, A. A., Galocy, R. M., Shalhav, A. L., & Zagaja, G. P. (2007). Da Vinci Robot Error and Failure Rates: Single Institution Experience on a Single Three-Arm Robot Unit of More than 700 Consecutive Robot-Assisted Laparoscopic Radical Prostatectomies. *Journal of Endourology*, *21*(11), 1341-1344. doi:10.1089/end.2006.0455

Appendix A. Patient Torso Model

The Mathematica expression to create the 3D torso shown in Figure 17 is as follows:

```
Manipulate[
 torso=ParametricPlot3D[{z,a*Cos[t], b*Sin[t]}, {t,
  0,2Pi},{z,-maxz,maxz},  Mesh->True, BoundaryStyle->
  Black][[1]];
 abdomen=ParametricPlot3D[{Sqrt[r^2-
  u^2]Cos[theta]+shiftx, Sqrt[r^2-
  u^2]Sin[theta]+shifty,u+shiftz},{u,0.5b,r},{theta,0,
  2Pi}, Mesh->True, BoundaryStyle->Black][[1]];
 rt=1;
 targetOrgan=ParametricPlot3D[{Sqrt[rt^2-
  ut^2]Cos[thetat]+shiftxx, Sqrt[rt^2-
  ut^2]Sin[thetat]+shiftyy,ut+shiftzz},{ut,-
  rt,rt},{thetat,0,2Pi}, Mesh->True, BoundaryStyle-
  >Black][[1]];
 Graphics3D[{{Opacity[0.5],abdomen},{Opacity[0.5],
  torso}, {Red, targetOrgan}},Background-
  >LightBlue,Axes->True],{{a, 25,
  "Width"},20,30,1},{{b,12,"Thickness"},10,20,1},
  {{maxz,20,"Torso Length"},10,50,1},
  {{r,20,"Radius"},10,40,1},
  {{curve,0.5,"Curvature"},0.1,0.9,0.1},
  {{shiftx,0,"Abdomen Longitudinal"},-
  20,20,1},{{shifty,0,"Abdomen Lateral"},-
  20,20,1},{{shiftz,0,"Abdomen Vertical"},-40,0,1},
  {{shiftxx,0,"Target Longitudinal"},-
  20,20,1},{{shiftyy,0,"Target Lateral"},-
  20,20,1},{{shiftzz,0,"Target Vertical"},-20,20,1},
  TrackedSymbols->Manipulate]
```

Subsequent prototypes were created that improved the approximation of the human abdomen with respect to shape including taper at the hips and rib cage. This is shown in Figure 96.

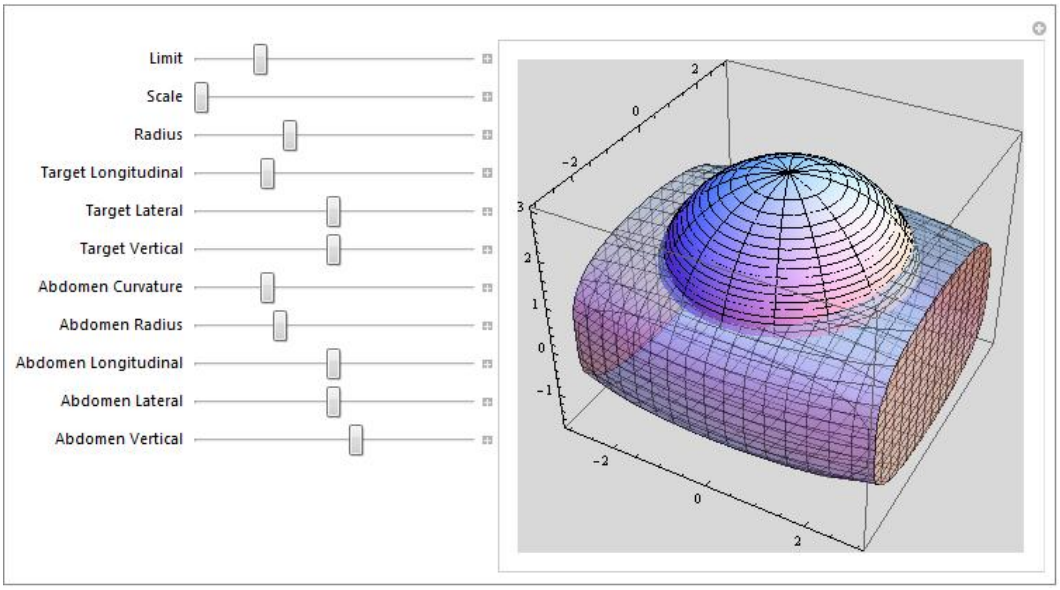

Figure 96. 3D Torso Model Interface Prototype

The Mathematica expression to create Figure 96 is as follows:

```
Manipulate[
 abdomen=ContourPlot3D[x^2+y^2+(z-za)^2==8, {x, -
  limit, limit}, {y, -limit, limit}, {z, 1.1,
  limit+za}, Mesh->True][[1]];
 target=ContourPlot3D[(x-shiftx)^2+(y-shifty)^2+(z-
  shiftz)^2==.1, {x, -limit, limit}, {y, -limit,
  limit}, {z, -limit, limit},Mesh->None][[1]];
 torso=ContourPlot3D[1/4(x)^2+(y)^2+(z)^4==3*limit,{x,
  -limit, limit}, {y, -limit, limit}, {z, -limit,
  limit}, Mesh->True][[1]];
 Graphics3D[{{Opacity[0.5],torso},target,{Opacity[0.5]
  ,abdomen}}, Background->LightBlue, Axes->True,
  Locator],
 {{limit,3,"Limit (3 is best.)"},1,10,1},
 {{shiftx,0,"Target Longitudinal"},-1.5,1.5,.1},
 {{shifty,0,"Target Lateral"}, -1.5,1.5,.1},
 {{shiftz,0,"Target Vertical"}, -1.5,1.5,0.1},
 {{za,-0.1,"Abdomen Height"}, -1/3limit, 1/3limit,
  0.1},
 TrackedSymbols->Manipulate]
```

The Mathematica expression to create Figure 18 is as follows:

```
Manipulate[
```

```
abdomen=ContourPlot3D[x^2+y^2+(z-za)^2==8, {x,-
 limit,limit}, {y,-limit,limit}, {z,1.1,limit+za},
 Mesh->False][[1]];
target=ParametricPlot3D[{Sqrt[r^2-
 u^2]Cos[theta]+shiftx, Sqrt[r^2-
 u^2]Sin[theta]+shifty,u+shiftz}, {u,-r,r},
 {theta,0,2Pi},Mesh->False][[1]];
torso=ContourPlot3D[1/4(x)^2+(y)^2+(z)^4==3*limit,
 {x,-limit,limit}, {y,-limit,limit}, {z,-
 limit,limit}, Mesh->False][[1]];
Graphics3D[{{Opacity[0.5],torso}, {Red,target},
 {Opacity[0.5],abdomen}},Background->LightBlue,Axes-
 >True], {{r,0.3,"Target Radius"},0.1,1,0.1},
 {{limit,3,"Torso Ratio"},3,5,0.5}, {{shiftx,-
 1,"Target Longitudinal"}, -limit,limit,.1},
 {{shifty,0,"Target Lateral"}, -limit,limit,.1},
 {{shiftz,0,"Target Vertical"}, -limit,limit,0.1},
 {{za,-0.1,"Abdomen Height"},-limit,limit,0.1},
 TrackedSymbols->Manipulate]
```

The model was exported to the Virtual Reality Modeling Language (VRML) file format into the three components for import into Blender as follows:

```
Export["abdomen.wrl",abdomen, "VRML"];
Export["torso.wrl",torso, "VRML"];
Export["target.wrl",target, "VRML"];
```

The components are processed and positioned into the scene with an example image created shown in Figure 19.

Appendix B. Usability Test Port Placement

B.1 Port Placement - Training

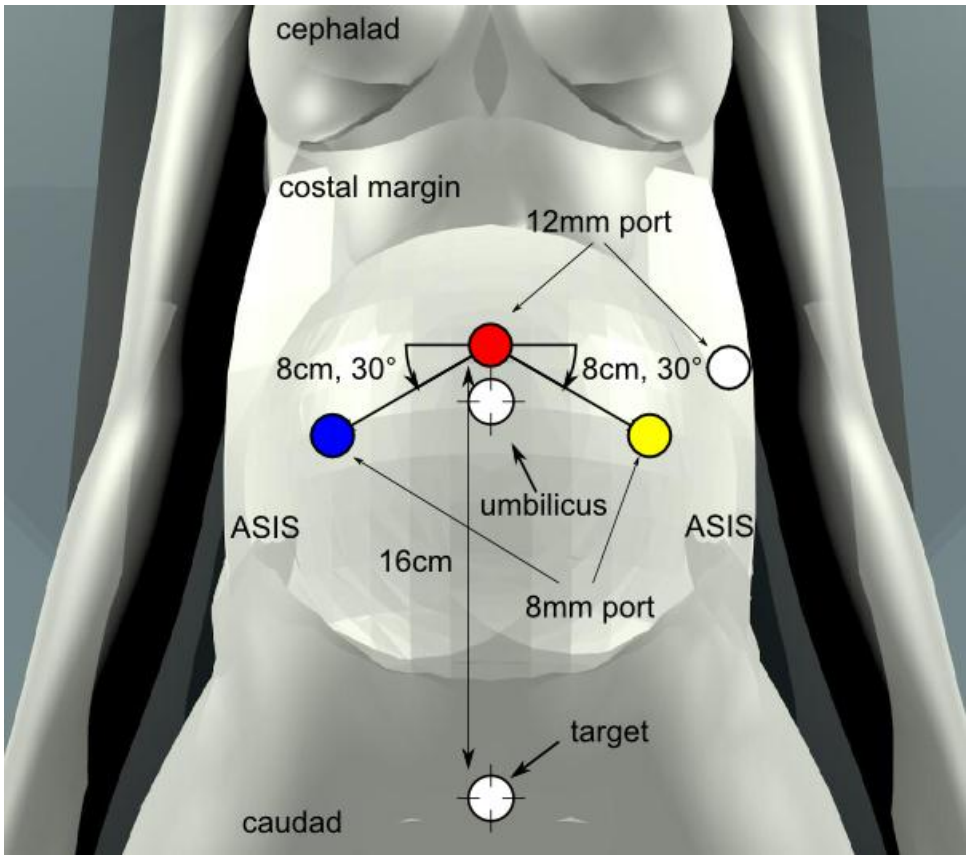

Figure 97. Example Port Placement - Sacrocolpopexy

B.2 Port Placement - Actual

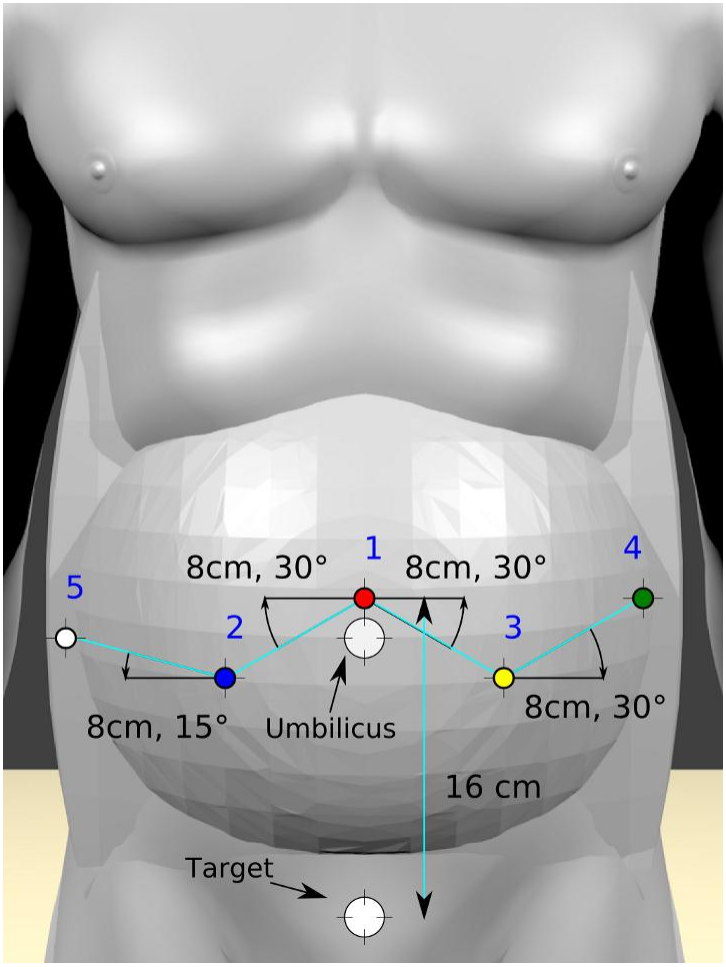

Figure 98. Example Port Placement - Radical Prostatectomy

Appendix C. Octave Program for Calculating Reachability and Interference

Listing 1. analysis.m

```
#Constants
distPorts = 8; # distance between port centers (8 - 10cm)
#distPorts = 10; # distance between port centers (8 - 10cm)
alpha15 = pi/12; # (radians) 15 degrees,
alpha30 = pi/6; # (radians) 30 degrees,
alpha45 = pi/4; # (radians) 45 degrees
# Radial Pattern
anglePort1 = alpha15;
anglePort2 = alpha15;
anglePort3 = alpha45;
offsetX = 2; # +/- distance offset from base port location for
x axis.
offsetZ = 2; # +/- distance offset from base port location for
z axis.

# Define the limits of analysis bounded by rectangular box
xmin = -20; # (integer) minimum x-axis
xmax = 20; # (integer) maximum x-axis
ymin = -6; # (integer) minimum y-axis
ymax = 14 ; # (integer) maximum y-axis
zmin = -6; # (integer) minimum z-axis
zmax = 20; # (integer) maximum z-axis
resolution = .1; # (integer) points per cm cube
totalVolume = (xmax-xmin)*(ymax-ymin)*(zmax-zmin);
boundary = [xmin xmax ymin ymax zmin zmax resolution
totalVolume];

# Locations
v0 = [ 0 0 0 ]; # center of target region sphere
targetRadius = 2; # radius of target region sphere
target = [v0 targetRadius];

# Constants for calculating y values
# Patient 1
torsoWidth = 30; # width of torso (cm)
torsoThickness = 22; # sagittal thickness of torso (cm)

# Patient 2
#torsoWidth = 40; # width of torso (cm)
#torsoThickness = 28; # sagittal thickness of torso (cm)

# Parameters for defining the elliptical cross-section of the
torso
semiMajor = torsoWidth/2; # semi-major axis
semiMinor = torsoThickness/2; # semi-minor axis
```

```
# Define endoscope port location based on endoscope location in
X-Z plane, torso width, and torso thickness.
portE = zeros (1,3);
portE(1) = 0; # x-axis position
portE(3) = 18; # z-axis position
portE(2) = ellipseY (portE(1), semiMajor, semiMinor);

# Calculate locations for ports 1, 2, and 3 based
# calculation based on the location of this port, e.g.,
endoscope port location
# distance between ports
# angle between ports from horizontal,
# offset from x (-1: to patient right, +1: to patient left)
# offset from z (-1: lower (caudad) , +1, higher (cephalad))
# half Torso Width
# half Sagittal Thickness
port1 = locatePort(portE, distPorts, anglePort1, -1,-1,
semiMajor, semiMinor);
port2 = locatePort(portE, distPorts, anglePort2, 1,-1,
semiMajor, semiMinor);
# Robot-Assisted Pattern
#port3 = locatePort(port1, distPorts, anglePort3, -1, 1,
semiMajor, semiMinor);
# Conventional Pattern
port3 = locatePort(port1, distPorts, anglePort3, -1, -1,
semiMajor, semiMinor);

#ports = [portE; port1; port2; port3];

# Define cone angles to axis in radians
#thetaE = pi/9; #20 degrees.  endoscope view angle is
approximately 40 degrees
thetaE = pi/12; #15 degrees
theta1 = pi/24; #7.5 degrees
theta2 = pi/24; #7.5 degrees
theta3 = pi/24; #7.5 degrees

thetas = zeros (1,4);
thetas(1) = thetaE;
thetas(2) = theta1;
thetas(3) = theta2;
thetas(4) = theta3;
```

```
# Different offsets for port 1
portOffsets1 = zeros(1,3);
portOffsets2 = zeros(1,3);
i = 1;
portOffsetsAll1 = zeros(9,3);
portOffsetsAll2 = zeros(9,3);
for dz = [-2*offsetZ, -offsetZ, 0, offsetZ, 2*offsetZ;]
 portOffsets1(3) = port1(3) + dz;
 portOffsets2(3) = port2(3) + dz;
 # For Patient 1, port 3 -offset will be outside of torso
 #for dx = [-offsetX, 0, offsetX;]
 for dx = [-2*offsetX, -offsetX, 0, offsetX, 2*offsetX;]
  portOffsets1(1) = port1(1) + dx;
  portOffsets1(2) = ellipseY(portOffsets1(1), semiMajor,
semiMinor);
  portOffsetsAll1(i,:) = [portOffsets1];
  portOffsets2(1) = port2(1) + dx;
  portOffsets2(2) = ellipseY(portOffsets2(1), semiMajor,
semiMinor);
  portOffsetsAll2(i,:) = [portOffsets2];
  i++;
 end
end
# Different offsets for port 3
portOffsets3 = zeros(1,3);
i = 1;
# use zeros(1,3) for fixed port 3
#portOffsetsAll3 = zeros(1,3);
# use zeros(9,3) for 9 positions of port 3
portOffsetsAll3 = zeros(9,3);
%{
for dz = [-offsetZ, 0, offsetZ;]
 portOffsets3(3) = port3(3) + dz;
 for dx = [-offsetX, 0, offsetX;]
 for dx = [-offsetX, 0, offsetX;]
  if (((port3(1) + dx) < -semiMajor) && ((port3(1) + dx) <
semiMajor))
   portOffsets3(1) = -semiMajor;
  elseif ((port3(1) + dx) > -semiMajor) && ((port3(1) + dx) >
semiMajor)
   portOffsets3(1) = semiMajor;
  else
   portOffsets3(1) = port3(1) + dx;
  end
  portOffsets3(2) = ellipseY(portOffsets3(1), semiMajor,
semiMinor);
  portOffsetsAll3(i,:) = [portOffsets3];
  i++;
 end
end
%}
```

```
T = size(portOffsetsAll1,1);
U = size(portOffsetsAll2,1);
%{
V = size(portOffsetsAll3,1);
%}

filename = 'analysisPatient1by08cmCby4.csv';
fid = fopen(filename, 'w');

columnHeader =
{"N","portEX","portEY","portEZ","port1X","port1Y","port1Z","por
t2X","port2Y","port2Z","port3X","port3Y","port3Z","thetaE","the
ta1","theta2","theta3","ptsTotal","ptsInSphere","ptsInConeE","p
tsInCone1","ptsInCone2","ptsInCone3","ptsInAll","ptsInst12Colli
de","ptsInst13Collide","ptsInst23Collide","ptsInstAllCollide","
reachability","pctTotalVol12Collide","pctTotalVol13Collide","pc
tTotalVol23Collide","pctTotalVolAllCollide","pctOverlap12","pct
Overlap21","pctOverlap13","pctOverlap31","pctOverlap23","pctOve
rlap32","pctVolCollide","errSphere","errConeE","errCone1","errC
one2","errCone3"};

fprintf(fid,'%s, %s, %s, %s, %s, %s, %s, %s, %s, %s, %s, %s,
%s, %s, %s, %s, %s, %s, %s, %s, %s, %s, %s, %s, %s, %s, %s, %s,
%s, %s, %s, %s, %s, %s, %s, %s, %s, %s, %s, %s, %s, %s, %s, %s,
%s\n', columnHeader{1,:});

%{
analysis = analyzePorts (boundary, target, ports, thetas);
fix(analysis);

fprintf(fid, '%d, %f, %f, %f, %f, %f, %f, %f, %f, %f, %f, %f,
%f, %f, %f, %f, %f, %d, %d, %d, %d, %d, %d, %d, %d, %d, %d, %d,
%f, %f, %f, %f, %f, %f, %f, %f, %f, %f, %f, %f, %f\n' , j,
portE(1), portE(2), portE(3), port1(1), port1(2), port1(3),
port2(1), port2(2), port2(3), port3(1), port3(2), port3(3),
thetas(1), thetas(2), thetas(3), thetas(4), analysis(1),
analysis(2), analysis(3), analysis(4), analysis(5),
analysis(6), analysis(7), analysis(8), analysis(9),
analysis(10), analysis(11), analysis(12), analysis(13),
analysis(14), analysis(15), analysis(16), analysis(17),
analysis(18), analysis(19), analysis(20), analysis(21),
analysis(22), analysis(23), analysis(24))
%}

fclose(fid);
```

```
j = 1;
for t = (1:T)
 for u = (1:U)
  %{
  for v = (1:V)
  %}
   fprintf('Processing combination %d ... \n', j)
   newPort1 = portOffsetsAll1(t,:);
   newPort2 = portOffsetsAll2(u,:);
   %{
   newPort3 = portOffsetsAll3(v,:);
   %}
   newPort3 = port3;

   ports = [portE; newPort1; newPort2; newPort3];
   analysis = analyzePorts (boundary, target, ports, thetas);

   fid = fopen(filename, 'a');
   fprintf('Writing to file %s.\n', filename)

   fprintf(fid, '%d, %f, %f, %f, %f, %f, %f, %f, %f, %f, %f,
%f, %f, %f, %f, %f, %f, %d, %d, %d, %d, %d, %d, %d, %d, %d, %d,
%d, %f, %f, %f, %f, %f, %f, %f, %f, %f, %f, %f, %f, %f, %f, %f,
%f, %f\n' , j, portE(1), portE(2), portE(3), newPort1(1),
newPort1(2), newPort1(3), newPort2(1), newPort2(2),
newPort2(3), newPort3(1), newPort3(2), newPort3(3), thetas(1),
thetas(2), thetas(3), thetas(4), analysis(1), analysis(2),
analysis(3), analysis(4), analysis(5), analysis(6),
analysis(7), analysis(8), analysis(9), analysis(10),
analysis(11), analysis(12), analysis(13), analysis(14),
analysis(15), analysis(16), analysis(17), analysis(18),
analysis(19), analysis(20), analysis(21), analysis(22),
analysis(23), analysis(24), analysis(25), analysis(26),
analysis(27), analysis(28))

   fclose(fid);
   #timeNow = fix(clock)
   j++;
  %{
  end
  %}
 end
end
```

Listing 2. analyzePorts.m

```
function output = analyzePorts(boundary, target, ports,
coneAngles)
# Constants
maxPoints = 25E6; # Maximum number of points in ndgrid

# Define the limits of analysis bounded by rectangular box
xmin = boundary(1);
xmax = boundary(2);
ymin = boundary(3);
ymax = boundary(4);
zmin = boundary(5);
zmax = boundary(6);
res = boundary(7);
analysisVolume = boundary(8);

F = [X,Y,Z] = ndgrid(xmin:res:xmax, ymin:res:ymax,
zmin:res:zmax);
pointsTotal = numel(F);
if (pointsTotal > maxPoints)
 printf("Too many points. Exiting.\n");
 break;
endif

#Target Region
v0 = target(1:3);
targetRadius = target(4);

#Endoscope and Instrument Ports
portE = ports(1,:);
port1 = ports(2,:);
port2 = ports(3,:);
port3 = ports(4,:);

# Define cone angles to axis in radians
thetaE = coneAngles(1);
theta1 = coneAngles(2);
theta2 = coneAngles(3);
theta3 = coneAngles(4);

vE = portE - v0;
v1 = port1 - v0;
v2 = port2 - v0;
v3 = port3 - v0;

# Calculate the points that are on or inside the target sphere
R = sqrt((v0(1) - X).^2 + (v0(2) - Y).^2 + (v0(3) - Z).^2);
insideSphere = R <= targetRadius;
outsideSphere = R > targetRadius;
```

```
# Calculate accuracy of sphere volume estimate
pointsInsideSphere = sum(sum(sum(insideSphere)));
errorSphere = accuracySphere (pointsInsideSphere, pointsTotal,
analysisVolume, targetRadius);

#Calculate height of cones and add radius of target sphere
magE = sqrt(vE(1)^2 + vE(2)^2 + vE(3)^2);
mag1 = sqrt(v1(1)^2 + v1(2)^2 + v1(3)^2);
mag2 = sqrt(v2(1)^2 + v2(2)^2 + v2(3)^2);
mag3 = sqrt(v3(1)^2 + v3(2)^2 + v3(3)^2);
dE = magE + targetRadius;
d1 = mag1 + targetRadius;
d2 = mag2 + targetRadius;
d3 = mag3 + targetRadius;

baseRadiusE = tan(thetaE)*dE;
baseRadius1 = tan(theta1)*d1;
baseRadius2 = tan(theta2)*d2;
baseRadius3 = tan(theta3)*d3;

# Find points inside angle of endoscope extended to infinity
dotProductE = (vE(1) * (vE(1) .- X)) + (vE(2) * (vE(2) .- Y)) +
(vE(3) * ( vE(3) .- Z));
magVPE  = sqrt((vE(1) - X).^2 + (vE(2) - Y).^2 + (vE(3) -
Z).^2);
denomE = magE .* magVPE;
angleE = acos(dotProductE ./ denomE);
scalarProjectE = dotProductE ./ magE;
insideConeE = (angleE <= thetaE) & (scalarProjectE <= dE);
pointsInsideConeE = sum(sum(sum(insideConeE)));

# Find points inside angle of instrument 1 extended to infinity
dotProduct1 = (v1(1) * (v1(1) .- X)) + (v1(2) * (v1(2) .- Y)) +
(v1(3) * ( v1(3) .- Z));
magVP1  = sqrt((v1(1) - X).^2 + (v1(2) - Y).^2 + (v1(3) -
Z).^2);
denom1 = mag1 .* magVP1;
angle1 = acos(dotProduct1 ./ denom1);
scalarProject1 = dotProduct1 ./ mag1;
insideCone1 = (angle1 <= theta1) & (scalarProject1 <= d1);
pointsInsideCone1 = sum(sum(sum(insideCone1)));

# Find points inside angle of instrument 2 extended to infinity
dotProduct2 = (v2(1) * (v2(1) .- X)) + (v2(2) * (v2(2) .- Y)) +
(v2(3) * ( v2(3) .- Z));
magVP2  = sqrt((v2(1) - X).^2 + (v2(2) - Y).^2 + (v2(3) -
Z).^2);
denom2 = mag2 .* magVP2;
angle2 = acos(dotProduct2 ./ denom2);
scalarProject2 = dotProduct2 ./ mag2;
insideCone2 = (angle2 <= theta2) & (scalarProject2 <= d2);
pointsInsideCone2 = sum(sum(sum(insideCone2)));
```

```
# Find points inside angle of instrument 3 extended to infinity
dotProduct3 = (v3(1) * (v3(1) .- X)) + (v3(2) * (v3(2) .- Y)) +
(v3(3) * ( v3(3) .- Z));
magVP3  = sqrt((v3(1) - X).^2 + (v3(2) - Y).^2 + (v3(3) -
Z).^2);
denom3 = mag3 .* magVP3;
angle3 = acos(dotProduct3 ./ denom3);
scalarProject3 = dotProduct3 ./ mag3;
insideCone3 = (angle3 <= theta3) & (scalarProject3 <= d3);
pointsInsideCone3 = sum(sum(sum(insideCone3)));

# Calculate accuracy of cone volume estimate
errorConeE = accuracyCone (pointsInsideConeE, pointsTotal,
analysisVolume, baseRadiusE, dE);
errorCone1 = accuracyCone (pointsInsideCone1, pointsTotal,
analysisVolume, baseRadius1, d1);
errorCone2 = accuracyCone (pointsInsideCone2, pointsTotal,
analysisVolume, baseRadius2, d2);
errorCone3 = accuracyCone (pointsInsideCone3, pointsTotal,
analysisVolume, baseRadius3, d3);

allInside = insideSphere & insideConeE & insideCone1 &
insideCone2 & insideCone3;
pointsInsideAll = sum(sum(sum(allInside)));
reachability = 100*pointsInsideAll/pointsInsideSphere;

instrument12Collide = outsideSphere & insideCone1 &
insideCone2;
instrument13Collide = outsideSphere & insideCone1 &
insideCone3;
instrument23Collide = outsideSphere & insideCone2 &
insideCone3;
# Volume of All Instruments Outside The Sphere
instrumentAllCollide = outsideSphere & insideCone1 &
insideCone2 & insideCone3;
# Volume of All Cones Combined
instrumentAll = insideCone1 | insideCone2 | insideCone3;

pointsInstrument12Collide = sum(sum(sum(instrument12Collide)));
pointsInstrument13Collide = sum(sum(sum(instrument13Collide)));
pointsInstrument23Collide = sum(sum(sum(instrument23Collide)));
pointsInstrumentAllCollide =
sum(sum(sum(instrumentAllCollide)));
pointsInstrumentAll = sum(sum(sum(instrumentAll)));

# Percent of Total Volume where two work volumes collide
pctTotalVol12Collide =
100*pointsInstrument12Collide/pointsTotal;
pctTotalVol13Collide =
100*pointsInstrument13Collide/pointsTotal;
```

```
pctTotalVol23Collide =
100*pointsInstrument23Collide/pointsTotal;
pctTotalVolAllCollide =
100*pointsInstrumentAllCollide/pointsTotal;

# Interference
# Percent of Instrument Work Volume Coinciding with another
instrument
pctOverlap12 = 100*pointsInstrument12Collide/pointsInsideCone1;
pctOverlap21 = 100*pointsInstrument12Collide/pointsInsideCone2;
pctOverlap13 = 100*pointsInstrument13Collide/pointsInsideCone1;
pctOverlap31 = 100*pointsInstrument13Collide/pointsInsideCone3;
pctOverlap23 = 100*pointsInstrument23Collide/pointsInsideCone2;
pctOverlap32 = 100*pointsInstrument23Collide/pointsInsideCone3;
# Percentage of total volume of all instrument cones with
collision
pctVolumeCollide =
100*pointsInstrumentAllCollide/pointsInstrumentAll;

#Output analysis as an array
analysis(1) = pointsTotal;
analysis(2) = pointsInsideSphere;
analysis(3) = pointsInsideConeE;
analysis(4) = pointsInsideCone1;
analysis(5) = pointsInsideCone2;
analysis(6) = pointsInsideCone3;
analysis(7) = pointsInsideAll;
analysis(8) = pointsInstrument12Collide;
analysis(9) = pointsInstrument13Collide;
analysis(10) = pointsInstrument23Collide;
analysis(11) = pointsInstrumentAllCollide;
analysis(12) = reachability;
analysis(13) = pctTotalVol12Collide;
analysis(14) = pctTotalVol13Collide;
analysis(15) = pctTotalVol23Collide;
analysis(16) = pctTotalVolAllCollide;
analysis(17) = pctOverlap12;
analysis(18) = pctOverlap21;
analysis(19) = pctOverlap13;
analysis(20) = pctOverlap31;
analysis(21) = pctOverlap23;
analysis(22) = pctOverlap32;
analysis(23) = pctVolumeCollide;
analysis(24) = errorSphere;
analysis(25) = errorConeE;
analysis(26) = errorCone1;
analysis(27) = errorCone2;
analysis(28) = errorCone3;
output = analysis;
```

Listing 3. accuracySphere.m

```
function output = accuracySphere(pointsInside, pointsTotal,
boundaryVolume, radius)

ratioPoints = pointsInside/pointsTotal;

actualSphere = (4/3)*pi*(radius^3);
actualRatio = actualSphere/boundaryVolume;

percentError = 100*((actualRatio - ratioPoints) / actualRatio);

output = percentError;
```

Listing 4. accuracyCone.m

```
function output = accuracyCone(pointsInside, pointsTotal,
boundaryVolume, baseRadius, height)

ratioPoints = pointsInside/pointsTotal;

actualConeVolume = (pi/3)*baseRadius^2*height;
actualRatio = actualConeVolume /boundaryVolume;

percentError = 100*((actualRatio - ratioPoints) / actualRatio);

output = percentError;
```

Listing 5. ellipseY.m

```
function output = ellipseY(x,a,b)
% This function calculates the positive y-values of an ellipse
given the x
% value, a (semi-major axis), and b (semi-minor axis).
y = b*sqrt(1-(x^2/a^2));
output = y;
```

Listing 6. locatePort.m

```
function output =
locatePort(basePort,distanceOffset,angleOffset,horiz,vert,a,b)
% This function calculates the port location based on input
variables
% basePort is an array of (x,y,z)
% horiz: negative = left, positive = right
% vert: negative = down, positive = up

if (horiz >= 0)
 x = basePort(1) + (cos(angleOffset)*distanceOffset);
else
 x = basePort(1) - (cos(angleOffset)*distanceOffset);
endif

if (vert >= 0)
 z = basePort(3) + (sin(angleOffset)*distanceOffset);
else
 z = basePort(3) - (sin(angleOffset)*distanceOffset);
endif

y = ellipseY (x,a,b);

port = zeros(1,3);
port(1) = x;
port(2) = y;
port(3) = z;

output = port;
```

Appendix D. Technology Stack

D.1 Hardware

3D Simulation and Development Platforms
Intel Core i5 M560 @2.67GHz, 8GB RAM
Intel HD Graphics
Windows 7 Professional Service Pack 1 64-bit

Intel Core i7 930 @2.8GHz, 18GB RAM
NVIDIA GeForce 6600 GT 128MB
Windows 7 Professional Service Pack 1 64-bit

Usability Testing platform
Lenovo Thinkpad X60-6364 Tablet
Intel Core Duo L2400 @1.66GHz, 2GB RAM
Gentoo Linux 3.2.1-R2 32-bit
Mozilla Firefox ESR 10.0.3

D.2 Software

3D Visualization
Software platforms were evaluated for the purpose of creating the 3D models. The platforms considered were Autodesk Maya, Autodesk 3ds Max, Blender, Crystal Space, Irrlicht, Mathematica, Matlab, Octave, Ogre3D, OpenSceneGraph and Unity. They were evaluated on operating systems supported, physics support, game engine, graphical user interface for modeling, and extensibility, license, cost. Based on the above criteria, Blender was chosen for the 3D visualization. Blender has the additional advantage of incorporating kinematics for simulation.

Blender
http://www.blender.org/
Starting with version 2.58a to current (2.61)

Computation of Work Volume
GNU Octave, version 3.4.3 configured for “x86_64-pc-linux-gnu”

Patient Image Processing
GIMP, the GNU Image Manipulation Program
http://www.gimp.org/

Patient Torso Model
Wolfram Mathematica 7

Robot Symbolic Parameters
SYMORO+: SYmbolic MOdeling of RObots. Version 1.3 for Windows

SYMORO+ was used to calculate the modified Denavit-Hartenberg parameters of the da Vinci Si Surgical System patient-side cart.

Statistical Analysis
Statistical analysis was performed using R version 2.10.1 (2009-12-14).

Decision Aid Wireframe
Axure RP version 6.0 was used to create the decision aid prototype. For the usability testing, the decision aid was displayed on Mozilla Firefox ESR version 10.0.3 on a Lenovo Thinkpad x60 with 1024x768 screen resolution